



**AFRICA CENTER OF EXCELLENCE FOR WATER MANAGEMENT
ADDIS ABABA UNIVERSITY
SCHOOL OF GRADUATE STUDIES
COLLEGE OF NATURAL AND COMPUTATIONAL SCIENCES**



**DE-FLUORIDATION OF GROUND WATER USING RAW AND MODIFIED
BENTONITE CLAY**

By

Adane Woldemedhin Kalsido

A PhD dissertation submitted to Africa Center of Excellence for Water Management, the School of Graduate Studies of Addis Ababa University in partial fulfilment of the requirements for The Degree of Doctor of Philosophy in Water Management (Water Science and Technology)

June, 2022

Addis Ababa, Ethiopia

Africa Center of Excellence for Water Management
Addis Ababa University
School of Graduate Studies

**DE-FLUORIDATION OF GROUND WATER USING RAW AND MODIFIED
BENTONITE CLAY**

By

Adane Woldemedhin Kalsido

A PhD dissertation submitted to Africa Center of Excellence for Water Management, the School of Graduate Studies of Addis Ababa University in partial fulfilment of the requirements for The Degree of Doctor of Philosophy in Water Management (Specialization in Water Science and Technology)

SUPERVISORS

Main Advisor: Prof. Dr.-Ing Esayas Alemayehu

Co-advisor: Dr. Beteley Tekola

June, 2022
Addis Ababa, Ethiopia

Declaration

I, Adane Woldemedhin Kalsido (GSR/5113/10), hereby declare that this thesis,
**“DEFLUORIDATION OF GROUND WATER USING RAW AND MODIFIED
BENTONITE CLAY**
” has been developed by me and has not been submitted, to this or any other University for any degree and is, except where otherwise stated the original work of the author. The content of the dissertation has not been plagiarized and where works of other researchers have been used, they have been appropriately cited.

Candidate Name

Adane Woldemedhin Kalsido

Signature



Date

21/03/2022

AFRICA CENTER OF EXCELLENCE FOR WATER MANAGEMENT

ADDIS ABABA UNIVERSITY

**DE-FLUORIDATION OF GROUND WATER USING RAW AND MODIFIED
BENTONITE CLAY**

By:


Adane Woldemedhin Kalsido

A PhD DISSERTATION SUBMITTED TO AFRICA CENTER OF EXCELLENCE
FOR WATER MANAGEMENT ADDIS ABABA UNIVERSITY

APPROVED BY BOARD OF EXAMINERS

This is to certify that we have read this PhD research and that in our opinion; it is fully adequate,
in scope and quality, as a PhD dissertation for The Degree of Doctor of Philosophy in Water
Management (Specialization in Water Science and Technology)


Main Advisor

Name Prof. Dr. Ing. Esayas Alemayehu Signature  Date _____


Co-Advisor

Name Dr. Beteley Tekola Signature _____ Date _____

External Examiner

Name Prof. Revocatus Lazaro Machunda Signature  Date 09-June-2022

Internal Examiner

Name Dr. Embialle Mengistie Signature  Date 10-June-2022

Chairperson

Name Dr. Feleke Zewge Signature _____ Date _____

Dedication

This research work is dedicated to my wife, children, parents, brothers, sister
and my supervisors

Acknowledgments

I wish to thank ALMIGHTY GOD for the gift of life and for granting me HIS GRACE and opportunity to pursue this research work. I would like to gratefully acknowledge the Africa Centre of Excellence for Water Management (ACEWM) through the World Bank ACEII project for funding this study. My special and heartfelt thanks go to Dr. Feleke Zewge, Center director & Dr. Beteley Tekola (Deputy Director), Africa Center of Excellence for Water Management those provided me scholarship opportunity to IIT-Delhi, India to conduct all my experimentation work.

I am heartily thankful to my supervisors Prof, Dr.-Ing Esayas Alemayehu and Dr. Beteley Tekola for giving me an opportunity to research in the area of drinking water treatment. Without their guidance and support, this research work would not have been possible. Long hours of in-depth discussion with them on Fluoride, adsorbents, drinking water treatment, and fixed bed column adsorption experiments have given me a comprehensive understanding of the issues, for which I will always be thankful to them. I express gratitude to my mentor during research stay at Indian Institute of technology delhi (IITD), India, Dr. Arun Kumar, for his guidance and thoughts on this research work. I would also like to express my thanks to Prof, Dr. Ing-Esayas Alemayehu & Dr. Feleke Zewge for guidance during the inception and design of this work at proposal level.

I am grateful to different faculties for sharing their knowledge and experience with me. I would also like to express thank to Mr. Netsanet Assefa, for his whole-hearted support and interaction throughout my stay.

To my wife Meron Seid, she has always stood by me and given support even during the hardest periods, children's Yodahe Adane, Edna Adane and Liana Adane for their prayers and patience when I was away.

Adane Woldemedhin Kalsido
ACEWM, AAU, 2022

Bio-Data

Adane Woldemedhin Kalsido is graduate of both Bsc and Msc in Water Supply and Sanitation Engineering from Arba Minch university, Arba Minch, Ethiopia in 2012. Worked as Lecturer at the same university since 2010 upto 2016. Later in 2017, joined Wachemo university as lecturer in Hydraulic and Water resources Engineering Department, and worked until 2018. In 2018, joined the Africa center of Excellence to do a PhD in Water Management (Specialization in Water Science and Technology). The following Articles and Proceeding are published from the research project titled “**De-fluoridation using Raw and Modified Bentonite Clay**” as a requirement for the completion of the program.

1. **AW Kalsido**, Beteley Tekola, Beshah Mogessie, and Esayas Alemayehu. *Excess fluoride issues and mitigation using low-cost techniques from groundwater: A review: Cost Effective Technologies for Solid Waste and Wastewater Treatment*. <https://doi.org/10.1016/B978-0-12-822933-0.00004-8>. Copyright © 2022 Elsevier Inc. All rights reserved.
2. **AW Kalsido**, Arun Kumar, Beteley Tekola, Beshah Mogessie, Esayas Alemayehu; Evaluation of bentonite clay in modified and unmodified forms to remove fluoride from water. *Water Sci Technol* 15 November 2021; 84 (10-11): 2661–2674. doi: <https://doi.org/10.2166/wst.2021.220>
3. **AW Kalsido**, Meshesha, B.T. Behailu, B.M.; Alemayehu, E. Optimization of Fluoride Adsorption on Acid Modified Bentonite Clay Using Fixed-Bed Column by Response Surface Method. *Molecules* 2021, 26, 7112. <https://doi.org/10.3390/molecules26237112>
4. **Adane Woldemedhin Kalsido**, Beteley Tekola, Beshah Mogessie, Arun Kumar, Esayas Alemayehu Fluoride removal from water using locally available bentonite clay in a continuous fixed-bed column: Adsorbent characterization: ***Proceedings of international Conference on Energy and Environment (ICEE 2021)***. <https://www.scribd.com/document/520140858/ICEE-2021-Proceedings>

List of Abbreviations

ANOVA	Analysis of variance
BBD	Box behnken design
CCD	Central composite design
FT-IR	Fourier transform tnfrared spectroscopy
CEC	Cation-exchange capacity
SSA	Specific surface area
WHO	World health organization
HSAB	Hard Soft acid basis
RO	Reverse Osmosis
NF	Nano filtration
ED	Electro -dialysis
pH	Power of hydrogen
pVA	Polyvinyl alcohol
SEM	Scanning electron microscopy
EDX	Electro-dispersive x-ray
RSM	Response surface methodology
XRD	X-ray diffraction
RB	Raw Bentonite
ATB	Acid treated bentonite
Alum-Mbent	Aluminum oxide modified Bentonite
SPADNS	p-sulfophenylazo)-1,8-dihydroxy-3,6-napthalenedisulfonic acid

Contents

Acknowledgments	iv
Bio-Data.....	v
List of Abbreviations	vi
Abstract	xvii
CHAPTER 1: INTRODUCTION AND LITRATURE REVIEW	1
1.0. Introduction	2
1.1. Statement of the problem	5
1.2. Objectives of the research	7
1.2.1. General objective	7
1.2.2. Specific objectives.....	7
1.3. Research questions	7
1.4. Significance of the study	8
1.5. Literature Review	10
1.5.1. Occurrence of Fluoride in water & its chemistry	10
1.5.2. Available fluoride removal technologies.....	12
1.6. Modeling and analysis of column data	22
1.6.1. Operational factors affecting adsorption performance	23
1.6.2. Clays as adsorbent for fluoride removal	25
1.7. Scope of the study.....	34
1.8. Thesis Outline.....	34
1.9. Conclusions and Future research areas	35
CHAPTER 2: MATERIALS AND METHODS.....	37
2.0. Materials and Methods.....	38
2.1. Reagents and Materials	38
2.2. Instruments and software	38

2.3.1.	Fluoride analysis	38
2.4.	Collection of adsorbent and preparation.....	40
2.4.1.	Non-modified adsorbent	40
2.4.2.	Modified adsorbent	40
2.5.	Adsorbent characterization	41
2.5.1.	Surface morphology study and identification of elements	42
2.5.2.	Measurement of physicochemical properties of the adsorbent	43
2.6.	Adsorption experimental setup.....	47
2.6.1.	Column adsorption study	47
2.7.	Investigation of the kinetic models	48
2.8.	Optimization of the Adsorption Conditions Using Response Surface Methodology	51
CHAPTER 3: PHYSICO-CHEMICAL CHARACTERIZATION OF MODIFIED AND UNMODIFIED BENTONITE CLAY FOR FLUORIDE REMOVAL		53
3.0.	Results and Discussion	54
3.1.	Determination of physical properties of the adsorbents.....	54
3.1.1.	Surface morphology	54
3.1.2.	Mineralogy.....	56
3.1.3.	Chemical composition (SEM-EDX analysis)	61
3.1.4.	FT-IR analysis.....	64
3.1.5.	Cation exchange capacity (CEC)	67
3.1.6.	Point-Zero charge Determination	69
3.2.	Summary	71
CHAPTER 4: MODELING OF THE ADSORPTIVE REMOVAL OF FLUORIDE BY ALUMINIUM AMENDED BENTONITE CLAY		72
4.1.	Results and discussions	73
4.1.1.	Breakthrough Curve determination.....	73

4.1.1.2.	Volumetric flow rate effect	76
4.1.1.3.	Adsorbent packed bed depth Effect.....	77
4.1.2.	Evaluation of interaction effect of process parameters on RB and ALUM-MBENT performance.	79
4.1.3.	Modeling of Breakthrough Curves.	82
4.1.3.1.	Thomas model.....	82
4.1.3.2.	Clark Model.....	82
4.1.3.3.	Yoon-Nelson Model.....	83
4.1.3.4.	Adams-Bohart model	84
4.2.	Adsorption capacity comparison by different low-cost adsorbents	86
4.3.	Summary	88
CHAPTER 5: OPTIMZATION OF FLUORIDE ADSORPTION ON TO FIXED BED COLUMN: A STATISTICAL APPROACH		89
5.0.	Results and Discussions	90
5.1.	Statistical Analysis.....	90
5.1.1.	Model fitting and analysis of variance (ANOVA), Quadratic model equations and selected model diagnostic test.....	90
5.1.2.	Analysis of Variance (ANOVA)	92
5.2.	Effect of Operating Condition on the Adsorption Performance of ATB.....	95
5.3.	Interaction Effect of Process Variables.....	97
5.4.	Optimization using the Desirability Function	100
5.5.	Model Validation	103
5.6.	Summary	105
CHAPTER 6: EFFECTS OF CO-EXISTING IONS ON FLUORIDE ADSORPTION AND RE-USABILITY.....		106
6.	Results and Discussions	107
6.1.	Effect of coexisting anions.....	107

6.2. Spent adsorbent regeneration.	112
6.3. Summary	113
CHAPTER 7: CONCLUSIONS AND RECOMMENDATIONS.....	115
REFERENCES	125

List of Tables

Table 1.1: Fluoride concentrations (mg/L) in deep and shallow wells in and outside Ethiopian Rift Valley	8
Table 1.2: The Nalgonda Technique basic operational parameters	14
Table 1.3: The advantages and shortcomings of coagulation-precipitation methods.....	14
Table 1.4: Comparison of different types of adsorbents used as fluoride adsorbent in batch and column study	31
Table 2.1: The models and equations used for the description of column adsorption	50
Table 2.2: Design experimentation variables and levels.....	51
Table 3.1: Identified Patterns List for Raw bentonite.....	58
Table 3.2: Identified Patterns List for Aluminum amended bentonite	59
Table 3.3: Crystallographic properties of raw bentonite determined by XRD analysis	61
Table 3.4: Elemental composition (% by wt.) of RB, ATB and ALUM-MBENT obtained from EDX characterizations.	62
Table 3.5: Values of SSA area and CEC by the Methylene blue adsorption method (particle size of 0.212mm)	68
Table 4.1: Times at the breakthrough points and end points of the experiments for both RB and ALUM-MBENT adsorbents.	74

Table 4.2:Criteria for removal of fluoride through ALUM-MBENT fixed bed column for various initial concentrations at a bed depth of 10cm were obtained.	75
Table 4.3:For different flowrates, the experimental evaluation of column parameters using ALUM-MBENT at a bed depth of 10cm packed bed column	77
Table 4.4:For different bed depths, variables were found for removal of fluoride in the ALUM-MBENT column at a bed flowrate of 15ml/min	78
Table 4.5: Performance evaluation of the RB and ALUM-MBENT column for both synthetic fluoride solution and real ground water samples	80
Table 4.6: Parameters of Clark, Thomas, Yoon-Nelson, and Adams-bohart models for adsorption of fluoride at the varied range of bed height (Z), influent flow rate (Q), fluoride concentration (C ₀) (experimental operating conditions ..	85
Table 4.7:Comparison of different types of adsorbents used as fluoride adsorbent in batch and column study	87
Table 5.1:Experimental runs and their predicted responses.....	91
Table 5.2:Analysis of variance values of experimental design for % fluoride removal and Adsorption Capacity.	92
Table 5.3:Constraints for desirability analysis selected.	101
Table 5.4:Optimization solutions provided by the model.	102
Table 5.5:Model validation.....	103
Table 5.6:Bentonite based adsorbent were compared by their adsorptive capacity	104

Table 6.1: Effects of co-existing ions on adsorption of fluoride onto ALUM-
MBENT: Model Water-Fluoride concentrations of 5mg/L, bed depth of 10cm and
15ml/min flowrate 110

List of Figures

Figure 1.1: A schematic diagram showing the fluoride-existing sources in the environment (Vithanage and Bhattacharya, 2015a)	10
Figure 1.2: The effect of pH diagram on Observed F speciation in aqueous suspensions of montmorillonite at varying pH [F] _{initial} =10 mg/L clay/water = 100 g/L, agitation period= 5–360 min (mean of data), temperature =30oC A: [F] _{sorbed} , B: [F] _{ionic} , C: [F] _{complexed} [.....	11
Figure 1.3:Principle of Nalgonda technique: Alum and lime are added to the fluoride water.....	13
Figure 1.4:Schematic flow diagram of donnan dialysis system: (a) open receiver circuit, (b) closed receiver circuit. Adapted from[60].....	17
Figure 1.5: Schematic principle of electro coagulation	19
Figure 1.6(a): Schematic diagram of column experiment.....	23
Figure 1. 7: Schematic representation of batch operation	23
Figure 2.1 : Schematic representation of the column set-up	48
Figure 3.1:SEM micrographs of the RB (A, B and C are magnified by 1000x , 5000x and 30,000 times respectively).....	55
Figure 3.2:SEM micrographs of the ALUM-MBENT (A, B and C are magnified by 1000x, 5000x and 30,000 times respectively.	55
Figure 3.3:SEM micrographs of the fluoride loaded ALUM-MBENT (A, B and C are magnified by 1000x, 5000x and 10,000 times respectively).....	56
Figure 3.4: XRD pattern of the adsorbents	58
Figure 3.5: Plot of Identified Phases for Raw bentonite.....	59

Figure 3.6:Stick pattern representation for SiO ₂ material	59
Figure 3.7: SEM-EDX micrographs of (a) RB with (b) elemental counts per second/eV for RB, and (c) ATB with (d) Elemental counts per second/eV for ATB, and (e) Alum-Mbent with (f) Elemental counts per second/eV for ALUM-MBENT.	64
Figure 3.8:FTIR spectra of modified and unmodified bentonite clay	67
Figure 3.9:Effect of particle size on CEC value by using pH equilibrium Method	68
Figure 3.10:Effect of particle size on CEC and CEC/SSA value by using methylene blue Method	69
Figure 3.11:Plot of pHZPC PH of modified and unmodified bentonite	70
Figure 4.1:Effect of concentration on the ALUM-MBENT breakthrough profile (, depth= 10 cm), treated volume = 4L, flow rate = 15 mL/min, and pH 7).....	75
Figure 4.2:Effect of flowrate on breakthrough profile of AL-BENT (pH = 7, treated volume = 6750 ml, bed depth = 10cm, and initial fluoride concentration = 5 mg/l).	77
Figure 4.3:Effect of bed height on breakthrough profile of ALUM-MBENT (pH = 7, treated volume =6750 ml, flowrate = 15ml/min, and initial fluoride concentration = 5 mg/l	78
Figure 5.1:Correlation of actual and predicted values for (a) removal efficiency (R) and (b) Fluoride adsorption capacity (Q _e).	95
Figure 5.2:Effect of initial concentration, flow rate and bed depth on % fluoride removal and adsorption capacity (mg/g.....	97

Figure 5.3:3D surface plots for interaction effect of operating conditions on Fluoride removal efficiency (R) and Adsorption Capacity (mg/g).....	100
Figure 5.4:Desirability ramp for optimization (R = 100% & Desirability = 1.00)	101
Figure 6.1:Effects of co-anions on fluoride removal by ALUM-MBENT co-ion concentrations for nitrate and phosphate that can be found in groundwater. Model water: Fluoride = 5mg/L, bed depth =10cm and Q = 15mL/min	108
Figure 6.2:Effect of individual co-existing anions.....	109
Figure 6.3:Effects of Co-existing anions a) C0 = 5mg/L, Q = 25mL/min & bed depth = 2cm b) C0 = 5mg/L, Q= 15mL/min & bed depth = 10cm.	112
Figure 6.4:Removal percentage of fluoride obtained using 0.1MNaOH regenerants at 10cm column depth, 5mg/l of fluoride concentration and 15ml/min flowrate conducted with three de-fluoridation cycles.....	113

Abstract

The presence of fluoride in groundwater sources of drinking water has posed a concern to global public health, particularly in the East African Rift Valley (EARV). The study's ultimate objective was twofold. First, investigate low-cost, locally available adsorbents for fluoride adsorption that could be used in Ethiopia's Rift Valley (which is the country's most fluorotic region), and second, contribute to the search for an appropriate and long-term fluoride removal technology for the treatment of fluoride-contaminated groundwater for drinking water for developing countries. Due to cultural beliefs and the terrible odor they emit, the use of bone char and the Nalgonda process for de-fluoridation is being rejected by users in the study area. Several researchers have advocated for the use of non-conventional low-cost adsorbents, such as natural materials and waste/byproducts from agriculture and industry, as effective adsorbents for the removal of fluoride from aqueous solution in recent years. Low-cost adsorbents, such as clay minerals, have emerged as a viable remediation technique for removing fluoride from polluted ground water. However, only a few clay minerals have been studied and investigated for their usefulness in removing fluoride from polluted water, either as is or after slight alteration. As a result, a new, cost-effective technology of fluoride removal is required. Therefore, in this study, the feasibility of fluoride adsorption from aqueous solutions using naturally available bentonite clay in both modified and unmodified forms is investigated. Scanning electron microscopy (SEM), energy dispersive X-ray (EDX), X-ray diffraction (XRD), Fourier-transform infrared spectroscopy analysis was applied to describe the structure and nature of modified and unmodified bentonite clay. The physicochemical characteristics of the adsorbent were also investigated for moisture content, pH, apparent density, specific surface area, cation exchange capacity and its point-of-zero charge. Results obtained from these studies are presented and discussed. These effects of treatment or modification have been discovered. The EDX analysis reveals a significant silica and alumina content, as well as trace amounts of Fe^{+3} , Ca^{+2} , and Mg^{+2} . The presence of the primary

minerals, silica and alumina, with a minor amount of hematite, was revealed by XRD analysis. Furthermore, the silica and alumina levels have increased due to modification of the original material. SEM scans revealed considerable alterations in the original pore structure. The research involves a series of adsorption experiments in a column mode to evaluate the ability of the adsorbents for fluoride removal from polluted water. The column operations were used to investigate the practical application of the produced low-cost adsorbents for removal effectiveness at greater fluoride concentrations under an ideal pH setting of 7.2, which is suitable for drinking. Under the optimized values of the process parameters of initial fluoride concentration (mg/L), Flowrate (mL/min) and bed depth (cm) under continuously flowing fixed bed column was determined. At optimized conditions, RB have shown very low fluoride removal efficiency (47.19%), whereas, modification of the clay surface with HCl and aluminum oxide, on the other hand, increased fluoride removal efficiency to 79.77% and 94.38%, respectively for the 5mg/L of initial fluoride concentration, 10cm bed depth and 15mL/min flowrate. The statistical model, central composite design (CCD) and mathematical models were applied to evaluate the column adsorption performance. The adsorption modelling study reveals that for all models such as Thomas, Clarck, Yoon-nelson and Adam-Bohart, the lower the flow rates with higher bed height leads to maximum fluoride uptake on to adsorbent. The analysis of variance was used to determine the importance of independent variables and their interactions on adsorption capacity and Fluoride removal. All the R^2 values indicate that the models match the experimental data well. Moreover, the study investigated the effects of co-existing ions in water on the performance of ALUM-MBENT, in column mode, the effects of anions on fluoride adsorption were investigated using concentrations of each anion of 0.1, 10, and 100 mg/L. When competing anions are present, the adsorption capacity of the adsorbent reduces, according to the findings. Multi-valent anions are more easily absorbed than monovalent anions. Carbonates and phosphate are the main anions that have the greatest influence on the fluoride adsorption. The fluoride adsorption is strongly affected by the concentrations of

competing anions. Phosphate, bicarbonate, and sulfate greatly reduced fluoride adsorption. However, chloride had little effect on the sorption. The impact of major anions on fluoride adsorption followed the order of $\text{Cl}^- < \text{SO}_4^{2-} < \text{PO}_4^{3-} < \text{CO}_3^{2-}$. The last objective reports on regeneration of the used adsorbent for fluoride adsorption in column mode. The addition of 0.1MNaOH was able to desorb fluoride. Meanwhile, the regenerated adsorbent showed reasonable removal of fluoride even after three consecutive cycles of experimentation. The degree of desorption varied between 94.5% and 68.5% from cycle 1 to cycle 3. When scaled up, the optimized ALUM-MBENT/ATB can be employed for fluoride treatment from polluted groundwater in EARV. Whatever the current fluoride adsorption capacity of ATB/ALUM-MBENT is encouraging, it is too early to conclude that ATB/ALUM-MBENT is directly applied in the field for treatment of fluoride, since the adsorbents are not tested at large scale in the field and may not sure about its regenerability after field application. Therefore, it is recommended that ATB/ALUM-MBENT should be tested at field level and hence possibly be developed further and it can most likely contribute to the provision of safe drinking water to some of the 16 million people still using unimproved sources, especially those living in rural fluoritic areas of RVLB.

CHAPTER 1: INTRODUCTION AND LITRATURE REVIEW

1.0. Introduction

Fluoride is widely distributed in the geological environment and generally released into ground water by slow dissolution of fluorine containing rocks. Various minerals, e.g., fluorite, biotites, topaz, and their corresponding host rocks such as granite, basalt, syenite, shale, contain fluoride that can be released into the groundwater [1]. Fluoride (F^-) contamination in groundwater has been recognized as one of the serious problems worldwide [2].

The United Nations Development Program has set a target of delivering wholesome or healthy water for drinking to all by 2030 as a sustainable development goal. In recent years, water quality problem has become a big problem all over the world. Aside from microorganism contamination, there are a variety of compounds that pose a significant risk to human health. The most significant problem with groundwater quality is fluoride pollution. Mostly, as consequence of natural and human activity causes, fluoride contamination of groundwater has already become a serious problem, posing health risks to humans [3]. Excessive exposure of fluoride can lead to a number of adverse effects on humans such as dental and skeletal fluorosis, though it has some beneficial effects for enamel strengthening at low concentrations. exposure for longtime leads to the risk of developing crippling skeletal fluorosis and other health effects such as endocrine distributions like renal, intestinal and immune systems [4, 5] [6] [6] . Today, in the world more than 200 million people are at risk of fluorosis and related health effects [7]. The World Health Organization (WHO) has set 1.5 mg/L as the maximum limit for fluoride in drinking water [8]. More than 70 countries of the world have drinking water supplies naturally contaminated with fluoride, and mostly countries belong to the Southeast Asia and South Asia [9]. In several countries of the world such as Chile, Taiwan, India, Bangladesh, Mexico and Hungary, the elevated level of fluoride (1.5 mg/L) has been reported [10]. Fluoride is widely distributed in the geological environment and generally released into ground water by slow dissolution of fluorine containing rocks. The East African Rift Valley zone is one of the locations having

high amounts of fluoride in its groundwater as a result of natural activity. The Rift valley zone is dominated by sedimentary and young volcanic rocks such as fluorspar (CaF_2), cryolite (Na_3AlF_6), and scorodite ($\text{FeAsO}_4 \cdot 2\text{H}_2\text{O}$). Natural processes such as mineral rock hydrolysis, water-rock interactions, desorption, dissolution, and sedimentation are frequent in many rift-valley zones [1, 11]. These mechanisms are to responsible for the observed high fluoride levels (> 1.5 mg/L) in Rift Valley groundwater. For example, fluoride levels have been recorded as high as 13 mg/L in Ethiopia [12] [13] ,13.6 mg/L in Tanzania (Thole, 2013), and 72 mg/L in Nakuru, Kenya [14], all of which occur in the Rift Valley zone. In Ethiopia, roughly 80% of persons living in the Ethiopian Rift Valley are exposed to high fluoride concentrations [15].

Hence, removal of fluoride from drinking water has to be taken as the primarily assignment in areas where the source of water supply is mainly from groundwater. There are a range of technologies exercised for reduction or removal of fluoride from drinking water. Numerous alternative water supply technologies have been identified and tested in different areas of the world to reduce the concentration of fluoride in water. These technologies for fluoride removal are as follows: adsorption, membrane tools, precipitation and coagulation , filtration and oxidation and biological oxidation and ion-exchange [16, 17] . Among these processes, adsorption is widely used due to availability of wide range of natural and synthetic adsorbents, ease of operation, cost effective and high efficiency depending on the nature of adsorbents [18, 19]. Because of its availability and cost, activated alumina is the most extensively employed of the studied adsorbents. However, because of frequent regeneration and limited adsorption capacity, activated alumina is difficult to operate and has a limited sustainability [20].

Several natural inorganic materials including clay minerals have been used in adsorption process for de-fluoridation of water [21] [22] investigated the potential applications of clay and clay minerals in de-fluoridation and indicated that clays have tremendous potential for fluoride adsorption due to their good specific surface area, chemical and mechanical stability, layered structure, and cation

exchange capacity. Clay and clay minerals are among the most abundant natural and inexpensive inorganic filler materials that have been extensively studied because of their strong adsorption and complexation ability. But, their effectiveness is limited only for fluoride concentrations < 1 mg/L [23]. Therefore, it may not be directly applicable to the groundwater in EARV as the majority of water wells are composed of fluoride > 5 mg/L [13]. Surface modification by loading a multivalent cations is vital thing to consider clay as an adsorbent in removing fluoride from drinking water especially for rural communities in less developed countries [6, 21]. Therefore, it is highly recommended to make an adsorbent suitable, if it has a good practical and economic viability for a sustainable use for groundwater de-fluoridation, particularly in developing countries like Ethiopia [24]. Bentonite is an alumino-silicate clay group made composed of layers of alumino-silicate sheets that has a high cation exchange capacity but poor permeability [25]. The bentonite clay's persistent negative charges are stabilized by accessible exchangeable cations. This improves the ability of cationic exchange to remove pollutants ([26]; [27]). Bentonite treated with high ionic density cations demonstrated increased anion adsorption capability. The aluminum oxide [28] and an acid treatment [29] have been proven effective on the removal of fluoride. As a result, one of the major purposes of this research is to emphasize on the surface modifications of bentonite in order to increase the adsorption performance for fluoride removal by applying acid treatment and aluminum Oxide. Acid treatments can often replace exchangeable cations with H^+ ions and Al^{3+} and other cations escape out of both tetrahedral and octahedral sites, leaving SiO_4 groups largely intact. This process generally increases the surface area and acidity of the clay minerals, along with the elimination of several mineral impurities and partial dissolution of the external layers [30]. And also, Al^{3+} is considered to be readily available, presumably in most developing countries, due to the use of aluminum bearing salts such as $Al_2(SO_4)_3$ in conventional water treatment. Thus, with regards to the search for appropriate materials for drinking water de-fluoridation, Al^{3+} could be a suitable for binding of fluoride ions and their subsequent removal from aqueous

environments. Al^{3+} does not occur naturally in the elemental form, but readily combines with oxygen and water to form oxides and/or hydroxides [31]. As a result, investigating optimal conditions for fluoride removal using modified and unmodified bentonite clay may be an appealing task toward gaining access to fluoride-free water in the EARV zone.

In terms of cost, efficiency, simplicity, power needs, availability of materials, know-how, and user acceptability, there is justifiable interest in a novel cost-effective technique to remove fluoride from polluted water. To the best of our knowledge, no research has been published on the removal of fluoride utilizing an acid and aluminum-oxide amended bentonite adsorbent as a possible filter. As a result, the goal of this study was to look at the best operational conditions, efficiency, and methods for removing fluoride from a continuously running fixed bed column. The optimized RB/ ATB/ALUM-MBENT was then evaluated for fluoride removal from underground water samples in the East African Rift valley locations of Ethiopia.

1.1. Statement of the problem

In locations where access to other water sources is restricted, removing fluoride from water is regarded the best approach. Fluoride may be removed from drinking water using a variety of ways. Among the de-fluoridation technologies implemented in Rift valley areas of Ethiopia, the Nalgonda technique takes a lead at the time due to the local availability of the chemical used. The technique works on co-precipitation from the mixing of Al-sulphate and Ca-hydroxide. In addition to the Nalgonda system, other de-fluoridation techniques/ alternatives to provide drinking water for households were studied and tested in the area. These are: Bone char, contact precipitation, Clay and soil, Reverse osmosis (RO) and rain water harvesting [24]. However, some users are opposed to bone-char because to cultural beliefs, the strong odor of treated water, and aesthetic issues. Nalgonda, on the other hand, is known for its huge sludge output, which poses a secondary environmental risk. This indicates that there is a need for obvious alternative cost-effective technique for reducing fluoride to levels safe for human

consumption (1.5 mg/L). Therefore, In this study, the adsorption technique through continuously flowing fixed bed column packed with modified bentonite clay was designed to reduce fluoride levels to WHO limits for drinking purposes. Since most experiments done so far have been in batch form using clay-based minerals, which results in shorter reaction times thus far from equilibrium & based on high fluoride concentrations (> 20mg/l), but the current study considers adsorption with low fluoride concentrations (5,10, and 12 mg/l) through continuously fixed bed column, which will help the scientific community understand under these conditions. In terms of cost, efficiency, simplicity, power needs, availability of materials, know-how, and user acceptability, there is justifiable interest in a novel cost-effective technique to remove fluoride from polluted water. To the best of our knowledge, no research has been published on the removal of fluoride utilizing an acid and aluminum-oxide amended bentonite adsorbent as a possible filter.

As a result, the goal of this study was to look at characterization of modified bentonite clay, the best operational conditions, efficiency, and methods for removing fluoride from a continuously running fixed bed column. The optimized RB/ ATB/ALUM-MBENT was then evaluated for fluoride removal from underground water samples in the East African Rift valley locations of Ethiopia. As a result, the goal of this research was to find the best operational parameters, efficiency, and removal method for low-cost adsorptive technology for fluoride remediation in polluted groundwater in Ethiopia's rift valley.

1.2. Objectives of the research

1.2.1. General objective

The main objective of this research was to modify bentonite clay, investigate for the optimal operation conditions, efficiency and adsorptive capacity through fixed bed column for fluoride removal from groundwater.

1.2.2. Specific objectives

- To **characterize** raw and modified bentonite clay based on their functional group, mineralogy, surface composition, specific surface area, cation-exchange capacity and moisture content.
- To investigate the **effects of operational parameters** by raw and modified bentonite clay through fixed bed column system.
- To examine adsorption data to **kinetic models** in order to describe fluoride adsorption processes
- To **optimize** fluoride adsorption parameters using response surface methodology.
- To determine the effects of **co- existing ions** on fluoride removal behavior of the adsorbents and its reusability

1.3. Research questions

1. What surface features of bentonites raw and modified will be suitable for de-fluoridation??
2. what operational parameters will facilitate the raw and modified bentonites to effectively de-fluoridate the water?
3. What are the optimal adsorption conditions effective for removal of fluoride from the groundwater?
4. Does the presence of common ions in the water affect removal efficiency of adsorbent fluoride?

1.4. Significance of the study

Groundwater is the primary supply of drinking water in Ethiopian rural communities because managing surface water systems, which require treatment, is frequently beyond their capacity. In the country's Rift Valley areas, rural villages are usually tiny and dispersed throughout a vast number of localities. Groundwater is considered the most feasible and cost-effective source of potable water under these conditions since the underlying aquifers may be accessed near to demand centers due to the scattered structure of rural populations. Fluoride is now generally understood as one of the most harmful inorganic pollutants in drinking water on a global scale. Fluoride levels in drinking water should not exceed 1.5 mg/L, according to the World Health Organization. In the Ethiopian Rift Valley, groundwater with fluoride levels above 1.5 mg/L has been recorded. Excessive fluoride in groundwater is a serious water safety problem, mainly affecting areas in the Ethiopian Rift Valley Regions, like Oromia, Afar, and the Southern Nations, Nationalities and Peoples Regional States. So far, groundwater provides drinking water is the sole source of drinking water mostly for many rural communities and in the Rift Valley. Increase in population density and scarcity of surface waters makes the use of groundwater very common. The existing fluoride concentration in different water sources are rich of fluoride for consumption as indicated in Table 1.1. Hence, it is often assumed that any water uses for drinking purpose from this source needs major treatment.

Table 1.1: Fluoride concentrations (mg/L) in deep and shallow wells in and outside Ethiopian Rift Valley

Fluoride (mg/l)	Within the Rift valley				Outside the Rift valley areas			
	Deep wells		Shallow wells		Deep wells		Shallow wells	
	No. of samples	%	No. of samples	%	No. of samples	%	No. of samples	%
<1	192	37.9	90	55.6	225	86.5	169	92.3
1.0 –1.5	61	12.1	28	7.3	25	9.6	4	2.2
1.51–3.0	93	18.4	19	11.7	9	3.5	10	5.5

3.1–7.0	2	20.2	15	9.3	1	0.4		
7.1–13.0	53	0.5	7	4.3				
>13.0	5	1	3	1.9				
Total	506	0	162	100	260	100	183	100

After many years of use of drinking water from drilled wells in the Rift Valley, Ethiopia, dental and skeletal fluorosis has become a serious medical problem [12, 32]. As can be observed in the Table 1.1, the percentage of fluoride exceeding the WHO guideline within the rift valley region is 40% for deep well users and 34% for shallow well users, which is a huge number. As a result, several otherwise successful boreholes (groundwater wells) have been blocked to human consumption (when the water quality analysis indicates the presence of fluoride contamination). This represents a financial loss to the government (cost of borehole drilling plus related/overhead costs). Aside from the economic loss, the circumstance impedes attempts by responsible water authorities to provide access to drinkable water in rural areas and small towns. As a result, the inability to provide clean water to portion of the population more quickly owing to the presence of high fluoride in the ground water supply remains a serious problem. Therefore, the current study is significant by introducing a low-cost de-fluoridation technology as alternative in the reduction of these elevated fluoride level from groundwater sources.

1.5. Literature Review

1.5.1. Occurrence of Fluoride in water & its chemistry

Fluoride in groundwater occurs as a result of weathering and leaching of fluoride-bearing minerals from rocks and sediments. Fluoride is useful in supporting dental health by decreasing dental caries when consumed in modest amounts (0.5 mg/L), but greater doses (>1.5 mg/L) may induce fluorosis [33-36]. Fluoride has been found in mineral rocks such as fluorite CaF_2 , apatite $(\text{Ca}_5(\text{PO}_4)_3\text{F})$, and micas [37]. Fluoride is also found in various minerals such as topaz, biotites, and their host rocks such as syenite, granite, basal, and shales. Thus, the major mechanisms for fluoride release into water are mineral dissolution and rock-water contact [38, 39] as shown in Figure 1.1. The hydrolysis of fluoride of these minerals under higher acidic conditions is responsible for the desorption of fluoride from metal oxide in igneous and metamorphic rocks that also contain fluoride, resulting in the release of fluoride into water [35, 40].

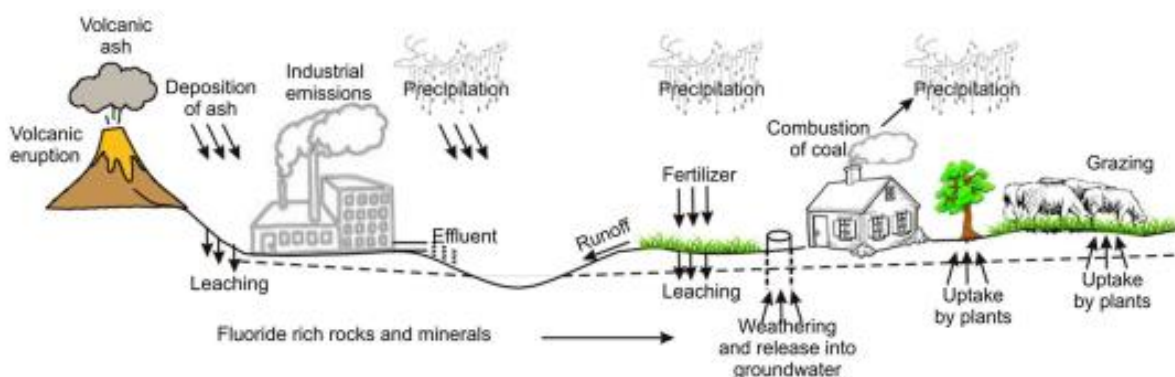


Figure 1.1: A schematic diagram showing the fluoride-existing sources in the environment (Vithanage and Bhattacharya, 2015a)

Different studies have been conducted to separate fluoride (F^-) from water using different sorbents. However, the application of any kind of adsorbent for the purpose of drinking water is linked with the risk of interaction of sorbent with water which could have bring unwanted impurities in the potable water [11, 41-46]. Fluoride exists in the form of (F^-), present in water, it gets easily combined with cations like Al^{3+} , Ca^{2+} , Mg^{2+} and Fe^{2+} . Fluoride is sensitive to mobilization

at the pH values typically found in groundwater (pH 6.5–10.2) and under both oxidizing and reducing conditions [47-51].

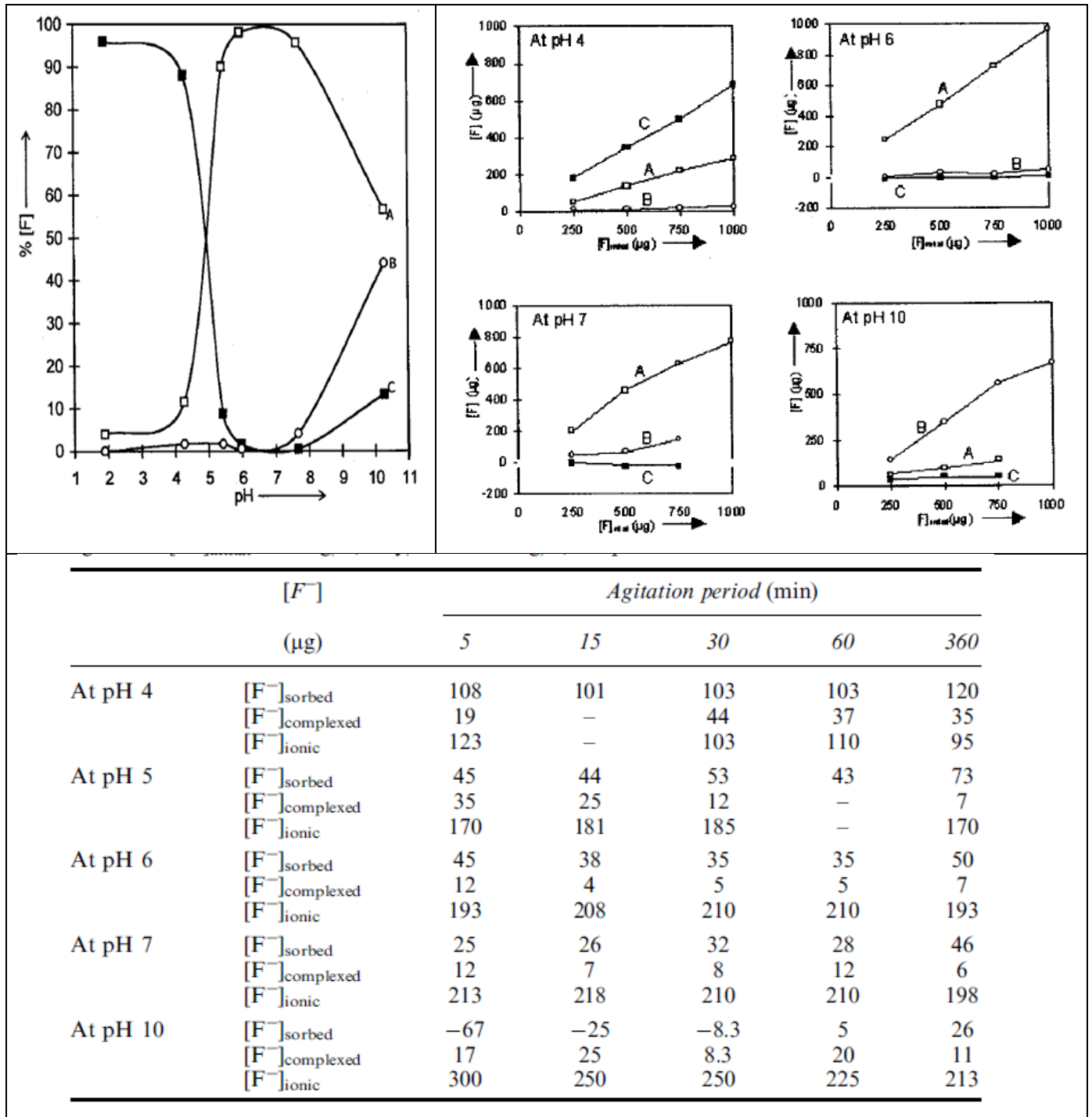


Figure 1.2: The effect of pH diagram on Observed F speciation in aqueous suspensions of montmorillonite at varying pH [F]_{initial} = 10 mg/L clay/water = 100 g/L, agitation period = 5–360 min (mean of data), temperature = 30°C A: [F]_{sorbed}, B: [F]_{ionic}, C: [F]_{complexed} [

The major part of the F⁻ sorbed is clearly shown at pH <4, which tells us that F⁻ exists in complexed form. However, the fraction of F⁻ existing in sorbed phase becomes significant in the pH range 5–7, maximum being at pH 6. At pH>7, while there is a significant decrease in sorbed fraction, a small rise in complexed F⁻ amount can again be seen. The fraction of fluoride existing as ionic F⁻ is almost nil in the pH range 2–7 and attains a significant value only at pH 10.

Under acidic (pH <4) or alkaline (pH>7) conditions the delayed attainment of equilibrium and observed fluctuations in F⁻ concentrations in solution phase even at 360 min of agitation, probably indicates the occurrence of several slow sequential and parallel reactions between the F⁻ and the species released from the disruption of clay lattice. In alkaline conditions OH⁻ ions also seem to play their role in this process as is clear from the decrease in sorbed F⁻ fraction as well as the increase in complexed F⁻ fraction at pH>7.

1.5.2. Available fluoride removal technologies

Improving and developing technologies to remove fluoride from aqueous solution has become a major interest of research in recent years. De-fluoridation is a process of removal of fluoride ion from drinking water. To overcome the hazardous health impact of fluorosis, different approaches for de-fluoridations are available. These are membrane separation processes, coagulation–precipitation, ion exchange, adsorption techniques, electro-dialysis, and electrochemical [52]. Each technology has their benefits and limitations and worked productively under ideal condition to remove fluoride to more noteworthy range. All the above approaches are examined briefly with their advantages and shortcomings.

1.5.2.1. Coagulation - precipitation method

Liming was the old-style method of removing fluoride from drinking water and accompanying precipitation was fluorites. The precipitation and coagulation process with Iron (III), activated alumina, alum sludge and calcium has been widely investigated (Abdollah Dargahi)[53]. The Nalgonda technique which uses Lime and alum are the most usually utilized coagulants for de-fluoridation of water. Development of lime stimuli precipitation of fluoride as insoluble calcium

fluoride and raises the pH value up to 11 – 12. A leftover of 8.0 mg/L leaves from lime, it is constantly connected with alum treatment to guarantee the best possible fluoride removal. As a first step, precipitation happens by lime dosing which is trailed by a second step in which alum is added to bring about coagulation. This technique is one of the widespread techniques broadly used for de-fluoridation of water in developing countries. The entire operation of a commonly used “fill and draw type” de-fluoridation unit for small community (around 200 people) can be completed within 2–3 h, with a number of batch performances in a day [54]. Figure 3 illustrates the scheme of mixing alum and lime based on Nalgonda technique and also the operational conditions with merits vs demerits are explained in Tables 1.2 & 1.3. The mixture is stirred and precipitates containing fluoride settle as sludge to the bottom of the solution [55]. When alum is added to water two reactions happen, In the first reaction, alum reacts with an alkalinity's portion to deliver insoluble aluminum hydroxide $[Al(OH)_3]$. In the second reaction, alum reacts with fluoride ions in the water. Best fluoride removal is proficient at pH range of 5.5 – 7.5 as indicated in Table 1.2 (Gan *et al.*, 2019).

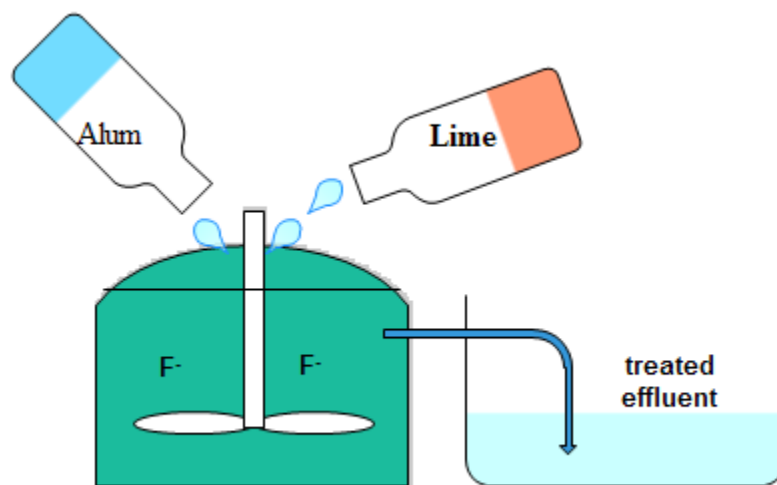


Figure 1.3: Principle of Nalgonda technique: Alum and lime are added to the fluoride water

Table 1.2: The Nalgonda Technique basic operational parameters

Operation parameters	Values
Effective PH range	5.5-7.5
Bleaching powder requirement	3mg L ⁻¹
Suitability	20 L day ⁻¹ utilization

In general, the advantages and shortcomings of coagulation-precipitation methods are summarized in Table 1.3.

Table 1.3: The advantages and shortcomings of coagulation-precipitation methods

Advantages	Shortcomings
Most widely used technique	High consumption of alum
The technology is more practical	Concentrate issue
Easy to use and operate	Health related issue with consumption of aluminum with finished water
The system is easy to understand	The utilization of aluminum sulfate as coagulant expands the sulfate ion concentration greatly which prompting cathartic impacts in human

1.5.2.2. Membrane process

The membrane separation process is more well-known for de-fluoridation of groundwater, wastewater treatment and sea water desalination. The most normally utilized membrane separation processes for removal of fluoride are reverse osmosis, nano-filtration, Donnan-dialysis and electro-dialysis. Each process is discussed below.

Reverse osmosis Technology

Reverse Osmosis technology is a physical process in which the anions are removed by applying pressure on the feed water to direct it through the semi permeable membrane. Reverse Osmosis operates at higher pressure with more protruding rejection of dissolved solids.

The membrane rejects the ions taking into account the size and electrical charge. Reverse Osmosis technology is the reverse of natural osmosis as a result of applied hydraulic pressure to the high concentration side of the solution, it forces solvent filter through the foils or tubes of the membrane, in contradiction of a pressure drop into the lower-concentration solution. In Reverse Osmosis, utilizing a mechanical pump, pressure is applied to a solution via one side of the semi-permeable membrane to overcome inalienable osmotic pressure. The process likewise removes soluble and particulate matter, incorporating salt from seawater in desalination.

Generally speaking, the RO process has proven to be a very efficient process for de-flouridation of drinking water supplies because it works at very low pressure and, in addition to fluoride, other inorganic pollutants are also removed without making any additional effort [56]. Advantages of RO system is summarized as follows.

- Proven technology,
- It removes chemical and biological contamination to WHO standards,
- Recognized and desired technology communities –willingness to pay,
- Widespread implementation – Supply chain and operational benefits.

Drawbacks of the RO system:

- The RO system is more costly to install when we compare with other de-flouridation technologies,
- It may remove nutritional minerals (like magnesium, potassium, and calcium) that our body needs,
- Removing minerals drops the pH of drinking water, which increase free radicals, with the protentional of the cancer risk,

- Heavily contaminated brine.

Nano filtration membrane process

As stated by Hu and Dickson (2006), Nanofiltration (NF) is the later innovation among all the membrane processes utilized for de-fluoridation of water. The essential contrast in the NF and RO membrane separation is that NF has somewhat bigger pores than those utilized for reverse osmosis and offer less resistance to entry of both solvent and of solute. As an outcome, pressures needed are much lower, energy pre-requisites are less, removal of solute is substantially less thorough, and flow are faster. Singh *et al.* 2016 [52] also confirmed Nano-filtration makes use of a similar overall development as reverse diffusion. For nano-filtration, the membranes have slightly larger pores than those used for reverse diffusion and provide less resistance to passage each of solvent and of solutes. As a consequence, pressures needed are a lot of lower, energy needs are less, NF operated at lower pressure and can yield same permeate flux at lower pressure.

The property of nano filtration relative to reverse diffusion may be a specific advantage, and experimental and theoretical analyses are being dedicated to getting a mechanism of substance retention to facilitate production and choice of targeted membranes in addition to optimization of conditions. The NF performance is usually described in terms of the pure water flux (J_w), the solution flux (J_v) and the rejection (R). Regarding to the studies on NF performance on fluoride removal from water is very limited as compared to the other types.

Dialysis

Dialysis separates solutes by transport of the solutes through a membrane instead of utilizing a membrane to hold the solutes while water goes through it as in reverse osmosis and nano-filtration. The membrane pores are a great deal less prohibitive than those for nano-filtration, and the solute can be driven through by either the Donnan effect or a connected electric field.

Donnan dialysis is otherwise called diffusion dialysis (Figure 1.4), is similar to ion exchange membrane however unique in relation to electro- membrane process in which the driving force is not a current from electric, but rather principally a distinction in chemical potential. Concentration difference is the most obvious driving force for ion transport in Donnan dialysis. A negative ion can be driven out of a feed solution through Donnan dialysis is equipped with anion exchange membrane by utilizing a second alkaline stream [57].

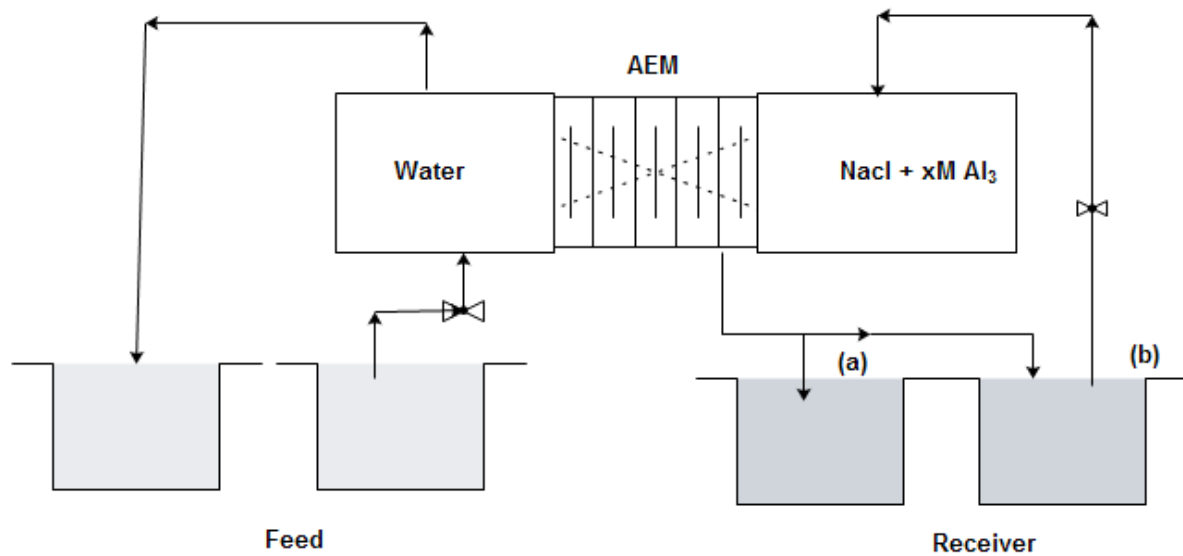


Figure 1.4: Schematic flow diagram of donnan dialysis system: (a) open receiver circuit, (b) closed receiver circuit. Adapted from [58].

Electro-dialysis

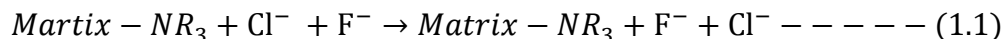
Electro-dialysis (ED) is a process that remove ionic components under the driving force of an electric current from aqueous solutions through ion exchange membranes. ED is separate ionic contaminants from water like reverse osmosis, except current, rather than pressure. Generally, ED is not suitable for rural water treatment because of use of Energy.

The ED processes presented in this literature is mainly explained in two different ways. These are with pretreatment and a chemical pretreatment. When we see the ED without pretreatment, the precipitation risk should be minimized. In this

case, it has been evaluated by Nowak *et al.* 2015 considering two steps. The first one is with 10V and ACS-CMX membrane is used to stop the bivalent ions. And the second one is a 10 V with a conventional membrane AFN-CMX in order to remove the ionic contaminants. Since the second method requires chemical additives in the pretreatment step and, consequently, has more impact on the environment than the first one, the first method which is (without pretreatment) is technical easy and preferable for ED process. However, the high-risk precipitation of the bivalent ions in the concentrate compartment is the major drawback of ED process.

1.5.2.3. Ion-exchange process

As explained by Zarrabi 2014[59], fluoride can be removed from water supplies with a strongly fundamental anion-exchange resin containing quaternary ammonium functional groups. The removal takes place according to the following reaction (Equation 1.1):

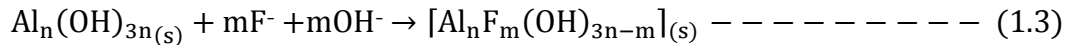
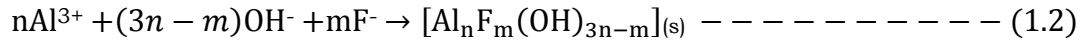


The fluoride ions substitute the chloride ions of the resin. This process proceeds until every one of the sites on the resin are possessed. Water that is supersaturated with dissolved sodium chloride salt can be used backwashed the resin. New chloride ions then substitute the fluoride ions prompting recharge of the resin and beginning the process once more. The driving force for the substitution of chloride ions from the resin is the stronger electro negativity of the fluoride ions.

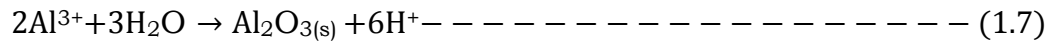
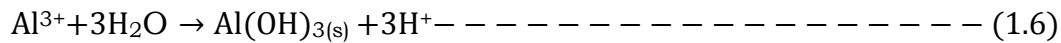
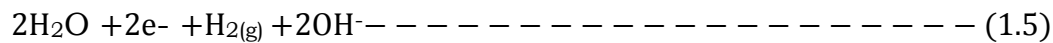
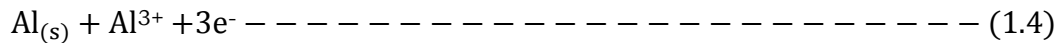
1.5.2.4. Electro-coagulation (EC) process

Electro-coagulation is a technique for applying direct current to sacrificial electrodes that are submerged in an aqueous solution. Electro-coagulation is a straightforward and efficient technique to remove the flocculating agent produced by electro-oxidation of a sacrificial anode and generally made of iron or aluminum. In this process, the treatment is performed without including any chemical coagulant or flocculants.

The mechanism of fluoride removal by EC-process is carried out through an electro chemical co-precipitation of fluoro-aluminium complexes (Equations 1.2 and 1.3, Figure 1.4) and by a chemical substitution reaction as stated in [60].



The EC process is governed by the following process at the Anode (Equation 1.4) and the cathode (Equation 1.5), respectively. In the bulk solution, at the PH-7, the aluminum flocs in the form of aluminum hydroxide and aluminum oxides will be formed as illustrated in Equations 1.6 and 1.7. These aluminum aggregates interact with the pollutants to produce flocs, and motivating the removal of pollutants.



In literature as Grich *et.al* 2019[61], it is also showed that the removal of fluoride is not attractive at $J > 7\text{mA cm}^{-2}$ (Figure 1.5), because the massive H_2 and O_2 bubble production at both the anode and the cathode, in the filter press cells, cause the rapture of aluminum aggregates.

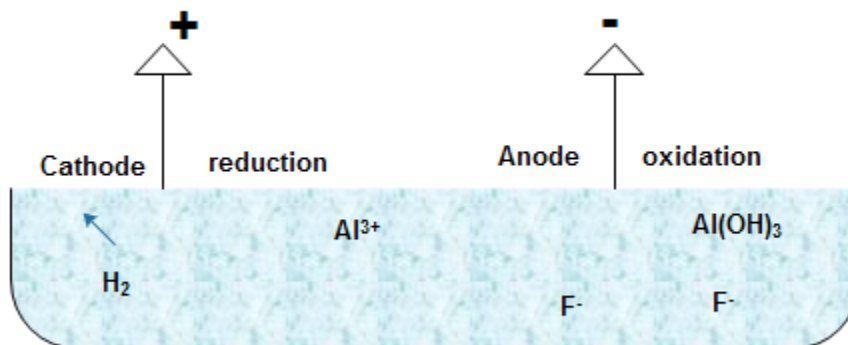


Figure 1.5: Schematic principle of electro coagulation

Due to surface activity, the fluoride ion gets preferentially adsorbed on the bed surface thereby causing a reduction of fluoride ion in the exit stream. In this particular review, an adsorptive method is discussed focusing on two adsorbents.

1.5.2.5. Adsorption technology

This technology is explained by the theory, which states that substances stick primarily because of intimate intermolecular contact. In adhesive joints this contact is attained by intermolecular or valence forces exerted by molecules in the surface layers of the adhesive and adherend. Adsorption processes have played a central role in water treatment for many years but their importance is on the rise with the continuous discoveries of new micropollutants in the water cycle

Adsorption Mechanism: Different researches are reported in literatures for the removal of anions like fluoride from aqueous environment using both modified and non-modified adsorbents. The mechanism of sorption is different for different anions and type of sorbents used till now [1, 62-74]. Generally, the adsorption process consists of three steps:

(i) diffusion within particle internal structure to transport adsorbate molecules to the available adsorption sites of adsorbents surface; (ii); external mass transfer of solute molecules from bulk solution to the sorbent particle surface by diffusion or turbulent movement and (iii) rapid uptake

The following adsorption mechanisms were reported and discussed as follows for fluoride adsorption from aqueous solution.

a) Van der waals forces (outer-sphere surface complexation)

This phenomenon is associated with van der Waals and electrostatic bonds between the adsorbate molecules or ions and the atoms or charges of the functional groups. Adsorbates are said to undergo physical adsorption if the forces of attraction include only physical forces such as coulombic attraction of unlike charges that exclude covalent bonding with the surface. In this case, the attraction between an adsorbate and adsorbent increases with increasing polarizability and size, which are directly related to van der Waals forces. The

larger the adsorbate size the greater the force of attraction. Therefore, adsorbates with high molecular weights such as dissolved organic matter are adsorbed on adsorbents having high surface area through van der Waals forces.

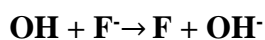
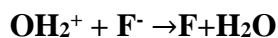
b) ion exchange (outer-sphere surface complexation)

The ion exchange process is rapid and reversible. Ion exchange tends to prefer counter ions of higher valency, higher concentration and ions of smaller hydrated equivalent volume ([59]). The order of selectivity for anions by anion exchange resins generally follows the order: [59]



c) ligand exchange (inner-sphere surface complexation)

The adsorption of fluoride on several multivalent metal oxides near neutral pH was reported to have increased the pH of solutions as a result of releasing OH⁻ ions from the adsorbents by ligand exchange of OH⁻ groups on the adsorbent surface with fluoride in solution.



Ligand exchange mechanisms fluoride (adsorbent) [21]

d) Diffusion and chemical modification of the adsorbent surface

The adsorption capacity of nitrate and fluoride on adsorbents can be increased by chemical modification of adsorbent surfaces [21]. This is particularly of advantage in the case of adsorbents possessing negative surface charges which tend to repel the similarly charged nitrate and fluoride ions. In such adsorbents, positively charged multivalent cations such as Al³⁺, La⁴⁺, Zr⁴⁺, Fe³⁺, and Ce³⁺ are impregnated onto the adsorbent to create positive charges on the adsorbent surface for attracting nitrate and fluoride by coulombic forces as well as producing adsorption sites capable of chemical interaction with nitrate and fluoride [75-77]. These metallic cations act as a bridge in adsorbing fluoride onto the adsorbent.

Adsorption types: There are mainly two types of adsorptions operations. The Batch and Column operations are mainly applied to determine the performance of adsorbents in adsorption systems.

I). Batch operations are usually performed to evaluate the ability of a material to adsorb as well as the adsorption capacity of the adsorbent[48, 50, 78-81] .The data obtained from batch operations are, in most cases, limited to a laboratory scale and thus do not provide data which can be accurately applied in industrial and household systems.

II). Column operations, on the other hand, provide data which could be profitable utilized in industries as well as household areas[48, 50, 78-81]. The schematic presentation of the column and batch operations are shown in Figures 5&6 respectively.

1.6. Modeling and analysis of column data

The practical application of the adsorption process for removing contaminants from water is accomplished by mixing the adsorbent with adsorbate either in a batch-type (Figure 1.7) contact unit operation or a continuous flow packed column bed system. Adsorption processes are characterized by adsorption equilibrium, adsorption kinetics and fixed bed adsorption.

Laboratory-scale column studies (Figure 1.6) simulate the dynamics of a fixed bed reactor that can be used to generate useful parameters, based on analysis of experimental breakthrough curves, which can be employed for design of full-scale water treatment systems [82-86]. The fluoride to be removed from solution in a fixed-bed column containing adsorbent was calculated by breakthrough curves.

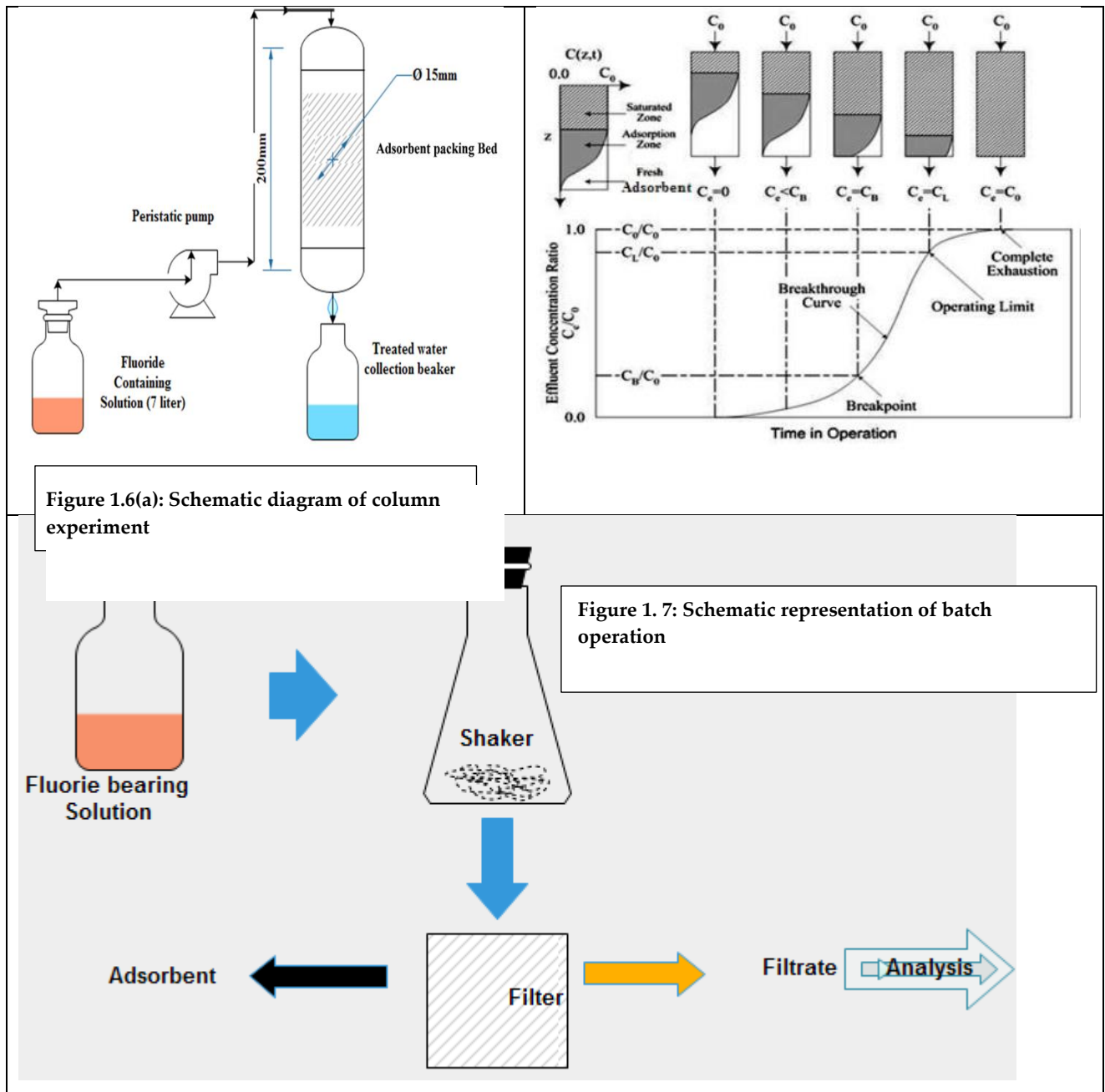


Figure 1.6(a): Schematic diagram of column experiment

Figure 1.7: Schematic representation of batch operation

1.6.1. Operational factors affecting adsorption performance

Most of the studies in adsorption were conducted by using synthetic metal or dye solutions. The effect of different process factors such as the starting adsorbate concentration, adsorbate flow rate in column, column bed height, adsorbate pH, adsorbent particle size, and system temperature were investigated, and breakthrough and exhaust points were observed. Each of these

factors are critical in determining the efficacy of an adsorbent in a continuous effluent treatment process on a pilot or industrial scale [87].

1.6.1.1. Effect of initial concentration

Because a significant number of empty sites were available at the start, adsorption was quick. Following that, raising the initial adsorbate concentration causes a larger driving force to overcome mass-transfer resistance in the liquid phase, and the sites are quickly depleted, resulting in a reduction in the amount of effluent treated. The most relevant feature of the parameter is expressed as with increased influent concentration, breakthrough and exhaustion points occur earlier. Following that, when the inflow concentration increased, the breakpoint time dropped [88, 89].

1.6.1.2. Effect of flow rate

With increasing flow rate, the amount of adsorbate adsorbed onto unit bed height (mass-transfer zone) increases, resulting in quicker saturation. With a reduced flow rate, the adsorbate has more time to contact the adsorbent, resulting in more adsorbate removal in the column. The major features of the parameters during operation is explained as with a larger flow rate, breakthrough points are more likely to occur. With a lower flow rate, the saturation of breakthrough time increases substantially [87, 90, 91].

1.6.1.3. Effect adsorbent packed bed depth

The increase in surface area and the number of binding sites accessible for adsorption was attributed to this. With increasing adsorbent packed bed depth, the time for adsorbate and adsorbent contact increased as well. The most common feature of these parameter during operation is with increased bed depth, breakthrough and exhaustion times take longer. It was also discovered that when the bed depth was raised, the volume of effluent treated increased [87, 92].

1.6.1.4. Effect of particle size of the adsorbent

Adsorption is a surface phenomenon, and the amount of adsorption should be proportionate to the surface area. To prevent problems related with solid-liquid separation, however, extremely tiny particle sizes are not explored. In the fixed-

bed column adsorbent, smaller particles also cause a high-pressure drop. The most common feature of these parameter during operation is with larger adsorbent particle sizes, breakthrough and exhaustion periods take longer. To improve adsorption capability, the largest particle size is preferred. For industrial applications, however, a modest flow rate is preferable [87, 93].

1.6.1.5. pH of adsorbate

It was determined by the type of the adsorbent and the adsorbate. The most common feature for these operational parameter is in certain cases, the highest adsorbate removals are found at acidic pH, whereas the highest adsorbate removals are found at alkaline pH [87, 94].

1.6.1.6. Temperature

It's possible that the increased operating temperature encouraged adsorbate to diffuse more quickly into the adsorbent, resulting in a shorter breakthrough and exhaust time. Furthermore, at high adsorption temperatures, less adsorbate was required to fulfill the adsorbent's maximal adsorption capacity, indicating an exothermic reaction. The most common feature observed during operation is that with rising system temperature, breakthrough and exhaustion times become slower. However, when the temperature rises, the adsorption capacity diminishes [87, 95].

1.6.2. Clays as adsorbent for fluoride removal

Ma and his co-workers in 2005 [96] synthesized granular Zr-loaded bentonite (GZLB) prepared with polyvinyl alcohol (PVA) for the removal of fluoride from aqueous solutions. Also, the regenerated spent bentonite by alum revealed the increase of the de-fluoridation capacity of prepared sorbent. Considering the pH 6.97 and inlet fluoride concentration of 6.34 mg L^{-1} , the adsorption capacity of 755 mg kg^{-1} was obtained.

Modification of bentonite clay with an electro positive atom (using lanthanum, magnesium and manganese), in order to enhance its adsorption capacity for fluoride ions from drinking water, was conducted by Kamble *et al.* 2009 [6]. High fluoride uptake was observed at 10% La-bentonite for de-fluoridation of drinking

water as compared to Mg-bentonite, Mn-bentonite and bare bentonite clay. At an adsorbent dose of 1.0 g L^{-1} , the maximum loading capacity of 10% La-bentonite was found to be 1.4 mg g^{-1} . Furthermore, the uptake of fluoride in acidic pH was higher as compared to alkaline pH and maximum fluoride removal was found at pH 5. The fluoride removal was decreased, due to the competition for adsorbent's active sites by excessive amount of hydroxyl ions at higher pH. The increase in the amount of positive charge in the presence of cations on the oxide surfaces and/or forming of a positively charged surface may helped the uptake of fluoride. The Langmuir maximum sorption capacity of 10% La-bentonite for fluoride was reported as 4.24 mg g^{-1} . The fluoride uptake mechanism was explained through exchange of OH^- ions from 10% La-bentonite surface, which was shown from the results of pH.

Fluoride removal by montmorillonite clay has been evaluated by Karthikeyan *et al.* 2005[97]. Effects of its particle size, temperature and pH were investigated and fluoride uptake was found maximum at pH 2, and it decreased with increase in pH. Particle size of $75 \mu\text{m}$ showed maximum uptake of fluoride when compared to the other particle sizes. At different temperatures, the Langmuir maximum sorption capacity was varied between $1.48\text{--}1.91 \text{ mg g}^{-1}$. The presence of trivalent ion (HCO_3^-) have adversely affected the adsorption of fluoride the study also reveals that adsorption occurred on the surface as well as through intraparticle diffusion pattern of the adsorbent material. Using X-ray diffraction, it is confirmed that the deposition of fluoride on the surface of the clay material was occurred. FTIR analysis also exhibited the involvement of hydroxyl group present on the surface as mechanism for the adsorption.

Another study was conducted by Tor 2006[98] for the de-fluoridation of aqueous solution using montmorillonite. At pH below 5, adsorption was not favorable due to the formation of weakly ionized hydrofluoric acid in acidic conditions, but at pH 6 the maximum removal of fluoride was obtained. The fluoride saturation capacity of montmorillonite was reported 0.263 mg/g at room temperature. The uptake of fluoride by the adsorbent was due to the interaction between the metal

oxides at the surface of montmorillonite and fluoride ions. Also, desorption was made by washing the adsorbent with a solution pH of 12.

Vhahangwele et al. 2014[5] introduced Al^{3+} bentonite clay (Alum-bent) by ion exchange of base cations on the matrices of bentonite clay for the removal fluoride. Modification of bentonite clay with Al^{3+} was performed in batch experiments. Parameters optimized include time, dosage, and Al^{3+} concentration. X-ray fluorescence, X-ray diffraction, energy dispersive X-ray spectrometry attached to scanning electron microscopy, Brunauer–Emmett–Teller analysis, cation exchange capacity (CEC) by ammonium acetate method, and pH_{pzc} by solid addition method was performed for the Physicochemical characterization of raw and modified bentonite clay. The effect of contact time, adsorbent dosage, adsorbate concentration, and pH were evaluated for fluoride removal, in batch modes at $(26\pm 2)^\circ \text{C}$ room temperature. The adsorption capacity of fluoride by modified bentonite clay was observed to be 5.7 mg g^{-1} . At 30 min, 1 g of dosage, 60 mg/L of adsorbate concentration, pH 2–12, and 1:100 solid/liquid (S/L) ratios maximum adsorption of fluoride was obtained. On the Kinetic studies, pseudo-second-order model was well fitted than pseudo first order fluoride adsorption. Monolayer and multilayer adsorption was confirmed due to the Langmuir and Freundlich adsorption isotherms were well fitted. Alum-bent showed good stability in removing fluoride from ground water to below the prescribed limit as stipulated by World Health Organization. We can say that Alum-bent is a potential de-fluoridation adsorbent for the application of point of use devices for de-fluoridation of fluoride-rich water in rural areas especially for the low-income developing countries. And hence, Alum-bent is a promising adsorbent with a high adsorption capacity for fluoride that may replace the expensive water de-fluoridation technologies.

Thakre and his associates 2010a[99] have studied the removal of fluoride by modification using magnesium chloride to enhance its adsorptive capacity. The Mg^{2+} -modified bentonite (MB) was characterized by using XRD and SEM techniques. Various operational parameters such as adsorbent dose, contact

time, pH, effect of co-ions and initial fluoride concentration were experimented by batch mode. The maximum fluoride removal capacity of 2.26 mg g^{-1} was observed over wide range of pH and initial fluoride concentration of 5 mg L^{-1} , which is much better than the raw bentonite. Langmuir adsorption isotherm and pseudo-first-order kinetics models well fitted into the experimental data. Thermodynamic study reveals that fluoride adsorption on MB is reasonably spontaneous and an endothermic process. MB exhibited meaningfully high fluoride removal in synthetic water as compared to real ground water. The study also considers desorption of MB in which that almost all the loaded fluoride was desorbed ($\sim 97\%$) using 1 M NaOH solution. The maximum fluoride removal of 73% after regeneration was applied. Therefore, chemical modification enhances the fluoride removal efficiency of bentonite and it works as an effective adsorbent for de-fluoridation of water.

Mn^{2+} modified bentonite clay was also used for groundwater de-fluoridation [100]. The effect of contact time at various adsorbent dosages, adsorption isotherms and the effect of pH on fluoride removal were evaluated by batch experiments. At first 30 min contact time and increased adsorbent dosage the percentage removal was achieved. The data fitted better to pseudo-second-order reaction indicating that F^{-} adsorption occurred via chemisorption. Both surface and intra-particle diffusion processes were involved during the F^{-} adsorption process as evaluation made by Weber-Morris model of intra-particle diffusion models. Furthermore, at pH 4 the optimum of 75.2% fluoride removal achieved. The acidic pH and at moderate to alkaline pH levels leads to the electrostatic attraction and ion-exchange process as the major mechanisms responsible for fluoride adsorption. Therefore, the study verified that Mn^{2+} modified bentonite clay has potential for application in de-fluoridation of groundwater.

In another study by Gitari *et al.* 2013[101] were studied the use of raw unprocessed bentonite clay and its Fe^{3+} -modified form for fluoride adsorption through a series of batch adsorption experiments to evaluate parameters that influence the adsorption process. Incarnation of Fe^{3+} on bentonite was attained

by mixing the crushed clay with 80 ppm Fe^{3+} solution for 15 min at ratio of 2 g 100 mL⁻¹. It was observed that the raw bentonite clay increases the pH of the F^- solution as opposed to the Fe^{3+} -modified bentonite. Fe^{3+} bentonite exhibited 100% F^- removal as different to raw bentonite, while the raw bentonite clay reveals release of F^- over the same pH range. This is critical to consider for the application of the adsorbent for de-fluoridation at the normal pH of the groundwater with no need for adjustment. Iron (III) -modified bentonite was effective in fluoride removal in high fluoride groundwater samples. The experimental data fitted well to Langmuir adsorption model that indicates a monolayer coverage of the adsorbent. Room temperature was also found to be favorable for the adsorption process. The results of the work indicated that Iron (III)-modified bentonite has possible for the use of onsite water de-fluoridation systems for household use in rural areas in South Africa.

Assaouj 2018[102] using natural bentonite clay (NBC) was investigated using batch adsorption experiments for wastewater de-fluoridation. X-Ray Diffraction (XRD), X-Ray Fluorescence (XRF), Energy Dispersive X-Ray attached to Scanning Electron Microscopy (SEM-EDX), BET Specific Surface Area (SSAN2BET) analysis and Fourier-Transform Infrared Spectrometry (FTIR) were applied for the determination of the mineralogical and physicochemical characterization of the adsorbent. Batch adsorption experiments were conducted to evaluate the effect of various operational parameters such as contact time, initial fluoride concentration, adsorbent dose and initial pH solution at room temperature (25 ± 2°C).

The experimentation results reveal that 30 min of contact time was sufficient for attaining equilibrium. For 5 mg L⁻¹ and 2 g L⁻¹ of initial fluoride concentration and adsorbent dose, the maximum wastewater de-fluoridation (52.2%) was obtained in the acidic conditions (pH=2). The pseudo-second-order kinetic adsorption model well fitted well to the experimental data. The maximum adsorption capacity achieved by applying NBC to be 4.4 mg g⁻¹. The Freundlich isotherm model well fitted with the adsorption data confirming multilayer

adsorption with heterogeneous energetic distribution of active sites and with interaction between adsorbed molecules. The adsorption mechanism might be through ion exchange adsorption, accompanied by interactions of fluoride with metal ions forming Metal-F complexes.

In the study conducted by Zhang and his associates in 2013[50], new adsorbent namely bentonite/chitosan beads have been synthesized and studied for its de-fluoridation efficiency. Following the preparation of beads using inverse suspension polymerization method, the bentonite/chitosan beads (bentonite dosage of 3.0 g) was used for de-fluoridation and showed an adsorption capacity of 0.895 mg g⁻¹ whereas chitosan beads had only 0.359 mg g⁻¹. The maximum de-fluoridation capacity of 1.164 mg g⁻¹ was observed at optimal pH value of 5. The adsorption capacity was evaluated by the process's parameters such as effect of temperature, contact time and initial fluoride concentration on the of the adsorbent. The mineralogical and physico-chemical characterizations were also made by Scanning electron microscopy (SEM), energy dispersive X-ray analysis (EDAX) and Fourier-transform infrared spectrometry (FTIR). Freundlich isotherm model and pseudo-second order kinetic model were well fitted with the adsorption data.

In another study done by Zhang *et al.* 2014 [51], a novel adsorbent, La(III)-loaded bentonite/chitosan beads (La-BCB) was prepared for de-fluoridation from aqueous solution. To examine the de-fluoridation behavior the adsorbent, the effects of various parameters such as dosage of La (III), pH, temperature, contact time, initial fluoride concentration and presence of co-existing anions were investigated. At pH 5 and temperature of 30 °C, the maximum de-fluoridation capacity of La-BCB of 2.87 mg g⁻¹ was achieved. The characteristics of La-BCB were analyzed by Scanning electron microscopy (SEM), energy dispersive spectroscopy (EDX) and Fourier transform infrared spectroscopy (FTIR). Both Langmuir and Freundlich isotherm models were fitted well with equilibrium fluoride adsorption data and pseudo-second order kinetic as well as particle and intraparticle diffusion models were fitted well. The presence of co-existing ions

(Carbonates and bicarbonates) reduced de-fluoridation capacity of La-BCB while sulphate, nitrate and chloride showed slight effect. Only a 17% loss was observed from the used adsorbent, but the rest was successfully regenerated using sodium hydroxide as a regenerant.

Table 1.4: Comparison of different types of adsorbents used as fluoride adsorbent in batch and column study

Adsorbent	Experiment Type	PH	Conc. range (mg L ⁻¹)	Ads. Capacity (mg g ⁻¹)	References
Al ³⁺ -modified bentonite clay	Batch	2-12	60	5.7	(Vhahangwele <i>et al.</i> , 2014)
Mg ²⁺ -bentonite clay	Batch	3-11	5	2.26	(Thakre <i>et al.</i> , 2010a)
Mn ²⁺ -modified bentonite	Batch	4	5	2.4	(Mudzielwana <i>et al.</i> , 2018)
Fe ³⁺ -modified bentonite clay	Batch	2	10	2.91	(Gitari <i>et al.</i> , 2013)
Natural Bentonite Clay	Batch	2	5	4.4	(Assaoui J*, 2018)
Bentonite/Chitosan Beads	Batch	5	100	1.164	(Zhang <i>et al.</i> , 2013)
La ³⁺ bentonite/Chitosan beads	Batch	5	15	2.87	(Zhang <i>et al.</i> , 2014)
Zr-loaded bentonite	Batch	6.97	6.34	0.755	(Ma <i>et al.</i> , 2005)
Granular acid treated Bentonite	Batch/Column	4.9	6	0.009	(Ma <i>et al.</i> , 2011)

As shown in table 1.4, bentonite clay was chemically modified by Al^{3+} by Vhahangwele and his co-workers in 2014[5]. The aluminum modified bentonite (Al-MB) exhibited significantly high fluoride removal efficiency over a wide pH range of 2–12. Maximum fluoride removal capacity of 5.6 mg/g was achieved at maximum fluoride concentration of 60 mg L⁻¹ which is much better than the raw bentonite.

For low concentrations of fluoride, bentonite clay modified by Thakre *et al.* 2010[103] are effective. In a wide pH range of 3–10, the magnesium incorporated bentonite (MB) showed significantly high fluoride removal efficiency. co-existing anions had no major effect on fluoride removal efficiency of MB except bicarbonate which has showed slight effect. A maximum fluoride removal capacity of 2.26 mg g⁻¹ was achieved at an initial fluoride concentration of 5 mg/L, which was reported better than the unmodified bentonite

The order of fluoride removal is presented as follows: bentonite > Charfines > Kaolinite > Lignites > nirmali Seeds.

Clay minerals has successfully been used as a method for removing fluoride from drinking water in domestic dwellings but it has not been used on a larger (village) scale. Many different forms of and differently treated clays have also been tested in a laboratory setting for their removal capacities; they can be effective fluoride removers at lower raw water concentrations of fluoride but their effectiveness in situ has not been widely tested through continuously flowing fixed bed column. The advantages of this treatment method are the low cost, ease of construction and ready availability of materials; the disadvantages are variable efficacy of the wide variety of media and the unproven scalability.

Among many clay minerals, Bentonite is considered in this study, which is a hydrous aluminum silicate, and it has been reported as effective and economical adsorbent for removal of fluoride from water through adsorption. However, the low adsorption capacity is the major problem for its possible application.

Therefore, it is important to modify the bare bentonite to overcome its drawbacks for fluoride removal.

The study explored the use of bentonite clay as base material for the synthesis of fluoride adsorbent which could have the potential for local production, hence a sustainable application for drinking water de-fluoridation.

The adsorption capacity of the synthesized adsorbents was studied in laboratory column experiments. The adsorbent characterization techniques and, several adsorption models were employed to understand the physico-chemical characteristics and fluoride adsorption capacities of the raw and synthesized adsorbent, as well as the mechanism of the fluoride removal. In addition to the adsorption performance, the potential for regeneration and the effect of regeneration on adsorption capacity also needs to be studied. Finally, the adsorbent should be tested in a continuously flowing fixed bed column to scale up to the pilot community filter plant in Ethiopian Rift Valley to evaluate the performance of the technology under real condition.

1.7. Scope of the study

The fluoride adsorption performance of the raw and synthesized adsorbents was studied. Various characterization techniques and, several kinetic and equilibrium isotherm models were employed to understand the physico-chemical characteristics and fluoride adsorption properties/capacities of the synthesized adsorbent, as well as the mechanism of the fluoride removal. The overall goal of the study was therefore twofold: (i) There is a need to **develop low cost adsorbents naturally available** materials for the removal of fluoride which are available in abundance (which is considered low-cost), (ii) Regeneration studies are carried out to obtain the reuse capacity of adsorbent which will reduce the environmental problem. and, (iii) to contribute to the search for an appropriate and sustainable fluoride removal technology for the treatment of the fluoride-contaminated groundwater for drinking water production in developing countries.

1.8. Thesis Outline

This dissertation work is made up of 7 chapters: **four** of the chapters represent the results and findings of different segments of the research, in addition to an introductory and conclusion chapters.

The first **Chapter 1** describes the general information as introductory part of the thesis and about literature review on the fluoride occurrence, fluoride health effects, and related works review on different low-cost fluoride removal technologies.

Chapter 2 comprises of the methods and materials employed. The rest of four chapters (3, 4, 5 & 6) present results from laboratory studies on the preparation of adsorbents for water de-fluoridation, that might have a potential for sustainable application in fluorotic areas of Rift Valley areas Ethiopia, based on surface modifications of indigenous/locally available material (bentonite clay) as base material.

Chapter 3 investigates the characterization and Properties of bentonite clay as adsorbent for removal of fluoride from water in fixed-bed column.

Chapter 4 evaluates an analysis for the Removal of fluoride from groundwater using Raw and Al-synthesized bentonite clay fixed bed column. It is mainly focused on the breakthrough Curve Analysis and adsorption modelling using different models.

Chapter 5 assesses the efficacy of ATB for water de-fluoridation under continuous flow conditions in laboratory- scale column experiments, and the optimization of the column using Response surface Methodology (RSM).

Chapter 6 studies the effects of co-existing anions on fluoride removal using Aluminum oxide modified bentonite clay and also the regeneration of the adsorbent for further use than disposal to the environment.

At the end, **chapter7** provides the overall conclusions, recommendation's and research outlooks for further research.

1.9. Conclusions and Future research areas

The following concluding remarks were derived from the review:

- I. Modification of minerals with metal oxide is a crucial matter for the actual application of Bentonite clay minerals for the removal of fluoride from groundwater.
- II. Tri-metal and Di-metal compounds are found to be more effective on filling the pores of bentonite minerals that enhance the surface area to adsorb anions.
- III. A promising result as indicated by different researchers because of it is the most active in the removal of fluorine from aqueous solutions.
- IV. Bentonite is an efficient de-fluoridating agent. In-situ production of adsorbents from low-cost materials may be an even better de-fluoridation technique. With proper sludge management, de-fluoridation by modified bentonite has a high potential for application.
- V. To maximize the adsorption capacity (low capacity of adsorption) of bentonite surface modification have shown significant changes in the physicochemical and adsorption structural characteristics of the samples; i.e., the ratio of the micro and mesopores and also the value of the specific

surface increase, the apparent density decreases, and the porosity of the sorbent grows and hence modification of the low-cost adsorbents is a paramount job for researchers on the field to have a good de-fluoridating agent.

- VI. Depending on the literatures result on de-fluoridating water, among the reviewed adsorbents in batch experimentation, Al-modified bentonite takes the lead. But the selectivity of the adsorbent depends on the availability and feasibility at the local level.
- VII. Almost above 98% of the literatures reviewed, the mode of experimentation was conducted using batch. This is therefore to enhance the applicability of the adsorbents at industry level, or community level water purification column operation has to be conducted.

CHAPTER 2: MATERIALS AND METHODS

2.0. Materials and Methods

2.1. Reagents and Materials

All reagents used in this study were of analytical grade except the raw bentonite. Here are the list of chemicals and reagents used throughout the research work. All chemicals were supplied by Merck S.P.L,Worli ,Mumbai India-400 01. Here are the list of chemicals and reagents used throughout the research work. Sodium Fluoride (NaF), Aluminum Sulphate $\text{Al}_2(\text{SO}_4)_3 \cdot 16\text{H}_2\text{O}$, SPANDS reagent, Zircony-chloride , Sodium-Arsenate, Methylene Blue (25gm), Hydrochloric acid (HCl), Sodium Hydroxide (NaOH), Potassium chloride(KCl), Potassium bromide (KBr), Acetic acid, Sodium carbonate (Na_2CO_3), Potassium dihydrogen phosphate (KH_2PO_4), Potassium Nitrate (KNO_3), Sodium Chloride (NaCl), Sodium Sulphate (Na_2SO_4), Sodium Carbonate (Na_2CO_3).

2.2. Instruments and software

A high precision electrical balance (Denver, SI-234 or Sartorius-312) was used for weighing of samples. The shaking samples for methylene blue experiments was conducted in a temperature controlled magnetic stirrer (Spinot, Cat No. 6040 or 6030). A UV-visible spectrophotometer (Systronics, Vis double beam Spectro 1203) with a 1cm quartz cell was used for quantitative determination of Fluoride in solution. A peristaltic pump (Mrclab, Model No. PP-X-10) was used for providing constant fluoride solution of fixed-bed column.

2.3. Determination of fluoride

2.3.1. Fluoride analysis

2.3.1.1. Fluoride model water

For determining fluoride ion in water, the electrode and colorimetric methods are the most satisfactory. Because both methods are subject to errors due to interfering ions, it may be necessary to distill the sample before determination. When interfering ions are not present in excess of the tolerance of the method, the fluoride determination may be directly without distillation.

This SPADNS method has an analytical range of 0 to 1.5 mg F /l with virtually instantaneous colour development. A curve developed from standards is used for determining the fluoride concentration of a sample by performing proper dilution. Fluoride reacts with the dye lake, dissociating a portion of it into a colorless complex anion (ZrF6⁻); and the dye. As the amount of fluoride increases, the colour produced becomes progressively lighter.

2.3.1.2. Apparatus for fluoride detection

Hitachi U-2000 spectrophotometer with 1.0 cm quartz cells was used for the absorbance measurements. Orion's Portable pH Meter with Orion Triode electrode was also employed for the pH, temperature and conductivity measurements of the influent solutions and effluent.

2.3.1.3. Determination of adsorption capacity and removal efficiency of fluoride

The fluoride concentrations before and after adsorption was recorded, and the percent of fluoride adsorption (removal efficiency) by the adsorbent was computed by using Equations 2.1.& 2.2.

All experiments were conducted in triplicates for better accuracy and the mean values were reported. Equations (2.1) and (2.2) were used to calculate the percentage removal and adsorption capacity, respectively.

The amount of F adsorbed, q_e (mg/g), was calculated from the expression (2.1): where Q = adsorption capacity (mg/g), C_o = initial F⁻ concentration (mg/L) , C_e = F⁻ concentration at equilibrium (mg/L), V = volume of solution in liter (L) and m = mass of adsorbent (g).

$$Q = \frac{V}{m} (C_o - C_t) \quad (2.1)$$

whereas, the percentage F adsorption from the relationship:

$$\% \text{ Removal} = \frac{(C_o - C_t)}{C_o} * 100 \quad (2.2)$$

2.3.1.4. Experimental data analysis

Design–Expert (Stat–Ease Inc., version 7.0.3, Minneapolis, USA) and Origin Pro 8 (Origin Lab corporation, Northampton, USA) software were used for the data analysis and fitting the values in various models.

2.4. Collection of adsorbent and preparation

2.4.1. Non–modified adsorbent

The most common and most effective type of clay used in water purification is bentonite which is an adsorbent and is generally impure clay consisting mostly of montmorillonite and also the structure of montmorillonite is a gibbsite layer sandwiched between two silica sheets to form the structural unit as described by [29].

Bentonite clay was collected from Geology laboratory of Indian institute of Technology Delhi which was stored for educational purpose. The raw bentonite clay samples were washed with ultra-pure water produced in IIT-Environmental engineering laboratory distiller. The washed bentonite was then dried in an oven for 24 h at 105°C. The samples were milled into a fine powder using hand crusher and made ready for use. This sample was named as RB.

2.4.2. Modified adsorbent

2.4.2.1. Preparation of Acid Treated bentonite clay

The modification of the surface of clay minerals through impregnation using acids, bases, and salts has been conducted by various researchers. Usually inorganic acid such as hydrochloric acid (HCl), sulfuric acid (H₂SO₄), nitric acid (HNO₃) are used for that purpose [104].

The Acid activation of the bentonite clay was conducted using the procedure reported by [29]. Data of surface area measurements have showed that with increase of concentration of hydrochloric acid, the surface area increased. The authors studied that differences of surface area at high acid concentrations (0.25 - 0.4 M) were caused by structural changes and partial decomposition of the samples. The maximum value (837.11 m²/g) was reached by the sample

activated with 0.4 M HCl. In contrast, activation with higher concentration (0.6 M) caused a decrease in the surface area

In this research, 0.4M HCl was used and a total of 150 g of ground bentonite was mixed with acid. Prior to modification, the clay was exposed for subsequent washing by ultra-pure (RO) water and calcinated in an oven at 300°C for 2 hours in order to remove some tedious material like carbonates from the surface. Then, the mixture was stirred at 60°C for 2 h using incubator shaker. Subsequently, the product was separated from the solution by filtration and washed several times with distilled water the pH of the filtrate ranges between 5.8 and 8.7, which is suitable for drinking water purpose and lies on permissible level. Subsequently, the sample was oven dried for 24 hours at 105°C, crushed and sieved to particle size ranges of 0.212mm-2mm and stored in PE bags. This sample was named as ATB.

2.4.2.2. Preparation of Al- Modified bentonite clay

1000mg/l of stock solution of Al^{3+} was prepared using $Al_2(SO_4)_3 \cdot 14H_2O$. From the prepared stock solution, appropriate dilutions were made using ultra-pure water. In order to make enough amount of sample, 20gm of $Al_2(SO_4)_3 \cdot 14H_2O$ was dissolved into 100ml of double distilled water in a beaker. Then 60gm of clay mineral was mixed with 900ml of double distilled water. Further, the clay solution was added slowly to the alum solution by continuously stirring for 60min using incubator shaker. The mixed solution was equilibrated for 24 hours before filtered and washed with deionized water, dried overnight at 105°C and stored in PE bags. This sample was named as ALUM-MBENT. This procedure is adopted from [5].

2.5. Adsorbent characterization

A wide range of researches have been conducted to quantitatively analyze and characterize bentonite samples using different instrumental techniques such as infrared spectroscopy (FTIR), energy dispersive X-ray spectroscopy (EDX), X-ray diffraction (XRD) and scanning electron microscopy (SEM). This study validates

the application of some of these techniques for comparative characterization of unmodified and modified bentonite clay.

2.5.1. Surface morphology study and identification of elements

2.5.1.1. Scanning electron microscope (SEM) study and EDX study

Scanning Electron Microscopy (SEM) coupled with Electro-Diffraction x-ray (EDX) was used to obtain information about the samples surface morphology, composition and properties. It helps in analyzing the structure and shape of the surface of bentonite[105].

In this study, samples of three materials (RB, ATB and ALUM-MBENT) were prepared to study the surface morphology by exposing it beams at magnifications of 1000x,5000x and 10000x.This samples were also subjected to EDX analysis for determining elemental analysis.

2.5.1.2. X-Ray Diffraction Analysis

XRD analysis was performed by PANalytical XRD instrument used for phase identification of a crystalline materials and can provide information on unit cell dimensions. The samples were cleaned with acetone solution and placed in aluminum specimen holder prior to analysis. The specimen holder was mounted inserted in the X-ray diffractometer for the analysis. The analysis was performed using Cu radiations of $K\alpha_1$ (Å): 1.54205, $K\alpha_2$ (Å): 1.544426, $K\alpha_2/K\alpha_1$; and intensity ratio of 0.50, $K\alpha$ (Å): 1.541874, $K\beta$ (Å): 1.392250. The X-ray tube was operated at 45 kV and 40mA where the 2θ angle of the diffractometer was stepped from 5° to 80.002° scan rate with a step size of 0.02° and time per step of 36.195 sec. The type of scan was continuous with minimum step size 2θ : 0.001, Minimum step size Ω : 0.001. The XRD data were analyzed and interpreted using X'pert high score plus software.

2.5.1.3. Functional group analysis: FT-IR Study

FTIR characterization of Adsorbents (a) before and (b) after fluoride adsorption was also employed to get an insight into the nature of Raw, ATB and ALUM-MBENT as well as its interaction with fluoride. The analysis was collected using Nicolet 6700 FTIR spectrophotometer (Thermo Instrument, USA).

2.5.2. Measurement of physicochemical properties of the adsorbent

2.5.2.1. Moisture content (%)

The oven-drying technique was used to determine moisture content.

In a Petri dish, 5.0 g of the adsorbent was precisely weighed. The dish was put in an electric oven set to 110°C for around 5 hours before being cooled in a desiccator and weighed. Heating, chilling, and weighing were performed every 30 minutes until the change in weight was less than 5 mg.

The moisture content of each adsorbent sample's was carried out and determined using the Equation (2.3) as per the standard set by American Standard testing Method [106].

$$\%MC = \frac{W2 - W3}{W3 - W1} \text{ --- (2.3)}$$

Where,

W1 weight of crucible (g)

W2 weight of crucible + wt of sample before oven dry

W3 weight of crucible + wt of sample after oven dry

2.5.2.2. Apparent density (g/cm³)

Apparent density of the adsorbent was determined as per literature reported by [107]. A slight compaction was applied on the cylinder to avoid void space between adsorbent particles before volume and mass measurements conducted. The final apparent density of the samples was determined by measuring in triplicates and values are reported.

Specific gravity bottle of 50 mL capacity without the stopper was weighed. Then it was filled with the adsorbent upto the edge of the neck tapping the bottle upto 20 times to ensure the absence of void spaces and weighed. The bulk or apparent density was obtained by dividing the weight of the adsorbent with volume of the adsorbent.

$$\text{Bulk density } \left(\frac{g}{cm^3} \right) = \frac{W_2 - W_1}{V}$$

Where e Weight of the empty bottle = W_1 ;

Weight of the bottle + adsorbent = W_2 ;

Volume of adsorbent = V .

2.5.2.3. Cation-exchange Capacity: Methylene blue method

The methylene blue (MB) method, adopted from by [108] study, gives a determination of the CEC value by determining the specific surface area.

To obtain the CEC by (MB) titration method, the clay was first mixed with deionized water until a homogeneous slurry was obtained. Then after, a known concentration of methylene blue (MB) was added to the mixture. The mixture was is then agitated for 1 minute using magnetic stirrer. And then, after taking a drop on a filter paper and observe a light blue halo around dark blue of the droplet. When the substitution between bentonite and methylene blue stops, the blue halo on the filter paper disappears. This analysis is repeated several times for the three adsorbents to keep it accurate. The average CEC values were calculated according to Equation 2.4.

$$\text{CEC (meq per 100 g of clay)} = \frac{100}{F * V * NMB} \text{ --- (2.4)}$$

Where, F is the sample weight, V is the required methylene blue volume at the time of titration, N is the normality of the MB solution is (i.e ,0.028 N) [109].

2.5.2.4. Cation Exchange Capacity: pH equilibration Method

In this method, the CEC values were determined by measuring pH change with pH meters. Measurements and calculations of CEC values were performed in accordance with procedures performed by [110]. 1 M acetic acid solution was prepared and 25 ml of acetic acid added into beaker glass containing 5 gm of bentonite with different particle size (0.212mm, 0.425mm, 0.6mm and 1.25mm). The mixture was then stirred for 1 hour using a magnetic stirrer and pH of supernatant was measured. All measurements were repeated three times and average CEC and standard deviations were reported. After doing experiments for the three adsorbents using mentioned particle sizes, a CEC particle size plot was determined. Values of CEC were calculated using Equation (2.5) where 22 is a derived conversion factor of the curve of Brown (1943).

$$\begin{aligned} &\text{CEC (meq per 100 g of clay)} \\ &= (\text{pH observed} - \text{pH acetic acid}) \times 22 \text{ --- (2.5)} \end{aligned}$$

2.5.2.5. Surface Area: methylene blue method

The methylene blue value for bentonites is determined as follows: 0.3 g both modified and unmodified bentonite was mixed ultrasonically with buffer for pH = 7 and dispersion agent (1 g sodium hexa metaphosphate) and 50 ml distilled water. With a burette a 0.01 M methylene blue solution was added in the slurry near the end point mixed using magnetic stirrer for 1 minutes. After each addition a drop of the suspension was taken and placed in a filter paper LS 14 (Schleicher and Schtill) and observed for the appearance of the halo. The consumption of methylene blue solution in ml corresponds with a weighted-in of 1 g clay to the exchange capacity in meq/100g clay and the surface area of modified and unmodified bentonite calculations were made as reported by [108, 109] and equation (4).

$$SSA = Mf * 130 * 6.02 * \frac{10^{-2}m^2}{g} \text{ --- (2.6)}$$

Where M_f is the methylene blue adsorbed per 100gm of clay. Hence, the specific surface area of the modified and unmodified bentonite clay was determined. And, hence, the halo method is the simplest routine analysis to be performed in the laboratory.

2.5.2.6. Surface charge density

The surface charge density was calculated using specific surface area (SSA) in m^2/g and Cation Exchange Capacity (CEC) in meq/g as per equation 2.7

$$\text{Specific Surface Charge } \left(\frac{meq}{m^2}\right) = \frac{\text{Cation Exchange Capacity}}{\text{Specific Surface Area}} \quad \text{--- 2.7}$$

2.5.2.7. Point of zero charge (pH_{zpc}) and pH determination

A). Point-Zero charge

The point of zero charge (pH_{pzc}) of raw, and Al^{3+} - amended bentonite clays were determined using the solid addition method [111]. 40 mL of 0.1 M KCl, 0.01MKCl and 0.001MKCl was transferred to a series of 100 mL of conical flasks. The initial pH (pH_i) of the solutions was adjusted between the range of 2-12 by adding 0.1M HCl and 0.1M NaOH solutions. The total volume of the solution in each tube was adjusted exactly to 50 ml by adding 0.1 KCl. Furthermore, 0.5 g of bentonite clay was added and the suspensions were then equilibrated for 48 h. After equilibration, the solutions were filtered and the final pH values (pH_f) of the filtrate were measured again. The difference between initial pH (pH_i) and final pH (pH_f) values ($\Delta pH = \Delta pH_i - pH_f$) was plotted against pH_i. The point of intersection of the resulting curve with abscissa (the co-ordinate that gives the distance along the horizontal axis), at which $\Delta pH = 0$, was an indication of PZC. The same procedures were repeated for Al^{3+} -amended bentonite. This procedure is also well implemented by [71] for investigation of pH_{PZC} of nano-alumina.

B) pH of Adsorbents

The pH of each samples was determined by putting 10 g of each samples into a 100-ml beaker and 20 ml of distilled water was added and stirred at 330 rpm for

30 min differently. Each adsorbent sample pH was measured with the pH meter WTW INOLAB pH 720 and measured triplicate [106] [112] .

2.6. Adsorption experimental setup

2.6.1. Column adsorption study

For column experiment, a borosilicate tube with an inner diameter of 1.5cm and height of 20 cm is used. The bottom of the column is sealed with wool to prevent the loss of the adsorbent during the infiltration processes. The illustrative design of the column experiment is shown in Figure 2.1. Known quantity of Bentonite adsorbent was filled in the column (different bed depths) and wetted with distilled water in the downward direction to withdraw the trapped air between the particles of the adsorbent. The fluoride solution was allowed to pass continuously in the downward flow direction using a peristaltic pump. At a predefined time, intervals of 30min samples were collected and the residual fluoride level was measured using spectrometer at known wave length (570nm). The breakthrough time (t_b) was recorded when the concentration reduced to 1.5mg/l (WHO guideline for drinking water of fluoride content). This point was called breakthrough point when the exhaustion time (t_E) capacity is 90-95% of influent concentration. The effect of bed height of the adsorbent, initial concentration, and flow rate of the column were investigated.

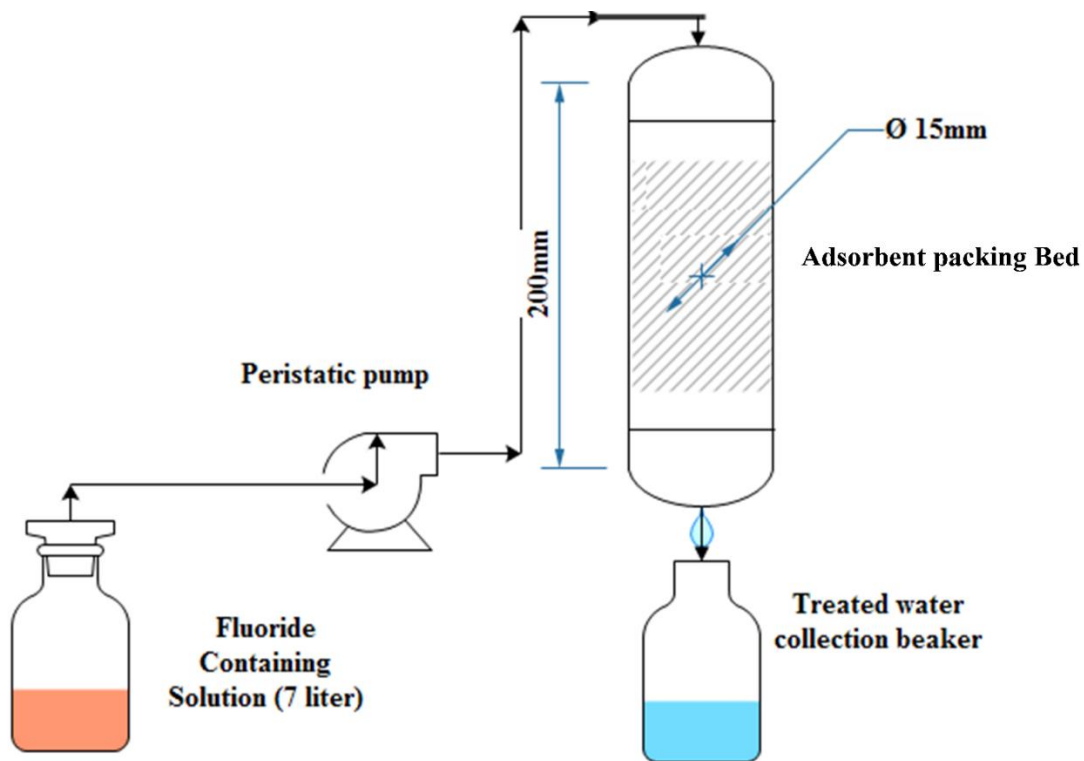


Figure 2.1 8: Schematic representation of the column set-up

2.7. Investigation of the kinetic models

2.7.1.1. Thomas Model

Thomas model is based on the assumption that the process follows Langmuir kinetics of adsorption-desorption with no axial dispersion. It describes that the rate driving force obeys the second-order reversible reaction kinetics[113]. And also, this column performance theory was developed to calculate the maximum solid phase concentration of the solute on an adsorbent and the adsorption rate constant for continuous adsorption process in column studies (Malkoc and Nuhoglu, 2006) . The linearized form of the Thomas model for an adsorption column is shown in equation 2.8.

$$\ln\left(\frac{C_0}{C_t} - 1\right) = K_{Th} * q_0 * \frac{M}{Q} - K_{Th} * C_0 * t \text{ --- (2.8)}$$

Where, k_{Th} (mL/min.mg) is the Thomas rate constant; q_0 (mg F/g) is the equilibrium fluoride uptake per g of the adsorbent; C_0 (mg/L) is the inlet Fluoride concentration; C_t (mg F/L) is the outlet Fluoride concentration at time t ; M (g) is the mass of adsorbent, Q (mL/min) is the filtration velocity and t (min) stands for filtration time.

A linear plot of $\ln\left(\frac{C_0}{C_t} - 1\right)$ against time (t) will be employed to determine values of k_{Th} and q_0 from the intercept and slope of the plot. The Thomas model is based

on the assumption that the process follows Langmuir kinetics of adsorption-desorption with no axial dispersion (Chu, 2010).

2.7.1.2. Yoon-Nelson Model

The Yoon-Nelson model is based on the assumption that the rate of decrease in the probability of adsorption for individual adsorbate practice is proportional to the probability of adsorbate adsorption and probability of adsorbate breakthrough on the adsorbent [114].

The model is described by equation 2.9.

$$\ln\left(\frac{C_0}{C_0 - C_t}\right) = k_{YN} * t - k_{YN} * \tau \text{ --- (2.9)}$$

Where k_{YN} (min^{-1}) is the Yoon-Nelson rate constant and τ (min) is the time required for 50% sorbate breakthrough.

On the study conducted by Tofan.et.al, 2015 describes the sorption of Cr (III) on modified hemp fibers showed that the values of the rate constant, k_{YN} , increase as the initial parameter increases. This may be due to the increases of competition between the adsorbent groups on the adsorption sites by increasing bed depth, which results in a higher rate of retention.

2.7.1.3. Clark model

It is explored because it considers the mass transfer and equilibrium adsorption to predict the nature of breakthrough curves [115]. The assumptions of this model are: (i) the nature of inflow in a column is piston type (ii) mass-transfer in column follows the Freundlich isotherm model [87]. Equation 2.10 shows the linearized representation of the model.

$$\ln\left(\left(\frac{C_0}{C_t}\right)^{n-1} - 1\right) = -rt + \ln A \text{ --- Eq. (2.10)}$$

where, ' C_0 ' (mg/L) and ' C_t ' (mg/L) designate the concentration of influent and effluent, respectively. The ' n ' designates the Freundlich constant determined experimentally in batch, r (min^{-1}) and A are constants of Clark model.

2.7.1.4. Bohart-Adams Model

The Adams-Bohart model is employed for describing the initial part of a breakthrough curve with the validity of the model being limited to the concentration range of $C_t C_0 < 0.5$ [116].

The model assumes the rate of adsorption is limited by external (film) mass transfer. The non-linear form of the model is given as equation (2.11), which can be linearized as equation 2.12.

$$\frac{C_t}{C_0} = \exp(KAB * C_0 * t - KAB * N_0 * \frac{Z}{v}) \text{ --- 2.11}$$

$$\ln\left(\frac{C_t}{C_o}\right) = K_{AB} * C_o * t - K_{AB} * N_o * \frac{Z}{v} - 2.12$$

where K_{AB} (L/mg h) is the kinetic constant, v (m/h) is the linear flow rate, Z (m) is a given column bed depth, N_o (mg/L) is the saturation concentration, and time t (h) ranges from the start to the fluoride breakthrough point. The linear flow rate was calculated from equation 2.13.

$$v = \frac{Q}{A} \text{ --- 2.13}$$

where Q (m³/h) is the volumetric flow rate, and A (m²) is the cross-sectional area of the bed.

Table 2.1 : The models and equations used for the description of column adsorption

Model	Linear Equation	Plot	Model Parameters	References
ClarkModel	$\ln\left(\left(\frac{C_o}{C_t}\right)^{n-1} - 1\right) = -rt + \ln A$		r, A	[84]
Thomas model (TM)	$\ln\left(\frac{C_o}{C_t} - 1\right) = K_{Th} * q_o * \frac{M}{Q} - K_{th} * C_o * t$	$\ln\left[\left(\frac{C_o}{C_t} - 1\right)\right]$	K_{Th}, q_o	[84]
Yoon-Nelson model	$\ln\left(\frac{C_t}{C_o - C_t}\right) = k_{YN} * t - k_{YN} * \tau$	$\ln\left(\frac{C_t}{C_o - C_t}\right) vs time$	K_{YN}, τ	[117]
Adams-Bohart Model	$\ln\left(\frac{C_t}{C_o}\right) = K_{AB} * C_o * t - K_{AB} * N_o * \left(\frac{Z}{U_o}\right)$	$\ln\left(\frac{C_t}{C_o}\right) vs Time$	K_{AB}, N_o	[118]

2.8. Optimization of the Adsorption Conditions Using Response Surface Methodology

The Central Composite Design (CCD) was employed to optimize the adsorption conditions to obtain the maximum amount of F removal using the Design-Expert 7 (DX7) software program [74, 119]. The benefits of CCD are seen in its usage in sequential experimentation [120-122]. The goal of this design experiment is to find conditions for a maximum amount of % removal and/or adsorption capacity with optimized initial fluoride concentration, flow rate, and bed depth. Based on the results found from the previous study of the authors [123, 124]; the workable range of the independent variables identified as Initial influent fluoride concentration (designated as A or 'X₁', (2-20mg/l)), Flow rate (designated as B or 'X₂', (6-20 l/min)), and Bed depth (designated as C or 'X₃', (2-10 cm)) are identified as shown in Table 2.2.

Table 2.2: Design experimentation variables and levels

Name	Units	Type	Low	High
Initial influent fluoride Concentration (A)	mg/l	Factor	2	20
Flowrate (B)	l/min	Factor	6	20
Bed depth (C)	cm	Factor	2	10
Fluoride removal (R)	%	Response		
Adsorption capacity (Q)	mg/g	Response		

The following is a representation (Equation 2.14) of the relationship between appropriate response and predictor variable:

$$Y = f(X_1, X_2, X_3 \dots \dots \dots X_n) + \epsilon \dots \dots \dots (2.14)$$

And Y stands for response, X denotes the predictor variables, n denotes number of factors under investigation, and ϵ denotes the sampling errors. The accompanying equation (Eq 2.15) was used to calculate the coded values of process variables:

$$Coded\ Value = xi = \frac{Xi - Xo}{\Delta X} (i = 1, 2, 3, 4 \dots \dots, K) \dots \dots (2.15)$$

Where xi is the coded variable, X_i is the actual value of an independent variable, X_o is the actual value of the independent variable at the center point and ΔX is the step change value of an independent variable. A total of 20 experimental runs

were defined by the CCD design model of which six of the experimental runs were replicates at the center point of the experiment. Based on this design, the number of the experimental run chosen is suitable for the assessment of quadratic response surface and to generate a second-degree polynomial model, which is used to optimize an adsorption process using a small number of experimental runs. The design was tested at 0.05 level of significance. The relation between the independent and the response variables was assumed to be quadratic, and its general form of expression is given in Equation 2.16.

$$Y = b_0 + b_1X_1 + b_2X_2 + b_3X_3 + b_{12}X_1X_2 + b_{13}X_1X_3 + b_{23}X_2X_3 + b_{11}X_1^2 + b_{22}X_2^2 + b_{33}X_3^2 \quad (2.16)$$

Where Y is the response (% Fluoride removal or Adsorption Capacity), b_0 is offset term, X_1 , X_2 , and X_3 are the independent variables, b_1 , b_2 , and b_3 are linear terms, b_{12} , b_{13} and b_{23} are interaction terms, and b_{11} , b_{22} , and b_{33} are quadratic terms.

CHAPTER 3: PHYSICO-CHEMICAL CHARACTERIZATION OF MODIFIED AND UNMODIFIED BENTONITE CLAY FOR FLUORIDE REMOVAL

3.0. Results and Discussion

3.1. Determination of physical properties of the adsorbents

RB, ATB, and Alum-Mbent had moisture content values of 1.67 percent, 0.345 percent, and 0.104 percent, respectively. In contrast to raw bentonite, acid and alum modification of the adsorbent did not appear to induce a noticeable difference in the moisture content of the adsorbents. The apparent density of RB, ATB, and Alum-Mbent, respectively, was found to be 2.62 g/cm³, 1.23 g/cm³, and 1.25 g/cm³ respectively. The raw bentonite was denser than the improved ones, since apparent density is a measurement of the compactness of clay minerals. The density difference between raw and modified bentonite may be due to the organic content of the clay. Some of the constituents found in the RB can disappear during modification resulting in lower apparent density. The pH value of the clay content was used to assess whether it was acidic or alkaline. RB, ATB, and Alum-Mbent had pH values of 7.16, 5.8, and 7.6, respectively, suggesting that the substance is more neutral. As per the literature [112], the pretreated clay samples have pH values that are similar to 7.2.

3.1.1. Surface morphology

The SEM results for the Bentonite samples at 1000x, 5000x and 1000x magnification (Figure 3.1,3.2& 3.3) were used to clearly identify all the morphological clay properties and larger interactions of the samples in SEM at higher resolutions. SEM Images indicate irregularity in shape and show the dispersion of clay minerals that could be predominantly Silica and alumina.

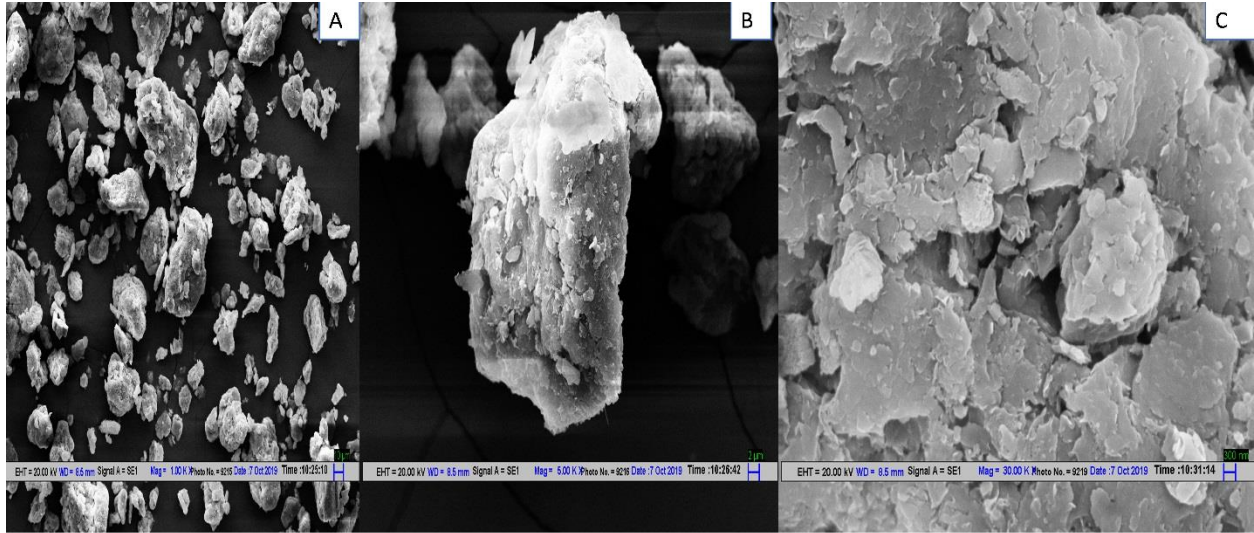


Figure 3.1: SEM micrographs of the RB (A, B and C are magnified by 1000x , 5000x and 30,000 times respectively).

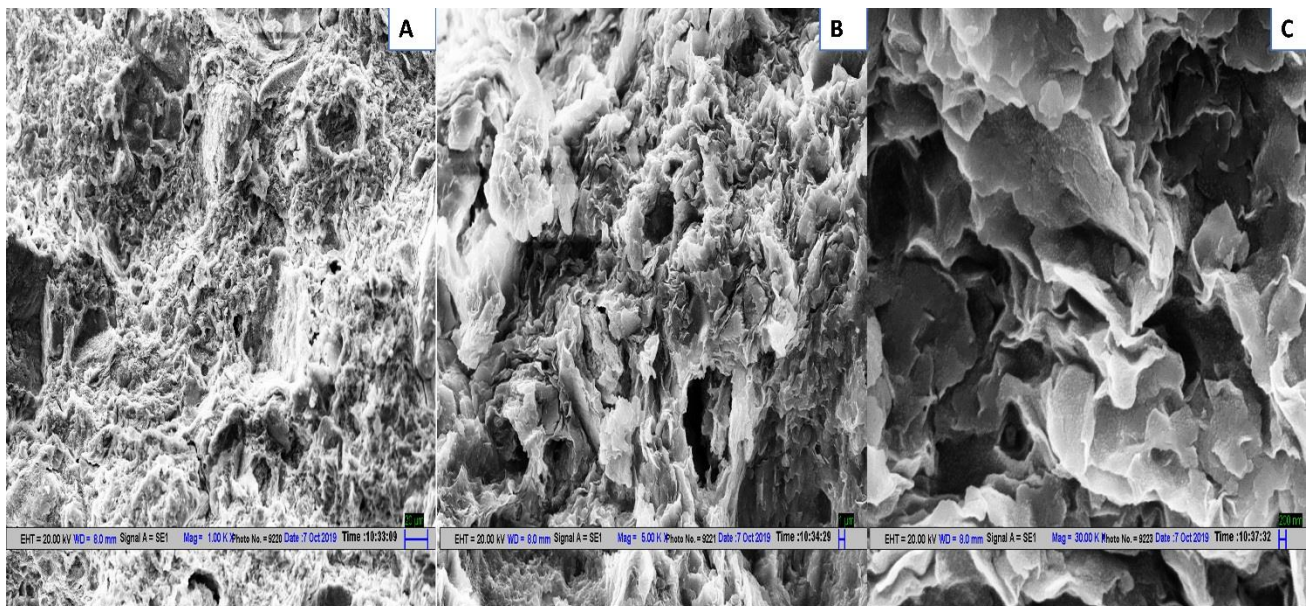


Figure 3.2: SEM micrographs of the ALUM-MBENT (A, B and C are magnified by 1000x, 5000x and 30,000 times respectively).

It is observed that the morphology of the bentonite clay is porous and irregularly shaped with large surface area. The modification was found to make the surface porous. The observed increase in surface area is expected to increase removal of anions such as fluoride. As shown in the figure 3.3 (A, B and C), the active sites on the surface of the aluminum amended bentonite adsorbent was fully

exhausted by fluoride ions after treatment through column bed experimentation. This indicates the materials is capable of removing anions like fluoride from aqueous solution.

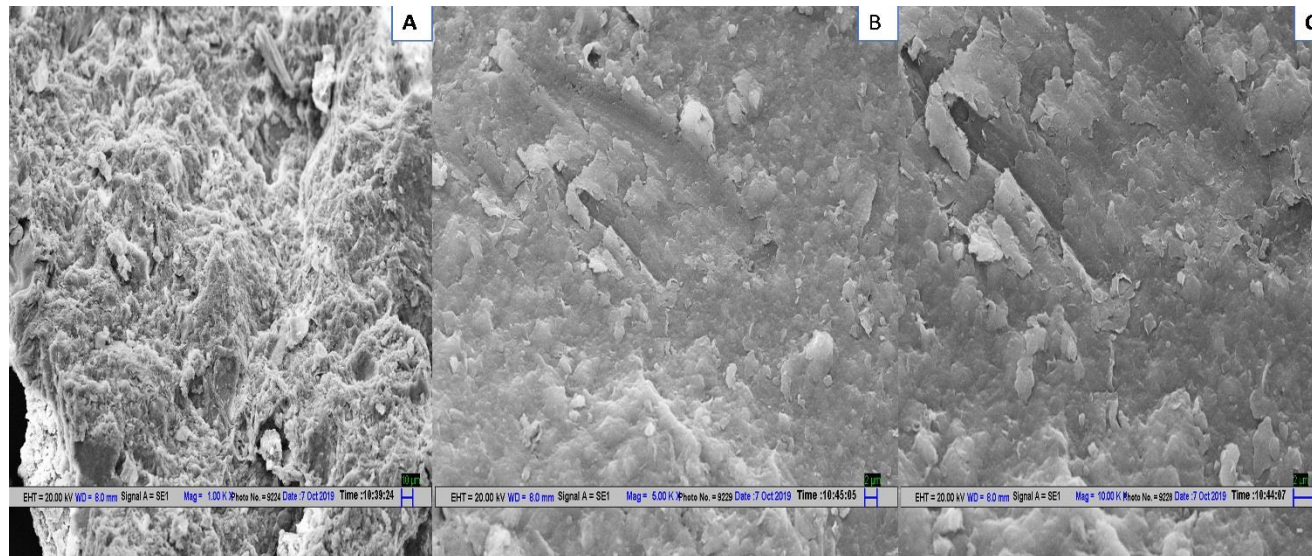


Figure 9: SEM micrographs of the fluoride loaded ALUM-MBENT (A, B and C are magnified by 1000x, 5000x and 10,000 times respectively).

The changes in the chemical composition of the bentonite clay after adsorption of fluoride exhibits significantly different physico-chemical characteristics compared to its fluoride unloaded adsorbents.

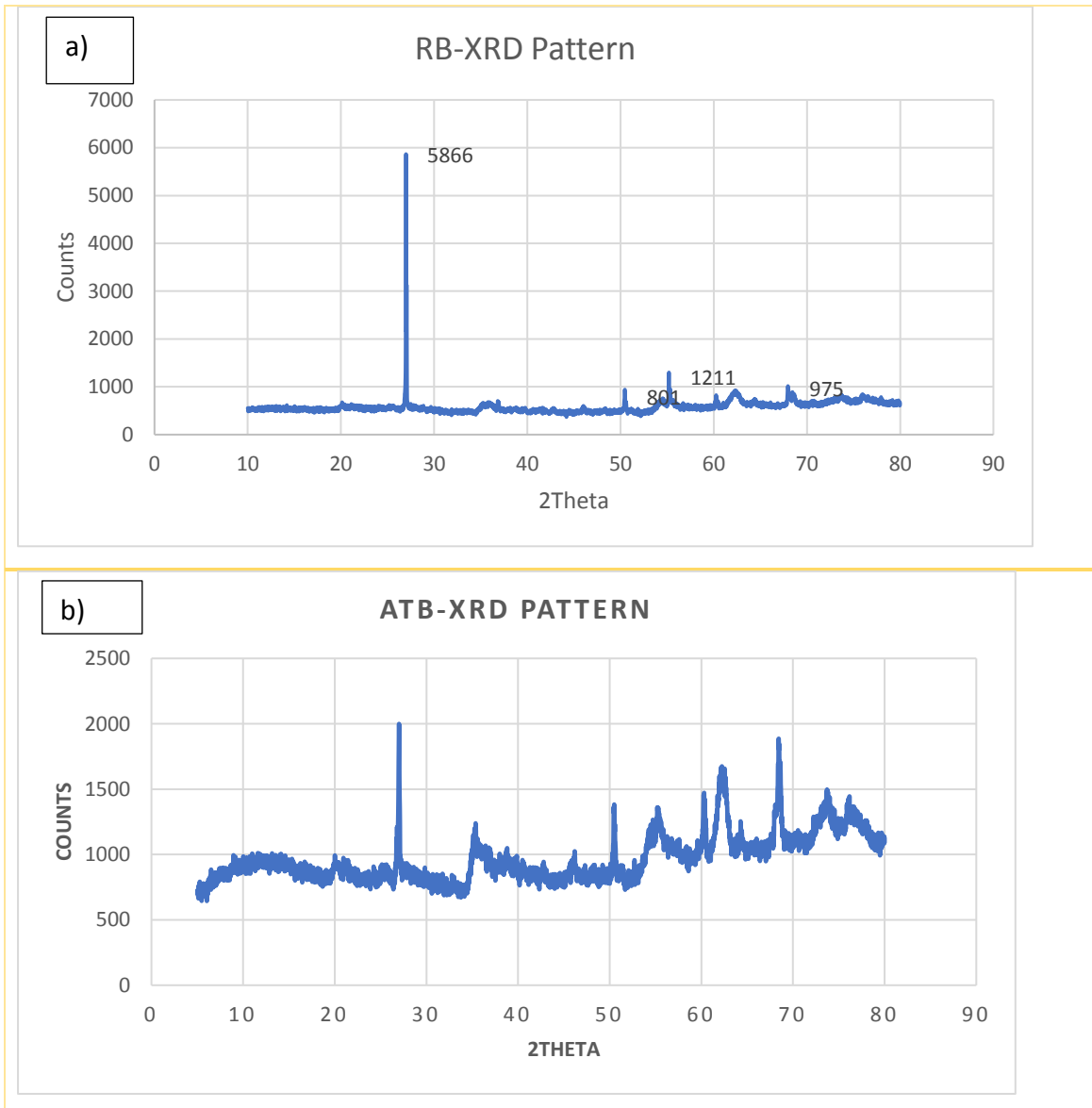
3.1.2. Mineralogy

The mineralogical and crystallographic characterization of the RB, ATB and Alum-Mbent clay were performed using X ray Diffraction method.

The results of the characterization of bentonite by X Ray Diffraction showed that bentonite of New Delhi area generally composed of 7 types of minerals. Alumina (Al_2O_3) = 17%, calcite (CaCO_3) = 22%, Silica (O_2Si) = 22%, bornite (Cu_5FeS_4) = 8 %, Hematite (Fe_2O_3) = 16%, Quartz (SiO_2) = 22%, Green cinnabar (Cr_2O_3) = 16% and burnt ochre = (Fe_2O_3) 20% (Figure 3.4). The other crystallographic parameters are shown in Table 3.3.

The phases were identified using x'pert Highscore software. Through executing search and match option from the data base of the tool, setting of the parameters

was conducted. The analysis reveals that hexagonal structure and inorganic material with compound named silica (SiO_2) and mainly iron oxide (Fe_2O_3) compound like burnt ochre and Hematite. The SiO_2 material is found at the d-spacings of mainly at 4.25499, 3.34347, 2.45687, 2.28149 and 2.23613 as depicted in Figure 3.4 a, b & c.



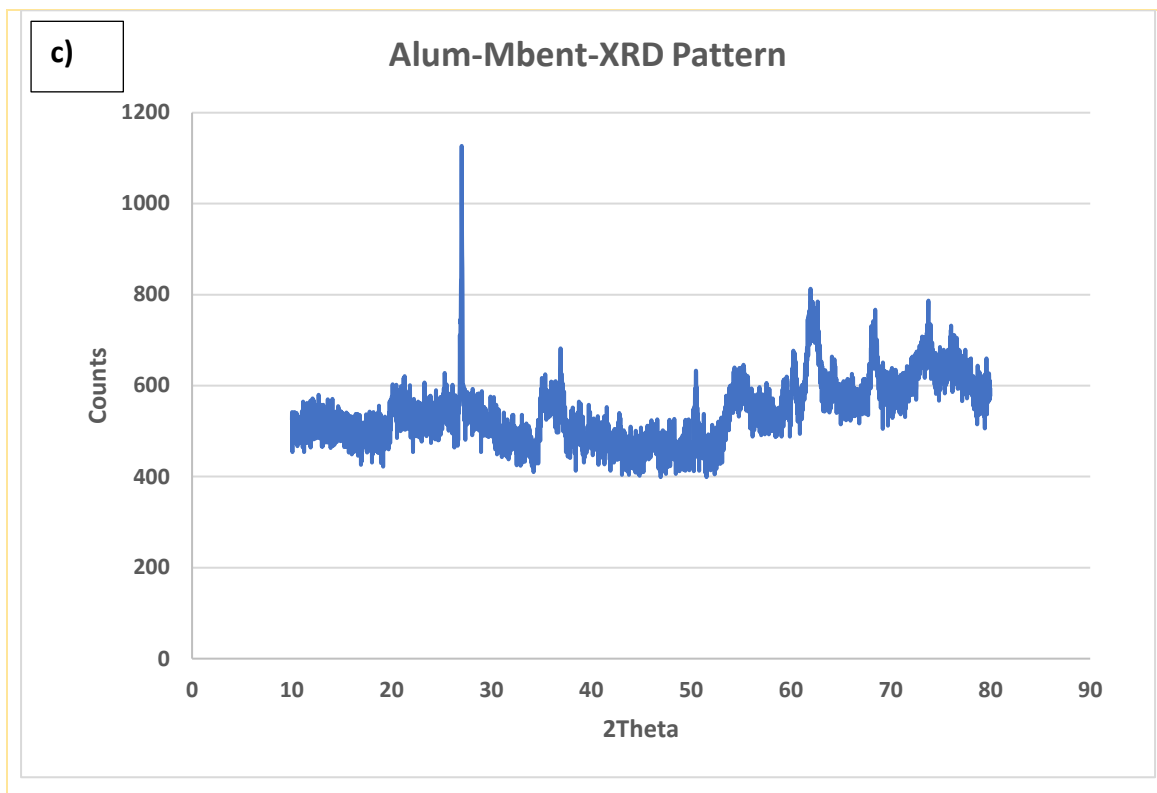


Figure 3.4: XRD pattern of the adsorbents

XRD also reveals the crystallographic parameters (figure) as a (Å): 4.9134, b (Å): 4.9134, c (Å): 5.4053, Alpha (°):90.0000, Beta (°):90.0000, Gamma (°):120.0000, Calculated density (g/cm³): 2.65, Volume of cell (10⁶ pm³): indicating the crystal system of Hexagonal structure . The maximum peak list that quartz, Silica and calcite (Table 3.1) exist is expressed in terms of d-spacing: 3.34200, 2Theta[deg]: 26.652 and intensity (%):100.

For the case of Alum-Mbent, the occurrence of Al₂O₃ (Alumina) is observed as shown in Table 3.1, this is due to the modification of the surface of the clay.

Table 3.1: Identified Patterns List for Raw bentonite

Visible	Ref. Code	Score	Compound Name	Displacement [°2Th.]	Scale Factor	Chemical Formula
*	00-046-1045	9	Quartz, syn	0.000	0.096	Si O ₂
*	00-033-0664	2	burnt ochre	0.000	0.034	Fe ₂ O ₃
*	00-033-1161	6	silica	0.000	0.009	Si O ₂

* 00-024-0072 2 Hematite 0.000 0.031 Fe₂O₃

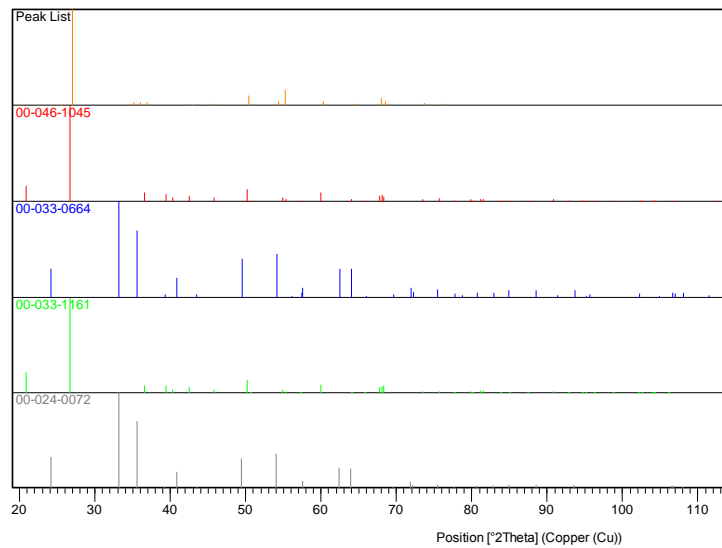


Figure 10: Plot of Identified Phases for Raw bentonite

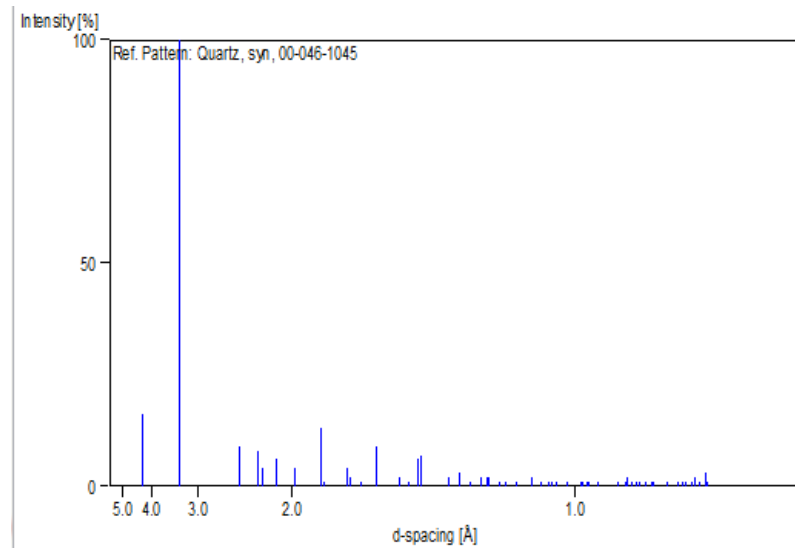


Figure 11: Stick pattern representation for SiO₂ material

Table 3.2: Identified Patterns List for Aluminum amended bentonite

Visible	Ref. Code	Score	Compound Name	Displacement [°2Th.]	Scale Factor	Chemical Formula
*	00-033-0664	7	burnt ochre	0.000	0.044	Fe ₂ O ₃

*	00-024-0072	5	Hematite	0.000	0.047	Fe ₂ O ₃
*	00-033-1161	4	silica	0.000	0.195	Si O ₂
*	00-046-1045	4	Quartz, syn	0.000	0.197	Si O ₂
*	00-010-0173	4	alumina	0.000	0.012	Al ₂ O ₃
*	00-005-0586	0	Calcite, syn	0.000	0.194	Ca C O ₃

Formation of CaF₂

For the case of used adsorbent characterization by XRD revealed that the formation of Fluorite (CaF₂) was there as a precipitation which might be formed due to the release of calcium cation from the surface of the clay layer to react with fluoride ion. The position of CaF₂ occurrence was detected at angles 26.9834, 36.8605, 45.9758, 50.4685, 54.3099, 54.3099, 55.1884, 60.2744, 62.4893, 67.9662, and 68.4494. This shows that at this diffractions angles Calcite (CaCO₃) has detected as an impurity for the clay material.

Table 3.3: Crystallographic properties of raw bentonite determined by XRD analysis

	Common name	Chemical formula	Crystallographic parameters									
			Crystal system	color	Empirical formula	Calculated density (g/cm ³)	a (Å):	b (Å)	c (Å):	Alp Ha (°):	Bet a (°):	Gam ma (°):
Alumina	Aluminum Oxide	Al ₂ O ₃	Rhombohedral	Yellow purple to violet	Al ₂ O ₃	3.99	4.758	4.758	12.991	90.000	90.000	120.000
calcite	Calcium carbonate	CaCO ₃	Rhombohedral	Colorless	CaCO ₃	2.71	4.989	4.989	17.062	90.000	90.000	120.000
Quartz	Silica	SiO ₂	Hexagonal	White	O ₂ Si	2.65	4.9134	4.9134	5.4053	90.000	90.000	120.000
Hematite	Iron Oxide	Fe ₂ O ₃	Rhombohedral	Dark reddish brown	Fe ₂ O ₃	5.26	5.038	5.038	13.772	90.000	90.000	120.000
Burnt ochre	Iron Oxide	Fe ₂ O ₃	Rhombohedral	Dark reddish brown	Fe ₂ O ₃	5.27	5.0356	5.0356	13.7489	90.000	90.000	120.000
Bornite	Copper Iron Sulfide	Cu ₅ FeS ₄	Cubic		Cu ₅ FeS ₄	5.09	5.470	5.470	5.4700	90.000	90.000	90.000
Silica	Silicon oxide	SiO ₂	Hexagonal	Colorless	SiO ₂	2.65	4.9134	4.9134	5.4053	90.000	90.000	120.000
Green cinnabar	Chromium Oxide	Cr ₂ O ₃	Rhombohedral	Dark grayish yellow-green	Cr ₂ O ₃	5.23	4.9588	4.9588	13.5942	90.000	90.000	120.000

3.1.3. Chemical composition (SEM-EDX analysis)

The EDX results for the three samples show that the major composition is Si, Al, and Fe with 23.79%wt, 10.55%wt, and 14.84%wt respectively for the RB samples

are shown in Table 3.4 and Figure 3.7 (A-F). The other elements like Cl, Na, Mg, Ti, Ca, and K exist at lower percentage weights. They are considered as impurities of the material and can be caused if the purification of bentonite is not clean and if the oven conditions are not correct. The SEM-EDX analysis revealed that surface of RB is smooth and flat compared to synthesized bentonite clay. This morphological variation may be the result of the modification of the raw bentonite with aluminum makes more porous. The major portion of the bentonite clay material is covered by silica material.

The EDX results confirmed Alum-MBENT samples enrichment in aluminum, which is associated with increase of oxygen abundance. This indicates that bentonite has incorporated together aluminum and oxygen. Moreover, lower variations of the relative abundance in EDX compared to XRD measurements suggest that aluminum oxide was not only deposited at the surface of the grain but also penetrated inside. It is expected that the fluoride ions would be adsorbed mostly by the oxides of aluminum.

Table 5:Elemental composition (% by wt.) of RB, ATB and ALUM-MBENT obtained from EDX characterizations.

Elements		O	Si	Fe	Al	Cl	Na	Mg	Ti	K	Ca
EDX (%wt)	RB	37.91	23.79	14.84	10.55	0	2.82	1.80	2.24	1.35	0.66
	ATB	24.04	10.95	9.36	6.59	3.8	3.4	0.84	0.75	0.24	0.11
	ALUM-MBENT	45.67	16.83	15.81	13	0	2.57	1.16	2.46	2.03	1.74

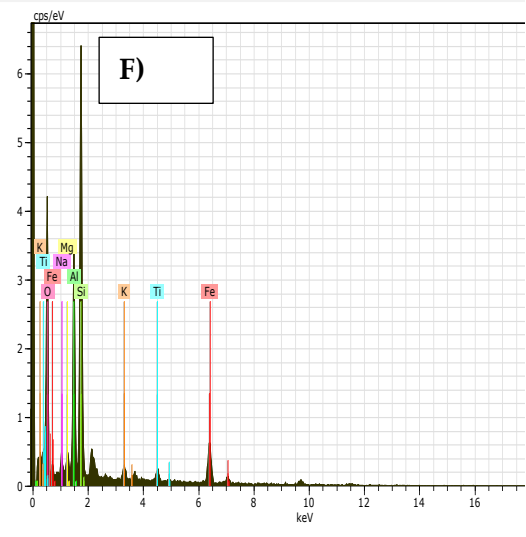
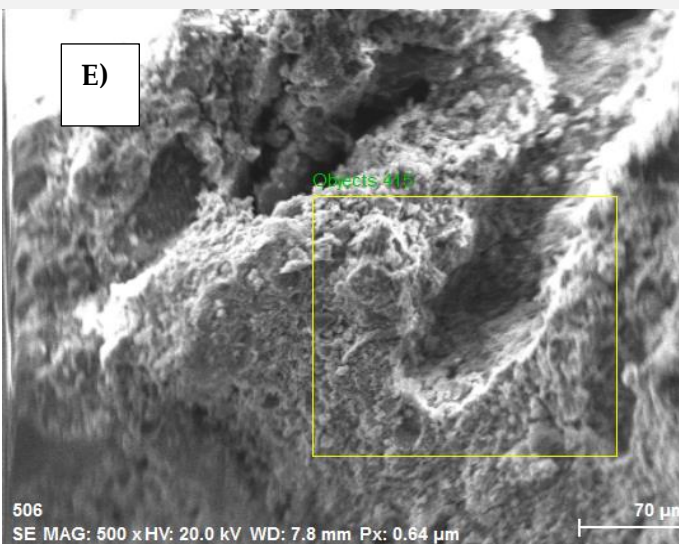
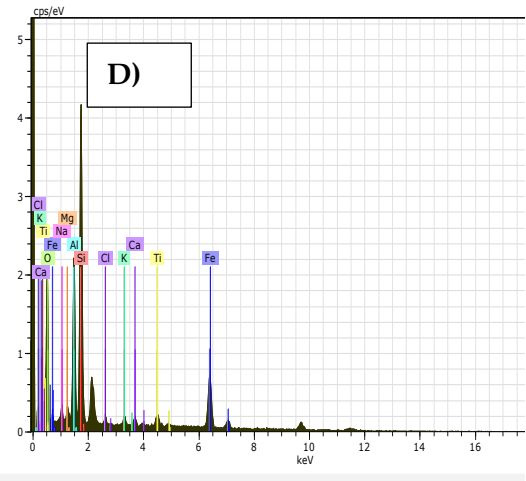
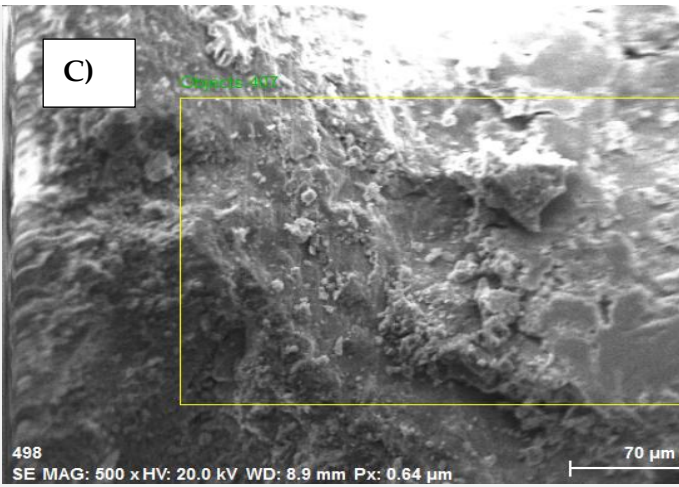
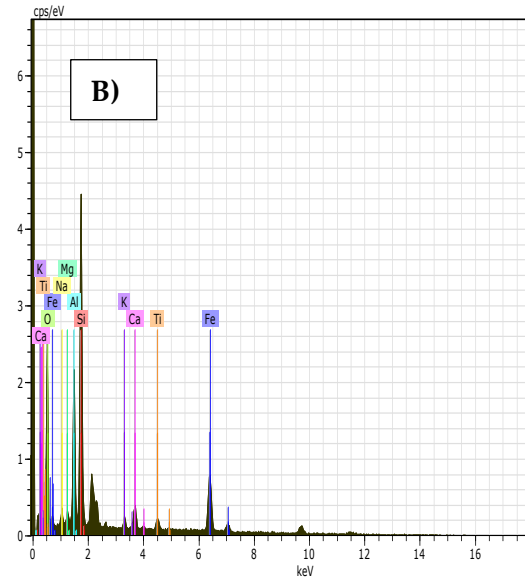
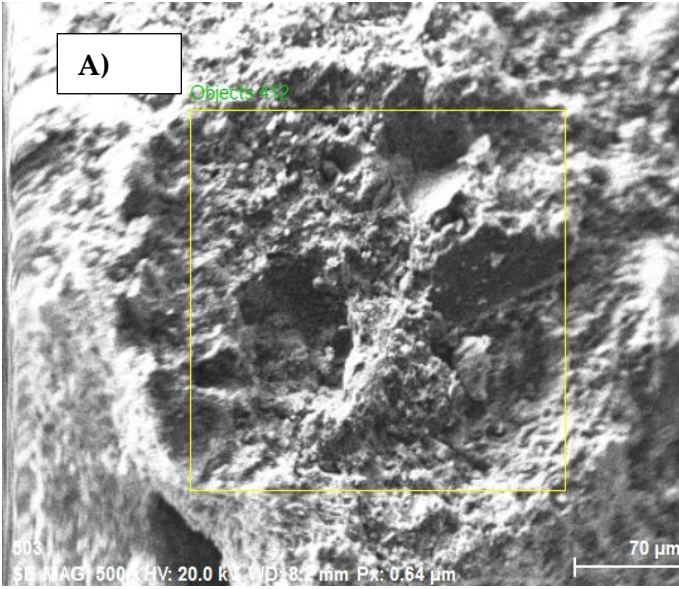


Figure 12: SEM-EDX micrographs of (a) RB with (b) elemental counts per second/eV for RB, and (c) ATB with (d) Elemental counts per second/eV for ATB, and (e) Alum-Mbent with (f) Elemental counts per second/eV for ALUM-MBENT.

3.1.4. FT-IR analysis

These characterization techniques are helpful for studying the nature of the adsorbent material and the possible types of surface functional groups present, and how they interact with the fluoride during the adsorption process. Figure 3.8 shows the FTIR spectra of, (a) RB before and after fluoride treatment, (b) ATB before and after fluoride treatment (C) Alum-Mbent before and after fluoride treatment.

The spectra of the samples reveal that the existence of several functional groups in the layer of the samples. The analysis of the spectra of the both modified and unmodified samples, revealed the presence, reduction or disappearance of the functional groups during modification of the samples Figure 3.8 (a,b, and c). There is a shift in the absorbance spectra in the same wavelength. This shows that modification has improved the surface activity of the adsorption onto clay minerals. The weakening or disappearance of these bands suggests the partial depletion of Al, Mg and Fe from the clay structure, in accordance with the change in the chemical composition and acidity shown above.

The peaks at 444.51 cm^{-1} , 464.01 cm^{-1} and $459.99.55\text{ cm}^{-1}$ are responsible for Al-Al-OH group deformation and are similar to those of 913 cm^{-1} and 914 cm^{-1} [5].

According to [125], the FT-IR spectrum of raw montmorillonite exhibits absorption bands at 3625cm^{-1} and 1640cm^{-1} which are assigned to the stretching and bending vibrations of the OH groups of the crystal and adsorbed water molecules, and a band at 3625cm^{-1} represents the stretching vibration of the OH groups in the silicate layers. The band at 1430cm^{-1} is due to the calcite impurity which was not removed during purification of the raw montmorillonite [97] . The bands at 915 , 880 and 843cm^{-1} , also observed in the unpurified raw clay, arise from the bending modes of the hydroxyl groups Al_2OH , AlFeOH and AlMgOH , respectively [97] [126].

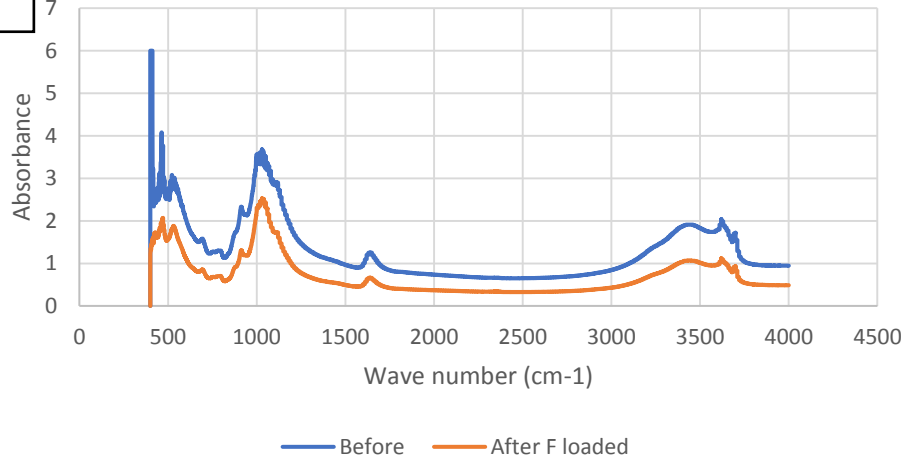
The presence of a band at 518cm^{-1} , which is the most sensitive to the presence of residual Al in the octahedral layer, suggests that the octahedral Al cations are retained. This means that the original structure of the bentonite clay was not fully disappeared, in agreement with the XRD result shown below. The absorption band at 792cm^{-1} is usually attributed to cristobalite and the band at 465cm^{-1} to a Si–O–Si bending vibration. After prolonged leaching, the band at about $792\text{--}800\text{cm}^{-1}$ strengthens and the intensity of the band at 1090cm^{-1} increases due to the formation of three-dimensional networks of amorphous Si–O–Si units [127] as a result of leaching of the octahedral layers in the raw montmorillonite. As in the non-purified montmorillonite, the Si–OH band is absent; this feature appears at 950cm^{-1} in other leached clay minerals such as kaolinite, vermiculite and talc. The reason for this behavior is presumably associated with the smaller extent of structural distortion in the present acid-leached montmorillonite[128].

The absorption band between 3619.12 and 3623.81 cm^{-1} could be ascribed to stretching vibrations of structural OH- groups of montmorillonite and water. At lower frequency (i.e. 999.10 cm^{-1}), bentonite showed a strong broadband this could be due to the stretching and vibration of Si–OH group. Band at 914.93 and 795 cm^{-1} could be attributed to Al–OH–Al group an Al–O and Si–O vibration, respectively, which indicates presence of quartz. Increase absorbance intensity was observed in Acid- modified bentonite at these peaks indicating the formation of new bonds such as; Ca–O, Mg–OH and Ca–H₂O. Increment in the absorption intensities of F- loaded Acid-modified bentonite was recorded. This could be attributed to the fact that structural hydroxide groups and water molecules contributed to F- adsorption process through the exchange of OH- in Mn, Al, Si oxides for F-.

The interaction of fluoride with hydroxyl ions indicated by the FT-IR analysis and the presence of bands indicating Al - F interactions, suggest that ligand exchange between F and hydroxyl groups on modified adsorbents surface may be involved in the adsorption mechanism.

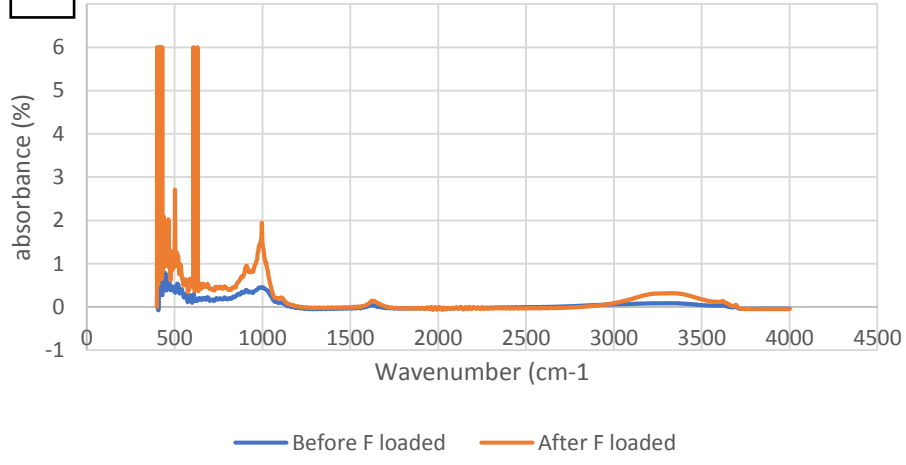
a

RB



b

ATB



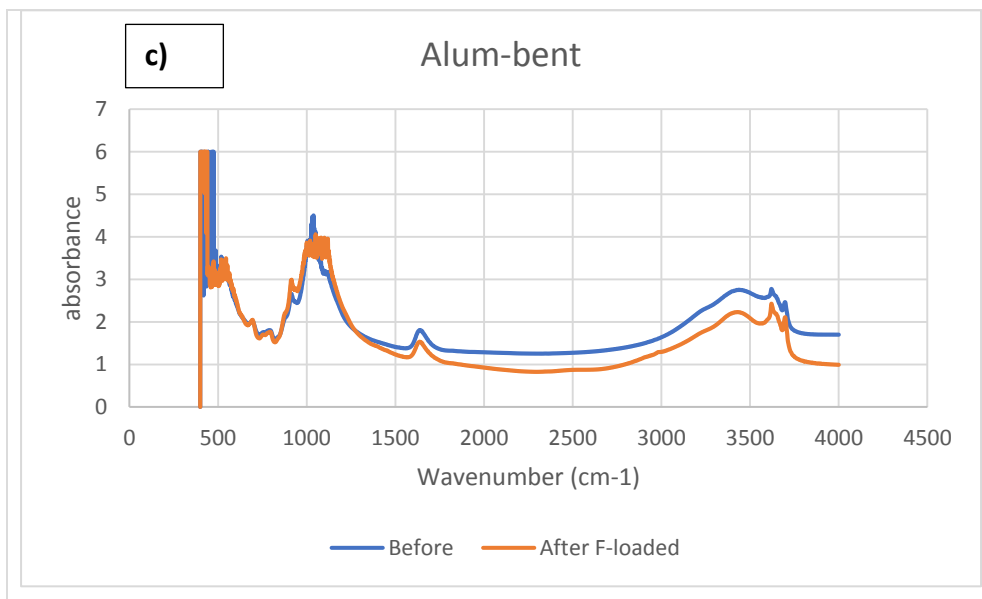


Figure 13: FTIR spectra of modified and unmodified bentonite clay

The interaction of fluoride with hydroxyl groups indicated by the FTIR analyses, suggests the mechanisms involved in the adsorption process may be columbic attraction of fluoride by protonated aluminol (AlOH) sites, and/or hydrogen-bonded complexation between fluoride and hydroxyl groups on the adsorbents surfaces, as well as ligand exchange reactions of fluoride with the hydroxyl groups. The applicability of FT-IR analysis suggested the adsorption mechanism is complex and involves both physical adsorption and chemical adsorption processes, and therefore supports/complements the thermodynamic and FTIR analysis.

3.1.5. Cation exchange capacity (CEC)

The determination of cation exchange capacity was determined for the three adsorbents using two well-known methods Methylene blue and pH equilibrium and results are presented in Table 3.5 and Figure 3.9 respectively. Higher CEC values shown in Table 3.5 by applying methylene blue method, implies surface activity with a greater layer charge and cation-exchange capacity. Therefore, Raw bentonite have a higher CEC, which shows the existence of the contact forces between the surrounding molecules and clay surface. A higher surface area was observed for ALUM-MBENT adsorbent.

Table 6: Values of SSA area and CEC by the Methylene blue adsorption method (particle size of 0.212mm)

Adsorbent	Volume of addition of methylene blue (ml/7.5gm)	Calculated (SSA) Specific Surface Area (m ² /g)	Calculated cation-exchange capacity (meq/100g)	Calculated cation-exchange capacity per SSA (meq/m ²)
RB	3ml	52	28.78	5.5*10 ⁻³
ATB	25ml	429	19.04	0.4*10 ⁻³
ALUM-MBENT	30ml	520	15.87	0.3*10 ⁻³

On the other hand, the results obtained by pH equilibration method (Figure 3.9) is also determined comparatively for different particle sizes. It is observed that both methods resulted (refer Table 3.5 vs Figure 3.10) similar CEC value for all adsorbents.

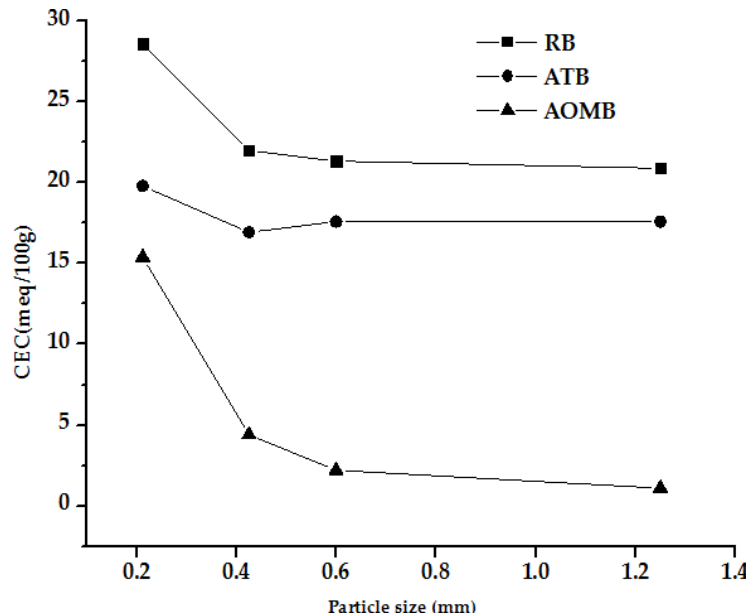


Figure 14: Effect of particle size on CEC value by using pH equilibrium Method

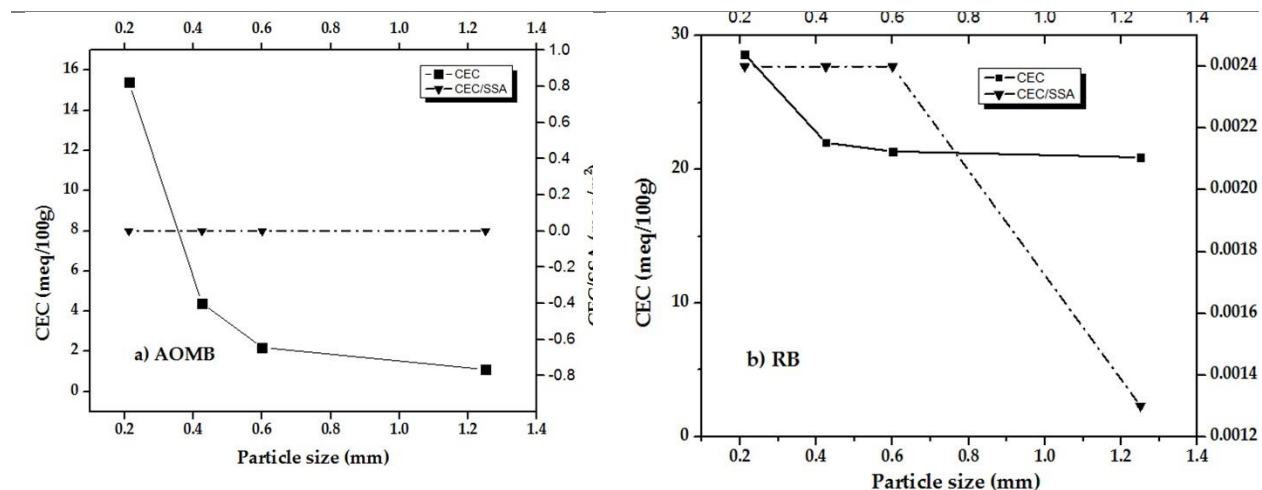


Figure 15: Effect of particle size on CEC and CEC/SSA value by using methylene blue Method

The smaller particle provides more surface area and leading to more sorption sites and to greater sorption. The increase in particle size from 0.212mm to 1.25mm doesn't show any change in CEC per SSA values for the case of ALUM-MBENT and slight decrease for the case of raw bent as shown in Figure 3.10 (a) and (b) respectively. As a result, increasing particle size decreases the material's sorption rate.

3.1.6. Point-Zero charge Determination

The effectiveness and efficiency of the adsorbent is dependent on the material reactivity of the adsorbent. pH value is a useful variable for the indication of the adsorption property. In this study, the behavior of the adsorbents was briefly elaborated on the basis of the pH_{PZC} (isoelectric point) and mean of pH value. The salt supplement method was used to determine the pH_{PZC} of the adsorbents. In the Figure 3.11, the pH_{pzc} of (a) RB (b) Alum-Mbent and (c) ATB are presented. The pH_{pzc} values for RB, ATB and ALUM-MBENT were found to be 7.1, 5.8 and 7.8, respectively. However, for Acid treated bentonite, ΔpH versus pH_i plot shows the pH_{pzc} touches the x-axis at 5.9. Both raw and Alum-Mbent clay have high pH_{pzc} indicative of clay dominated by aluminosilicate materials and other cations or oxides. Modification of the raw bentonite clay with acid and aluminum oxide increases the pH_{pzc} and which extends the pH range for adsorption of anions. This output reveals that the Alum-Mbent clay is expected to have high

adsorption capacity for fluoride ions than the raw bentonite clay. An increase in pHPzc of bentonite clay after modification has also been reported for Al³⁺-amended bentonite by [5] Also, Kim (2005), observed a pHPzc of 8.0 for Korean bentonite clay [129]. The pHPzc results for Korean clay was reported to be nearly the same value with the New Delhi area bentonite clay used in this study. Generally, adsorption is caused by the electrostatic attraction between the fluoride ion and the main constituents of Bentonite clay

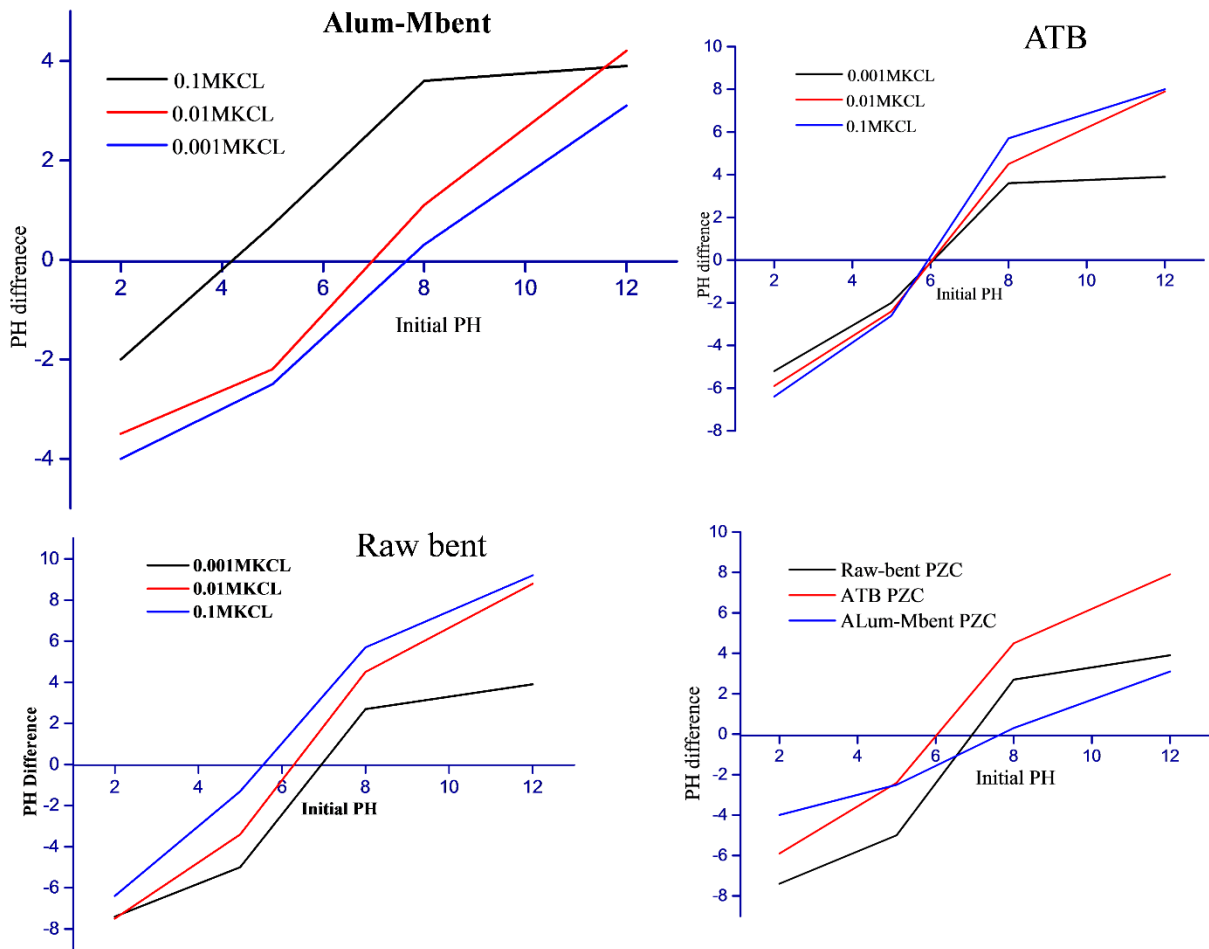


Figure 16: Plot of pHPZC PH of modified and unmodified bentonite

3.2. Summary

SEM micrographs confirmed that the RB surface was rough, which favors the uniform application of aluminum surface coating. The EDX spectra shows Al^{3+} was successfully deposited on the clay material surface, which was confirmed by the presence of more aluminum spectra on the modified bentonite clay than on the RB. The uptake of fluoride occurred at $pH_{PZC} > 7$ for RB, $pH_{PZC} > 5.9$ for ATB, $pH_{PZC} > 7.8$ for ALUM-MBENT by established hydroxyl groups between the fluoride ions and sorbent surface in the fluoride-contaminated drinking water. Because of their surface structure, bentonites have a lot of potential as adsorbents. Modification of the surface of bentonite enhances the adsorptive capacity by increasing surface binding sites. The presence of exchangeable cations on its surface makes alteration easier. The acidic and neutral surfaces of the samples examined indicate a positive capacity to remove different contaminants such as anions like fluoride in this case. SEM images reveal that particles are dispersed homogeneously and are irregular in shape. XRD and EDX analysis reveals that the bentonite is composed of major minerals such as SiO_2 , Al_2O_3 , Fe_2O_3 , and $CaCO_3$ and other impurities. The application of the advanced technologies for fluoride removal specially for small communities residing in rural areas is not feasible due to its complexity and affordability. In developing countries like Ethiopia, application of cost effective and simple de-fluoridation technologies like aluminum modified bentonite clay minerals as reported in this work may be preferable than advanced technologies. The output of this chapter tells us that, locally available materials can be considered as a proven filter for anions removal from drinking water.

CHAPTER 4: MODELING OF THE ADSORPTIVE REMOVAL OF FLUORIDE BY ALUMINIUM AMENDED BENTONITE CLAY

4.1. Results and discussions

4.1.1. Breakthrough Curve determination

The findings of fluoride adsorption onto ALUM-MBENT under continuous flow conditions are given in Table 4.1 as breakthrough curves for the three bed depths. The loading behavior of fluoride ions from solution onto the ALUM-MBENT column filter is depicted by the breakthrough curves, which are given as the ratio of effluent to influent fluoride concentration (C_t/C_o) as a function of time. The curves were discovered to have the usual "S" form of perfect adsorption systems [130]. The space underneath the breakthrough curve equals the maximum column potential for a specific variable, $q_e(\text{mg/g})$. When the effluent fluoride concentration reached 1.5 mg/L, the WHO guideline threshold, the breakthrough was achieved (WHO, 2011). This equated to a C_t/C_o of 0.3. Continuous flow column experiments were employed to generate the figures required to calculate the curves plotted at breakthrough points and the assessed result is shown in Figures 4.1-4.3. The breakthrough curve and breakthrough time are actual key aspect for determining the system behavior of the sorption column using packed adsorbent bed [130]. The breakpoint time refers to the period of adsorption when the column's outlet concentration was about 1-5 percent of the inlet concentration [131]. The breakthrough time for RB and ALUM-MBENT were determined as indicated in Table 4.1. At shallower bed depths (Figure. 4.3), axial dispersion phenomenon presumably dominates the mass transfer process and reduces the diffusion of fluoride ions into the mass of AOMP. Moreover, at shallower bed depths which correspond to shorter adsorbent exhaustion times, the fluoride ions do not have enough time to diffuse deeper into the whole of the ALUM-MBENT mass for increased uptake. These factors most likely contributed to a reduction in the breakthrough volume of treated water, when the bed depth decreased for both adsorbents from 10 cm to 2 cm with better performance for ALUM-MBENT than RB.

Table 4.7: Times at the breakthrough points and end points of the experiments for both RB and ALUM-MBENT adsorbents.

Adsorbent packed depth (cm)	ALUM-MBENT			RB		
	2	6	10	2	6	10
tB = Time at breakthrough (min)	75	115	150	95	295	360
tE = Time at exhaustion (min)	120	160	220	80	320	400
tE-tB = Elapsed time between CB and CE	25	45	70	5	40	40

4.1.1.1. Effect of Fluoride ion concentration.

The outcome of inlet concentration of fluoride on breakthrough profile at 5, 10, and 12 mg/L was investigated at a flow rate of 15 mL/min and bed height of 10 cm with the results revealed in Table 4.2 and Figure 4.2. Transition mechanism was obviously visible in the breakthrough curve at various initial fluoride concentrations. Exhausted and breakthrough times to individual adsorbent was calculated using 5 mg/l as the initial concentration. With inlet fluoride concentrations of 5gm/l, 10mg/l, and 12mg/l, respectively, the C_t/C_0 value reached 0.25, 0.35, and 0.65 after a 230-minute interval. Figure 21 indicates that ALUM-MBENT had a breakthrough time of 250 minutes and was exhausted after 390 minutes. Breakthrough times and exhausted times were 150 and 330 minutes, respectively, at of 10 mg/L fluoride concentration. Meanwhile, at 12 mg/l fluoride concentration, ALUM-MBENT breakthroughs in 120 minutes and exhausts in 310 minutes. Based on the findings, it may be inferred that shorter breakthrough time was achieved as the initial fluoride concentration increased. Breakthrough curves were strewn about, and at lower initial fluoride concentrations, breakthrough happened more slowly. Since the volume of adsorbate increased as the concentration increased, vigorous places were engaged at a quicker pace. In a shorter period as influent fluoride concentration rises to achieve the breakthrough time [47, 132]. Chen et.al [47] found a similar pattern with this output of the research using Kanuma mud for fluoride removal and by Nur et.al [132] for hydrous ferric oxide. Table 13 lists all of breakthrough and exhaust times for ALUM-MBENT.

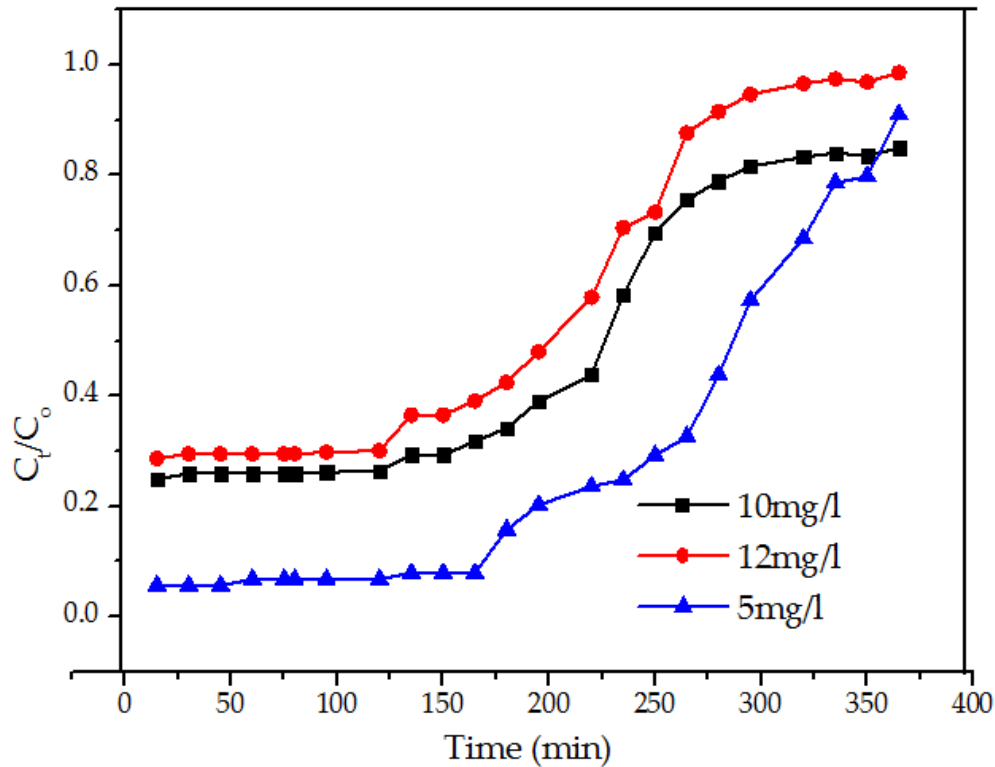


Figure 17: Effect of concentration on the ALUM-MBENT breakthrough profile (, depth= 10 cm), treated volume = 4L, flow rate = 15 mL/min, and pH 7)

Table 8: Criteria for removal of fluoride through ALUM-MBENT fixed bed column for various initial concentrations at a bed depth of 10cm were obtained.

C ₀ (mg/L)	(Q) (mL/min)	(C _e) (mg/L)	(t _b) (min)	(t _e) (min)	Δt (min)	Z _m (cm)	V _{eff} (ml)	q _e (mg/g)
5	15	0.28	250	390	40	8.975	6000	1.32
10	15	1.62	150	330	50	8.453	4950	1.99
12	15	2.89	120	310	55	8.195	4650	2.45

As a result, both exhaustion and breakthrough points occurred earlier as inlet concentration increased. Following that, the increase in inlet concentration, decreased breakthrough time.

By way of the initial fluoride concentration rises from 5.0 to 12 mg/L, adsorptive potential (q_e) raised from 1.32 mg/g of fluoride adsorbed to 2.88 mg/g Fluoride adsorbed, owing to the greater fluoride concentration.

4.1.1.2. Volumetric flow rate effect

Using the ALUM-MBENT, the outcome of flowrate on sorption was examined by differing of (15, 20, and 25 mL/min) flow rate while maintaining a 10 cm constant packed bed depth and an inlet concentration of 5 mg/L as revealed in Figure 4.2 through the breakthrough curve. Whenever it increases from 15 to 25 mL/min, adsorption equilibrium capacity of fluoride declined from 1.32 to 1.001 mg/g. The following facts should justify the increase in absorptive potential: The adsorbate employs extra time on to bed due to the low flow, allowing the adsorbent ample retention to contact with the adsorbate for actual interaction, follow-on in the persistent sorption process finding more penetrating time. When flow rate increased, the solution's retention period during filtering at a column is shorter, resulting in less contact between the adsorbate and adsorbent. Additionally, increasing flow rate from 15 to 25ml/min (Figure 4.2), the overall breakthrough profile shifts to the left, resulting in decreased fluoride removal over the same column operating period. This means that axial dispersion dominates the interaction between the adsorbent and the fluoride ion.

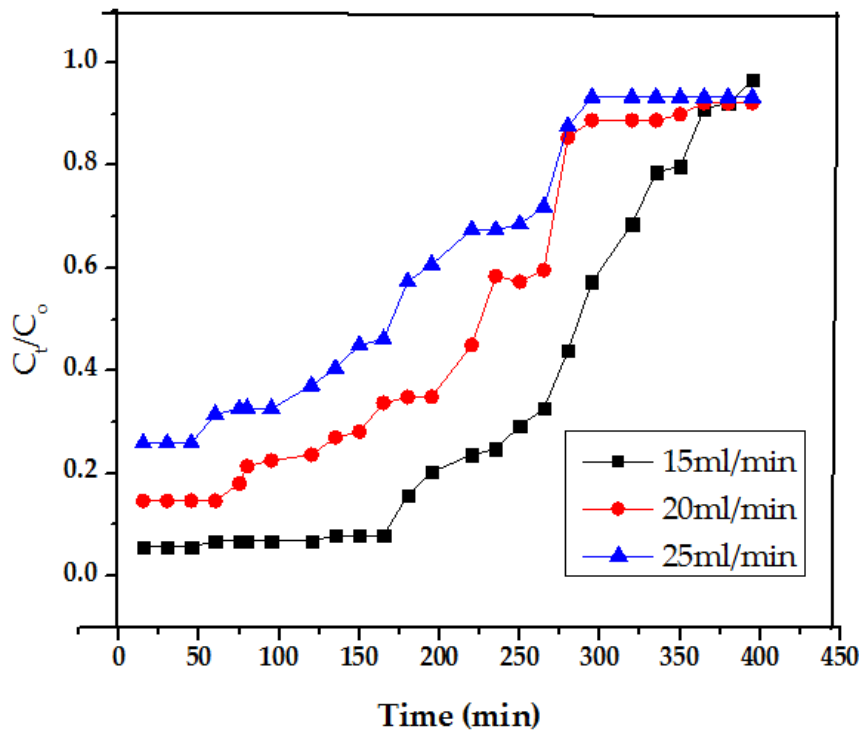


Figure 18: Effect of flowrate on breakthrough profile of AL-BENT (pH = 7, treated volume = 6750 ml, bed depth = 10cm, and initial fluoride concentration = 5 mg/l).

Table 9: For different flowrates, the experimental evaluation of column parameters using ALUM-MBENT at a bed depth of 10cm packed bed column

Flowrate (ml/min)	C ₀ (mg/l)	C _e (mg/l)	t _b (min)	t _e (min)	Δt (min)	Z _m (cm)	V _{eff}	q _e (mg/g)
15	5	0.28	360	400	40	8.975	6000	1.32
20	5	0.73	270	310	40	8.677	6200	1.76
25	5	1.29	180	270	90	6.629	6750	1.001

At larger flow rates, the shorter period for saturation could be due to the bed's fixed saturation potential for the same difference in concentration, resulting in a shorter time for saturation. The decline in removal efficiency (94.38 percent to 74.15 percent through the rise in flow rate (15 to 25 mL/min) may be clarified as a consequence of the adsorbate ion containing solution saturating the fixed-bed adsorption column as soon as retention period of fluoride ions in the column isn't really extended time for equilibrium of adsorption to be achieved for larger flow rate (Table 4.3).

Another explanation for faster inundation may be that higher flow rates improve mixing, which lowers the breadth of the liquid film covering the adsorbent, lowering the film transfer resistance and thereby increasing the mass transfer rate.

4.1.1.3. Adsorbent packed bed depth Effect

At a steady 15 mL/min flow rate and an influent fluoride 5 mg/L concentration, the breakthrough curves for fluoride adsorption for various column depths of 2, 6, and 10cm are shown in Figure 4.3. Exhaustion time (t_e), breakthrough time (t_b) and size of the fluoride solution (V_{eff}) all increase when depth packed bed increases. When packed column bed depth increases from 2 to 10 cm, bed sorption capacity increases from 0.51 to 1.32 mg/g (Table 4.4). Since higher

adsorption layer allows the fluoride ions to move through the packed material, the fluoride ions get higher residence time on the packed material, resulting in a greater amount of treated fluorine water. Another thing to keep in mind is that this was discovered during the service of the column that a higher bed depth made it simpler to trigger the flow to slow down after a while. It may be attributed to the propagation of ALUM-MBENT particles in the column as they are immersed in water, resulting greater decline in pressure and a reduction in flow rate in the column.

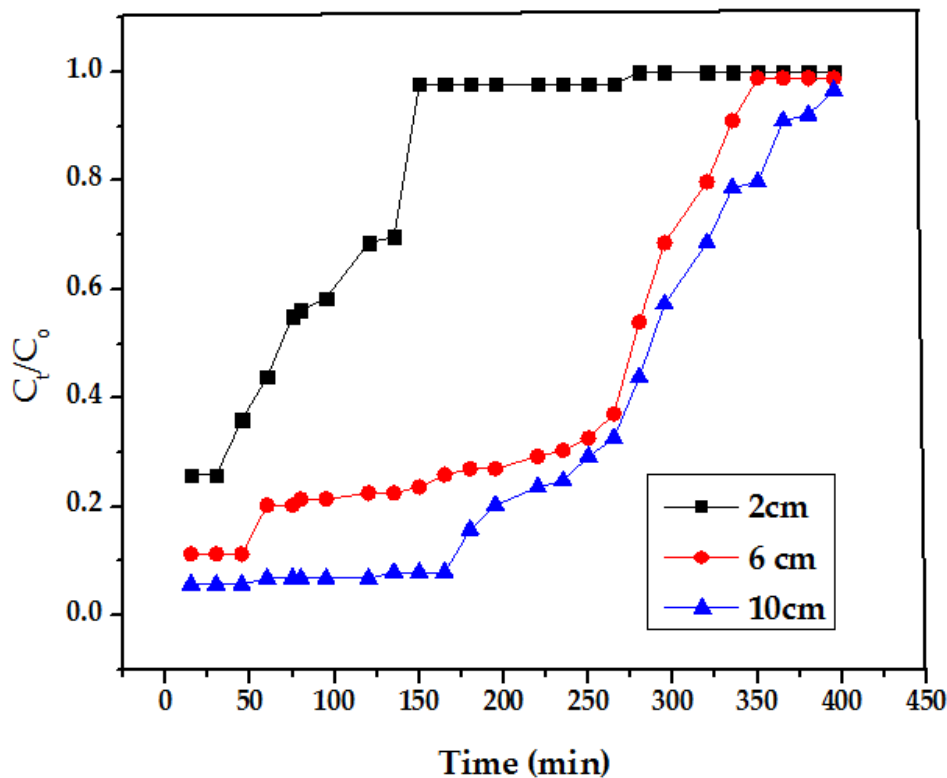


Figure 19: Effect of bed height on breakthrough profile of ALUM-MBENT (pH = 7, treated volume = 6750 ml, flowrate = 15ml/min, and initial fluoride concentration = 5 mg/l)

Table 10: For different bed depths, variables were found for removal of fluoride in the ALUM-MBENT column at a bed flowrate of 15ml/min

Bed depth (cm)	C ₀ (mg/l)	C _e	t _b (min)	t _e (min)	Δt	Z _m (cm)	V _{eff} (ml)	q _e (mg/g)
2	5	2.86	75	80	5	1.85	1200	0.51

6	5	0.56	295	320	25	5.51	4800	1.19
10	5	0.28	360	400	40	8.975	6000	2.88

4.1.2. Evaluation of interaction effect of process parameters on RB and ALUM-MBENT performance.

To study effect lower and higher bed depth versus corresponding flowrate with maximum adsorbate concentration on the column performance, the worst-case scenario was studied on both raw and ALUM-MBENT into a 1.5cm diameter borosilicate glass column and operated at a varied flow rates of 15ml/ and 25ml/min considering the real groundwater compositions was presented in Table 4.5.

Table 11: Performance evaluation of the RB and ALUM-MBENT column for both synthetic fluoride solution and real ground water samples

Adsorbent	solution	Operation conditions		Estimated parameters											
		Q (ml/min)	D (cm)	V of bed (m3)	C ₀ (mg/l)	t _b (min)	t _e (min)	q _e (mg/g)	V _{eff} (ml)	(BV)	EBC T	R (%)	Y	AE R	
RB	Synthetic F Solution	15	10	0.0176	12	150	220	1.45	3300	187.5	12.5	65.0	0.63	7.5	
		25	2	0.0035		75	78	0.05	1950	557.14	22.29	37.77	0.81	2.63	
	Real Ground Water Composition	15	10	0.0176		170	305	0.93	4575	259.94	17.33	41.48	0.58	5.46	
		25	2	0.0035		90	105	0.16	2625	750	30	51.31	0.78	2.11	
	ALUM-MBENT	Synthetic F Solution	15	10		0.0176	175	260	3.91	3900	221.59	14.77	75.15	0.57	6.45
			25	2		0.0035	32	45	1.32	1125	321.43	12.86	21.06	0.92	4.42
Real Ground Water Composition		15	10	0.0176	360	400	3.94	6000	340.91	22.73	94.15	0.1	4.16		
		25	2	0.0035	45	170	0.29	4250	1214.29	48.57	43.66	0.89	1.19		

The mass of the adsorbent divided by the volume of water treated at breakthrough is defined as adsorbent exhaustion rate (AER) and the empty bed contact time (EBCT) are two important design parameters. The empty bed contact time (EBCT) has an impact mostly on system's bed lifespan (the amount of bed volumes (BV) of water handled until breakthrough), and it must be properly selected to fully exploit the adsorbent potential [133]. The impact of EBCT on the ALUM-MBENT consumption rate, which defines how much the adsorbent needs to be recycled or regenerated. With rising EBCT, the associated RB and ALUM-MBENT exhaustion rates decreased, reaching a minimum value of 2.1 and 1.19 g/L, respectively, according to the performance assessment shown in Table 16. Similarly, bed lifespan increased with increasing empty bed contact time until a highest value of 1214.28 BV was reached at an EBCT of 48 minutes, after which it began to decline. Depending on the design flow (Q_d) used in this analysis, 48 minutes was believed an empty bed contact time for maximizing the use of ALUM-MBENT adsorption capability and might be a good approach during scale up of the system at large scale.

And for case of real ground water sample, the portion of idle bed length (Y) at breakthrough point rises from 0.574 to 0.922 with increasing of 15 to 25 mL/min flow rate, and sorbents exhaustion rate (AER) is reduced from 6.45 to 4.4 via rising of flow rate from 15 to 25 ml/min on to ALUM-MBENT.

4.1.3. Modeling of Breakthrough Curves.

Determination of the breakthrough curves is critical during efficient design of large-scale water purification systems. In this analysis, models like Clark model, Adams-Bohart, Thomas, Yoon-Nelson are used to forecast the dynamic behavior of the column filter. These models were used for column evaluation and are suitable for sorption process that are not constrained by external or internal diffusion [134]. Furthermore, these models are commonly used only for modeling the adsorption mechanism throughout column systems, so they deliver essential column variables that serve as the foundation for developing the column for field use.

4.1.3.1. Thomas model

For three different bed depths, K_{TH} and q_{th} values of the Thomas model parameters (Table 4.6), were calculated using non-linear optimization techniques based on Equation (2.8).

K_{TH} values decreased as input variables increased, but q_e values increased as parameter values increased. This implies that rising bed depth (D) produces a higher mass transfer driving force, which increases fluoride ion contact and thus raises the concentration gradient and adsorption potential. The decrease in K_{TH} as 'Depth of bed' rises due to an increase in flow resistance, which declines the mass transfer effect [135]. With the bed depth, the values of the maximum equilibrium uptake potential, q_e , calculated using the Thomas model, increased. The trend is similar with Chen et.al results [136]. The R^2 value of 2, 6 and 10cm bed depth is 0.96, 0.97 and 0.99 respectively. The conclusion is that the experimental breakthrough data closely matches Thomas' model.

4.1.3.2. Clark Model.

It was calculated using Equation (2.10). This model is developed to estimate how much the adsorbent can adsorb that adsorbate from aqueous solution until it becomes exhausted [86]. The Clark model, in this study, has been explored at

the value of ($n = 1.53$) Freundlich constant. The value was determined through batch test at room temperature of $27\text{ }^{\circ}\text{C}$. The model performs admirably and offers excellent column modeling. Table 3.7.3.1 shows the model parameters and coefficient of determination (R^2). The high R^2 result depicts Clark model is appropriate for telling or reflecting fluoride adsorption onto modified and unmodified bentonite packed column beds in continuous flow. The correlation coefficients of breakthrough curves to Clark model represent the good fitting ($R^2 > 0.90$). It implies that experimental data of column study is following the Clark model too. The enhancement of adsorbent bed height (z) and fluoride concentration (C_0) of influent has led to rise in the value of 'A' and 'r'. Whereas, the increase of influent flow rate leads to decrease in the values of 'A' and 'r'. Parallel order of variation for 'A' and 'r' is also mentioned by other researcher [135] [73, 137, 138].

The model variables could be useful for scaling up the treatment system using ALUM-MBENT column filters (for different concentrations and flow rates) without the need for additional experiments, potentially saving time and money.

4.1.3.3. Yoon-Nelson Model

According to Equation 2.9, this model is also useful to test the process parameters in the column. With the rise of variables, the increase of K_{YN} values was observed [139].

A graph against $\ln[(C_t/(C_0-C_t))]$ versus t as slope and intercepts, is used to measure K_{YN} and for various bed heights and initial concentrations.

K_{YN} values were found to decrease as bed height increased, whereas, as bed height increased, values that represent the time required for breakthrough showed a rising trend. It was discovered that the adsorbate breakthrough took longer when bed depth was raised. These results matched those reported by Chowdhury et al [140]. Meanwhile, K_{YN} increased as C_0 increased, and decreased as the C_0 decreased.

4.1.3.4. Adams–Bohart model

It defines the portion at the beginning of the curve, with model's reliability restricted to C_t/C_0 is 0.5 concentration range[116].

External (film) mass movement, according to the argument, limits the rate of adsorption. The linearized version of the model is used in the analysis.

K_{AB} and N_0 , constants of the model and Table 4.5 summarizes all of the data. The R^2 values ranged from 0.68 to 0.977. Table 4.5 clearly shows that K_{AB} values increased as bed height increased, while N_0 values declined with rise of bed depth. K_{AB} and N_0 , on the other hand, were affected by the initial fluoride concentration. K_{AB} value reported declining values as the initial concentration increased, but a growing pattern for N_0 . The pattern is similar to the outputs of a study that used nanoparticles to extract methylene blue and a commercial Bio-F adsorbent to remove fluoride from fixed-bed fluoride removal[141].

The model's validity also reinforces the role of external mass transfer in the fluoride adsorption process' rate limiting phase [142, 143]. Model's reliability is, indeed, constrained by the concentration range used (i.e. $C_t/C_0 = 1.1$).

Table 12: Parameters of Clark, Thomas, Yoon-Nelson, and Adams-bohart models for adsorption of fluoride at the varied range of bed height (Z), influent flow rate (Q), fluoride concentration (C₀) (experimental operating conditions)

D(cm) Q (mL/min) C ₀ (mg/L)			Clark model			Thomas model			Yoon-Nelson model			Adams-Bohart model		
			Ar	r	R ²	K _{th} *10 ⁻² (mL.mg ⁻¹ min ⁻¹)	Q _{th} (mg/g)	R ²	K _{YN} (min ⁻¹)	τ (min)	R ²	K _{AB} (L/mg·min)*10 ⁻⁵	N ₀ (mg/L)	R ²
2	15	5	3.286	0.0332	0.689	1.52	-0.88	0.59	0.0138	73.62	0.57	74.8	138.72	0.57
6	15	5	17.92	0.0041	0.95	1.6	3.37	0.77	0.016	206.25	0.77	93	43.01	0.77
10	15	5	21.07	0.0058	0.92	1.53	4.053	0.89	0.0168	187.5	0.94	350	6.62	0.89
10	15	12	2.066	0.0017	0.946	0.9	1.809	0.9	0.009	201	0.9	71.12	12.65	0.69
10	15	10	1.997	0.0019	0.96	1.58	2.249	0.89	0.0158	141.77	0.89	175	13.67	0.889
10	25	10	1.49	0.0011	0.717	0.92	0.03	0.87	0.008	1.63	0.8	1.91	1052	0.80
10	20	5	11.96	0.0077	0.92	1.30	2.54	0.93	0.013	172.3	0.93	230	349.84	0.89
10	25	5	3.61	0.0037	0.87	1.1.3	1.52	0.93	0.0113	106.93	0.93	64.6	251	0.93
6	15	12	3.918	0.0012	0.42	0.13	0.88	0.04	0.00113	780	0.3	78.2	3.61	0.04
2	25	10	1.864	0.0055	0.83	1.55	0.17	0.72	0.0156	10.95	0.72	0.6	32916	0.72

Finally, the results of an experimental analysis using continuous sorption of fluoride ions passing through aluminum modified bentonite clay (ALUM-MBENT) showed that it was effective at removing fluoride ions.

4.2. Adsorption capacity comparison by different low-cost adsorbents

Table 4.7 compares the fluoride adsorption potential of various low-cost adsorbents in column process. Many studies looked into the effectiveness of various low-cost adsorbents in batch mode for eliminating fluoride ions from ground water. However, only a small number of adsorbents were examined in a continuously flowing fixed bed system using clay minerals. Table 10 depicts the capacities of low-cost adsorbents on adsorption for several operating conditions. Based on the results, modified bentonite clay may be taken as a viable alternative to apply as fluoride ions removing adsorbent from drinking water.

1 Table 13: Comparison of different types of adsorbents used as fluoride adsorbent in batch and column study

S.No	Adsorbent	Bed Height (cm)	Concentrations range (mg/L)	Q _e (mg/g)	References
1	ALUM-MBENT	10	12	2.88	Current study
2	Quaternized palm kernel shell	6	6	0.99	[144]
3	Hydrous ferric oxide	12	30	7.06	[132]
4	Slow Pyrolyzed Okra Stem and Black Gram Straw Bio-chars	6	2	6	[145]
5	Surface-Tailored Zeolite (Al-F9)	15	20	4.93	[85]
6	Bio-F sorbent	10	30	9.87	[141]
7	Granular acid treated Bentonite	4.95	6.34	0.009	[146]
8	Coconut husk activated carbon	5	10	1.3	[86]
9	Kanuma mud	10	20	1.6	[47]

2

4.3. Summary

The aluminum-amended bentonite clay (ALUM-MBENT) adsorbent was discovered as functioning for removal of fluoride ion from drinking water. Fluoride ion using ALUM-MBENT bed column was found to be 95% removed. At room temperature, flowrates and bed depth were found to have an effect on removal. Only fluoride spiked water solution on ALUM-MBENT column were nearly completely removed. Breakthrough was achieved after treating 5 L of water for approximately 110 minutes with synthesized bentonite clay concentrations of 5 mg/L. Only fluoride spiked solution achieved breakthrough faster (90 minutes) than other anions mixed solutions (240min).

The C_t/C_0 ratio (adsorbate concentration) rises quickly, resulting in a faster breakthrough period. With concentration of fluoride as 5 mg/L, breakthrough time (t_b) for only fluoride spiked solution onto ALUM-MBENT were 120, 145, and 160 minutes, respectively, and for real ground water, they were 250, 260, and 300 minutes for flowrates 15, 20, and 25 mL/ min, respectively. For flowrates of 15, 20, and 25 mL/ min, the times to hit $C = C_0$ (max) or the exhaustion period (t_e) were 250, 270, and 295 minutes for only fluoride spiked water, and 315, 345, and 390 minutes for actual groundwater, respectively. The effluent concentration of the adsorbate decreases more quickly at higher bed heights than at lower bed heights. Higher feed concentrations resulted in relatively steep breakthrough curves with a shorter breakthrough time. Fixed bed sorption data has shown a high level of agreement with well-known column models like the Thomas and Clark.

CHAPTER 5: OPTIMZATION OF FLUORIDE ADSORPTION ON TO FIXED BED COLUMN: A STATISTICAL APPROACH

5.0. Results and Discussions

5.1. Statistical Analysis

Implementing Central Composite Design with RSM process for optimization comprises four main steps: (i) Generate a statistical experimental plan based on the independent variables and execute the experiment according to the plan. (ii) Propose a mathematical model according to the responses of the experimental results and elaborate the result of analysis of variance. (iii) Check the accuracy of the model through diagnostic plots (iv) Execute response analysis of the model and predict optimal conditions, and confirm the model through running an experiment.

5.1.1. Model fitting and analysis of variance (ANOVA), Quadratic model equations and selected model diagnostic test

Single and interaction effects of the independent factors on the % Fluoride removal and Fluoride adsorption capacity were studied by employing the CCD with RSM [74]. The CCD is frequently used for modeling and optimization, and it requires minimal number of experiments. In general, the CCD is made up of three types of runs: factorial runs, axial runs, and center runs [147, 148]. A total of 20 experimental run accordingly were performed and the actual and predicted value of the responses along with the experimental conditions are summarized in Table 5.1.

Table5.1: Experimental runs and their predicted responses.

Category	Run	Factors			R%			Qe(mg/g)		
		A	B	C	Observed	Anticipated	Residual	Observed	Anticipated	Residual
Factorial points (8 runs)	3	10	15	10	87	61.901	-25.099	2.11	2.10825	-0.00175
	5	10	25	2	10	-37.349	-47.349	0.3	0.33295	0.03295
	14	5	15	2	55	41.31	-13.69	1.3	1.21145	-0.08855
	15	10	15	2	25	-6.975	-31.975	0.6	0.38445	-0.21555
	16	5	15	10	95	82.706	-12.294	2.45	2.35525	-0.09475
	17	5	25	10	68	49.786	-18.214	1.6	1.75375	0.15375
	19	5	25	2	35	9.886	-25.114	0.9	0.83995	-0.06005
	20	10	25	10	76	30.031	-45.969	1.8	1.82675	0.02675
Central point (5 runs)	2	7.5	20	6	86.5	58.322	-28.178	2.11	2.096175	-0.01383
	6	7.5	20	6	87	58.322	-28.678	2.11	2.096175	-0.01383
	11	7.5	20	6	88.6	58.322	-30.278	2.3	2.096175	-0.20383
	13	7.5	20	6	89	58.322	-30.678	1.3	2.096175	0.796175
	1	7.5	20	6	87	58.322	-28.678	2.1	2.096175	-0.00383
Axial points (6)	8	7.5	12	6	76	60.9836	-15.0164	1.3	1.572735	0.272735
	4	3	20	6	85	69.5	-15.5	2	1.9596	-0.0404
	7	12	20	6	55	8.264	-46.736	1.3	1.281	-0.019
	9	7.5	20	1	20	1.5795	-18.4205	0.5	0.816925	0.316925
	12	7.5	20	13		61.3215	61.3215	2.45	2.358325	-0.09168
	18	7.5	25	6		33.6485	33.6485	1.1	1.626425	0.526425

5.1.2. Analysis of Variance (ANOVA)

The effect of main and interaction effects factors on % fluoride ion (R%) and adsorption capacity (mg/g) were analyzed by performing the analysis of variance (ANOVA) at 0.05 level of significance. The result of the analysis of variance (ANOVA) for the response surface quadratic model both for responses are given in terms of F and p-value (Table 5.2). The main and interaction effects of each factor having P values <0.05 are considered as having significant effect on the responses.

Table 5.2: Analysis of variance values of experimental design for % fluoride removal and Adsorption Capacity.

Source of Variance	% fluoride removal		Adsorption Capacity (q)	
	F value	p-value prob > F	F value	p-value prob > F
Model	110.29	< 0.0001	23.84	< 0.0001
A	59.62	< 0.0001	13.1	< 0.0047
B	77.32	< 0.0001	9.23	0.0125
C	645.56	< 0.0001	137.25	< 0.0001
AB	4.04	0.0723*	1.34	0.2744*
AC	27.69	0.0004	4.39	0.0625*
BC	0.082	0.7800*	0.69	0.4262*
A ²	38.63	< 0.0001	0.824	< 0.0166
B ²	83.39	< 0.0001	35.63	< 0.0001
C ²	167.63	< 0.0001	23.89	0.0006
Lack of fit	4.88	0.0533*	1.38	0.3961*

*Not significant model terms.

As the value of F-values or Sum of Squares rises, so is the relevance of that variable to significantly impact the % fluoride removal or Adsorption capacity. The three factors are designated as initial fluoride concentration (A), flow rate (B), and bed depth (C). It was observed that A, B, C, AC, A², B², and C² impart significant effect on % Fluoride removal. From the table it can be observed that only the interaction of initial concentration and bed-depth has significant effect

on fluoride removal. The "Lack of Fit F-value" for the % fluoride removal model is not high indicating the good fitness of the model. A significant "Lack of Fit F-value" has a 5.33 percent chance of being caused by noise in case of fluoride removal. Furthermore, the adsorption capacity is significantly affected by A, B, C, A², B², and C². The "Lack of Fit F-value" for both % fluoride removal and adsorption capacity is not high indicating the good fitness of the model. All for adsorption capacity, all interaction effects are insignificant. Therefore, the insignificant interactions will not be included in the model equation. The experimental data was analyzed and the quadratic model was suggested to best fit both % fluoride removal and fluoride adsorption capacity. To know whether the quadratic model is significant or not, use a sequential model sum of squares was applied. For instance, for % fluoride removal, according to model summary statistics, the quadratic model had the highest adjusted R² 0.981 and projected R² 0.9356 values for % fluoride removal. The 0.9356 "Pred R-Squared" and the 0.9810 "Adj R-Squared" values are in reasonable agreement since the rule of thumb for the adjusted R-squared basically plateaus when insignificant terms are added to the model, and the predicted R-squared will decrease when there are too many insignificant terms [149]. Furthermore, a smaller coefficient of variation (CV = 5.47%) suggests that the experiments were done with more precision and reliability [150]. As a consequence, the quadratic model was chosen to describe the relationship. Using the results of the experiment, a regression model linking the response (Y) to the variables (X) relationship in terms of actual significant factors is expressed in Equation (5.1 and 5.2).

$$\text{Fluoride removal} = -93.73425 + 7.26 * \text{Initial Fluoride Concentraion} + 12.41 * \text{Flow Rate} + 12.57 * \text{Bed Depth} + 0.69 * \text{Initial Fluoride Concentration} * \text{Bed Depth} - 0.97 * \text{Initial Fluoride Concentration} - 0.36 * \text{Flow Rate} - 0.92 * \text{Bed Depth} \quad (5.1)$$

$$\text{Adsorption Capacity} = -4.56 + 0.28 * \text{Initial Fluoride Concentration} + 0.46 * \text{Flow Rate} + 0.39 * \text{Bed Depth} - 0.024 * \text{Initial Fluoride Concentration} - 0.012 * \text{Flow Rate} - 0.018 * \text{Bed Depth} \quad (5.2)$$

The fitness and suitability of the developed regression models to the experimental results were further analyzed by the coefficients of determination (R^2). An R^2 value of 0.985 is reported for % fluoride removal model. An R^2 value of 0.985 means that the model can explain 98.5% of the variation in % fluoride removal, and only 0.15% was as a result of chance. In addition to this, the predicted R^2 ($R^2_{pre} = 0.949$) is in a reasonable agreement with the adjusted R^2 ($R^2_{adj} = 0.978$) implying the high correlation between the actual and predicted values of % fluoride removal. The adequate precision value measures the signal to noise ratio and, a ratio greater than 4 is always desirable. In the case of % fluoride removal model an adequate precision value of 34.32 is obtained that indicates an adequate signal. Hence, this model can be used to navigate the design space. Similarly, for the Adsorption Capacity (mg/g) developed quadratic model the coefficient of determination ($R^2 = 0.927$) indicates an excellent fit, meaning that the fitted model explained about 92.7% of the total variation in the Adsorption Capacity (mg/g). In addition to this, the difference between the adjusted R^2 ($R^2_{adj} = 0.893$) and that of predicted R^2 ($R^2_{pred} = 0.817$) is in reasonable agreement, that means high correlations existed between the actual and predicted value of % removal of Fluoride. Finally, the adequate precision of the model is 15.7 hence, the suggested quadratic model is a good fit to the experimental data and can be used to navigate the design space. The model diagnostic test was performed using the predicted and actual values of for both responses as is shown in Figure 5.1(a) shows the predicted vs actual value of the % Fluoride removal response. All data points are either near to or laid on the $y = x$ line, which indicates that the model is well fitted. Similarly, Figure 5.1(b) shows the predicted vs actual values of Adsorption capacities. Here again, all the data points lay near to the $y = x$ line, which indicates the variability of the data is well explained by the generated model.

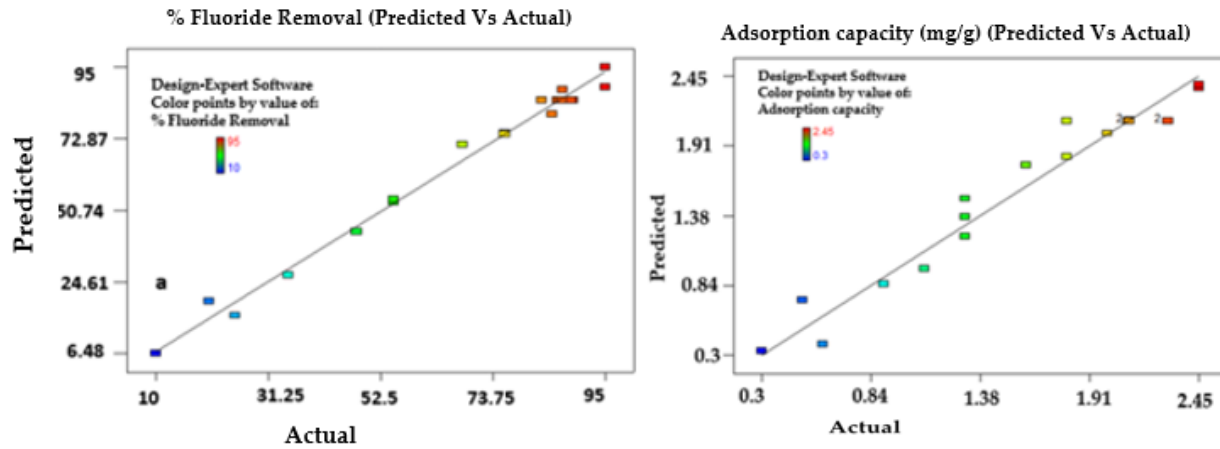
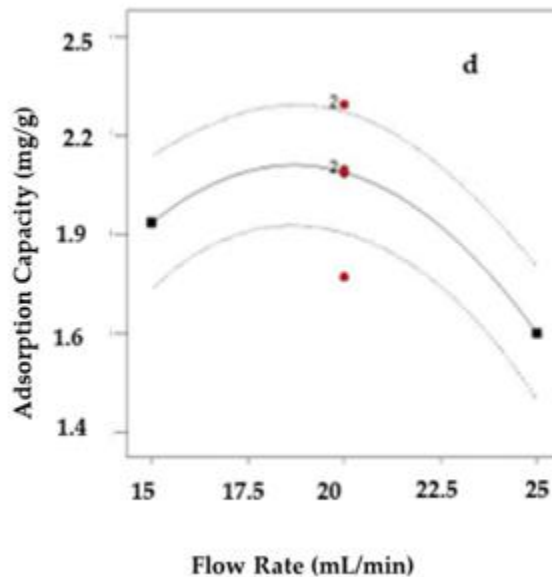
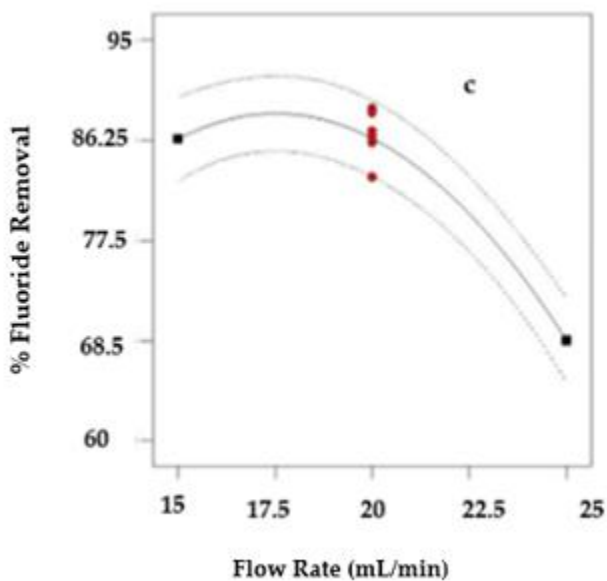
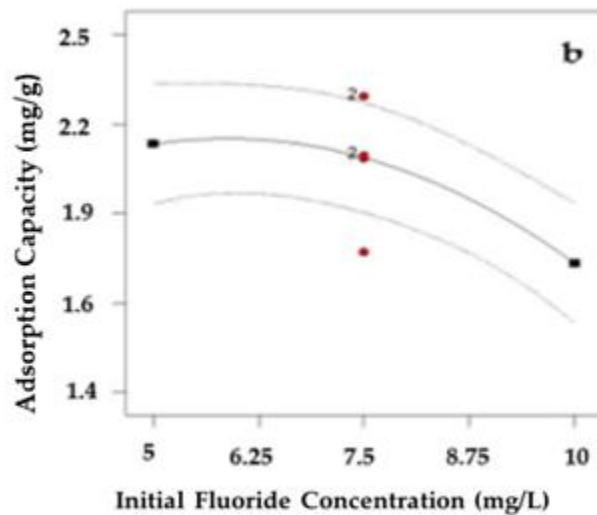
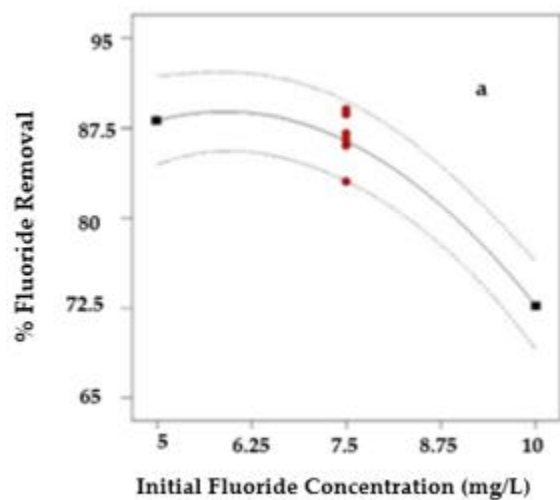


Figure 20: Correlation of actual and predicted values for (a) removal efficiency (R) and (b) Fluoride adsorption capacity (Qe).

5.2. Effect of Operating Condition on the Adsorption Performance of ATB

Figure 20 shows the singular effect of operating parameters on removal efficiency & adsorption capacity. It was observed that the three parameters have significant singular effect on removal efficiency and in any of the factors reasonably increases the removal efficiency. As shown in Figure 5.2 e & f, the increase in bed depth increased % removal & adsorption capacity. Fluoride removal efficiency decreased from 92.5 % to 70.2 % with the increase of flow rate from 15 to 25 mL/min, respectively as shown in Figure 5.2 c. Varying the initial fluoride concentration revealed (Figures 5.2 a & b) very small effect on percent removal of fluoride and adsorption capacity. It was also observed that adsorption capacity is significantly increased with increase in bed depth whereas increase initial concentration results in relatively very small increase in adsorption capacity.



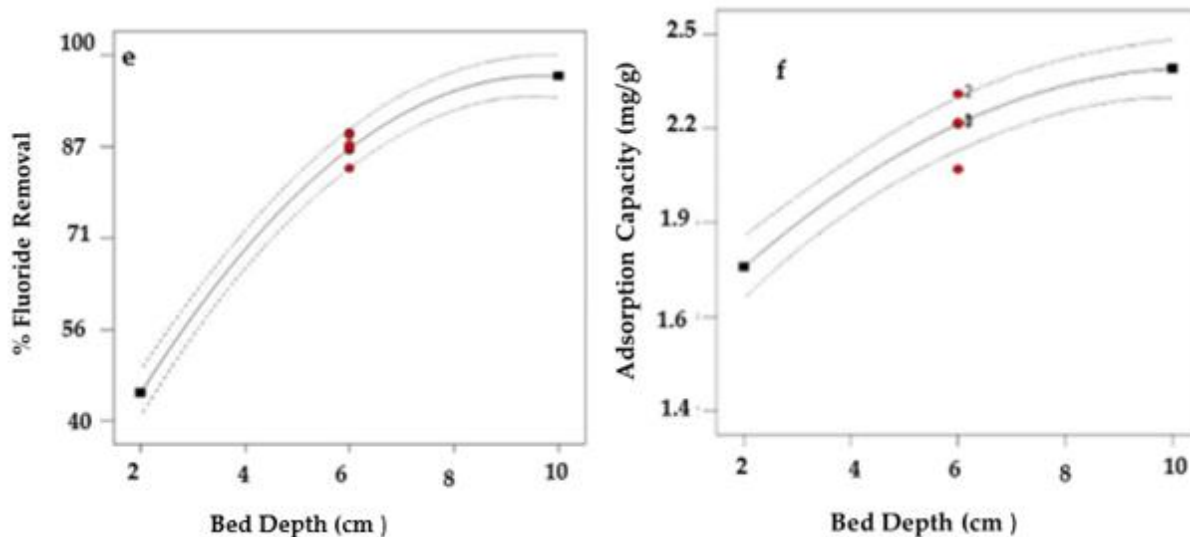
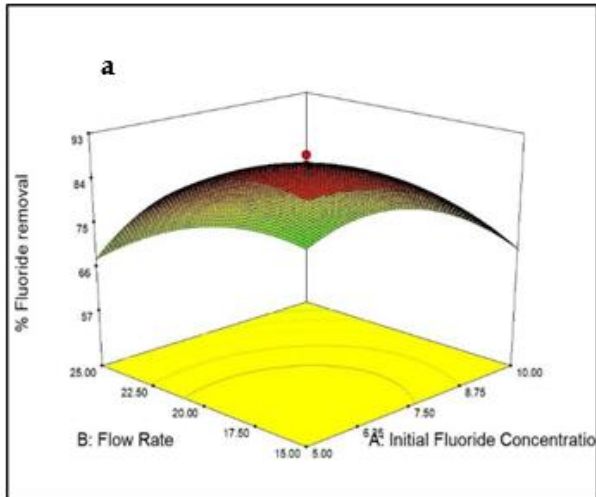


Figure 21: Effect of initial concentration, flow rate and bed depth on % fluoride removal and adsorption capacity (mg/g).

5.3. Interaction Effect of Process Variables

To evaluate the interaction effect of the three independent parameters on the adsorption productivity through fixed bed column operations, a number of experiments with 1 cm to 13 cm of adsorbent packed bed depth at flow rate of 12, 15, 20, 25 mL/min and initial fluoride concentrations 3, 5, 7.5, 10, 12 mg/L were conducted. In order to present the regression model output, graphical explanation using 3D response surface plots were shown for the optimization of fluoride adsorption on to acid treated bentonite clay through fixed bed column. The influences of the three different process variables (initial concentration, volumetric flow rate, and adsorbent bed depth) on removal efficiency (R) and fluoride adsorption capacity (Qe) as responses plot were determined. Figure 5.3a demonstrates that at lower levels, the combined effects of flow rate and initial fluoride concentrations have a considerably greater combined influence on removal efficiency. It was discovered that the influence of flow rate is greater than that of initial fluoride concentration, and that lowering any of these two parameters improves removal efficiency. The combined effect of flow rate and initial fluoride concentration on adsorption capacity is shown in Figure 5.3b. The combined effect of the two variables was found to be mostly controlled by flow rate, with the starting fluoride content having very little influence. It was also discovered that as the flow rate is increased, the adsorption capacity decreases. And hence, within the experimental range, the % fluoride removal dropped as both the starting fluoride concentration and the flow rate grew. The reality that almost all adsorbents have such a limited number of binding sites that become

saturated at a particular concentration may explain this phenomenon. The binding sites on the adsorbent surface became more quickly saturated as the incoming fluoride concentration increased, ensuing in an earlier breakthrough. Also, with increased flow rates, the fluoride solution's retention time in the column reduced, resulting in fluoride molecules not having enough time to grab binding sites on the surface of the adsorbent or penetrate into the adsorbent pores, exiting the column before equilibrium was reached. Initial concentration and bed depth have a substantial combined influence on removal efficiency, as seen in Figures 5.3 c and d, with bed depth having the biggest effect, but initial concentration has a decent effect as well. At higher levels of the two variables, the total effect was shown to be larger. It was also discovered that raising any of the parameters improves the efficiency of removal. Figure 5.3 depicts the combined effect of the two variables on adsorption capacity. It was discovered that at higher starting concentrations, increasing bed depth considerably reduces adsorption capacity, but at lower initial concentrations, increasing bed depth greatly increases adsorption capacity. This tendency can be explained by the fact that increasing bed height increases the number of binding sites available for the adsorption process. Since this is because of the fluoride molecules had more time to contact the adsorbent. The increased number of active sites available for adsorption might explain the first rise in fluoride ion adsorption. The adhering potential is high at the beginning phase, when the adsorbent surface is empty, and therefore sorption occurs at a faster rate. However, due to the saturation of active sites, the subsequent adsorption rate was sluggish, and equilibrium was only established over time [151]. Figure 5.3(e & f) shows the interactive effect of flow rate and bed height on % fluoride removal for dynamic adsorption of fluoride by ATB in a 3D plot. The % fluoride removal was significantly influenced by the interaction of flow rate and bed height. The percentage fluoride removed dropped as the flow rate rose, but it increased as the bed height grew. This trend may be explained by the fluoride molecules' residence duration in the column as well as the presence of binding sites.



Design-Expert® Software

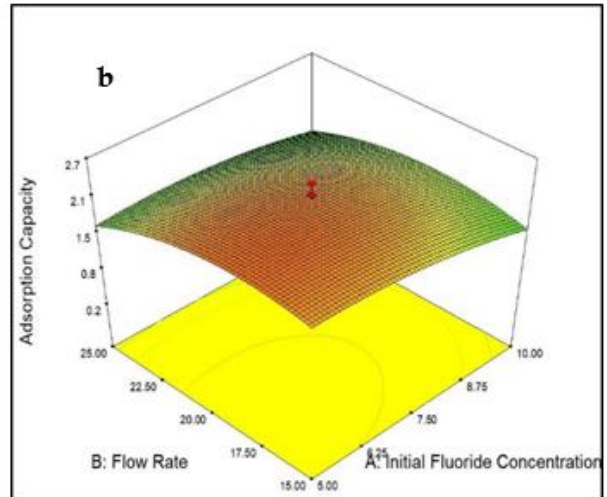
Fluoride removal

- ◆ Design points above predicted value
- ◇ Design points below predicted value



X1 = A: Initial Fluoride Concentraion
X2 = B: Flow Rate

Actual Factor
C: Bed Depth = 6.00



Design-Expert® Software

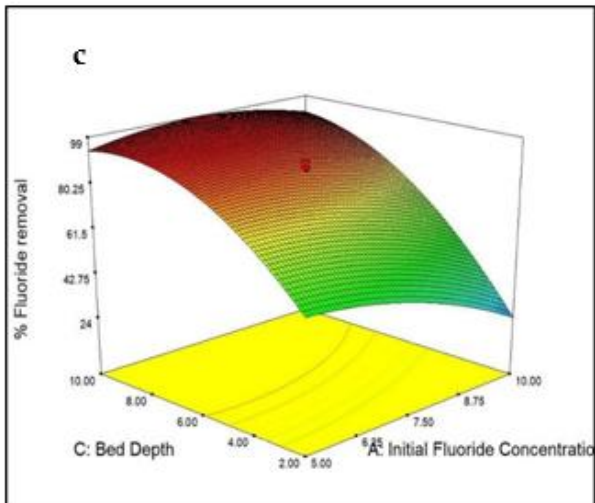
Adsorption Capacity

- ◆ Design points above predicted value
- ◇ Design points below predicted value



X1 = A: Initial Fluoride Concentraion
X2 = B: Flow Rate

Actual Factor
C: Bed Depth = 6.00



Design-Expert® Software

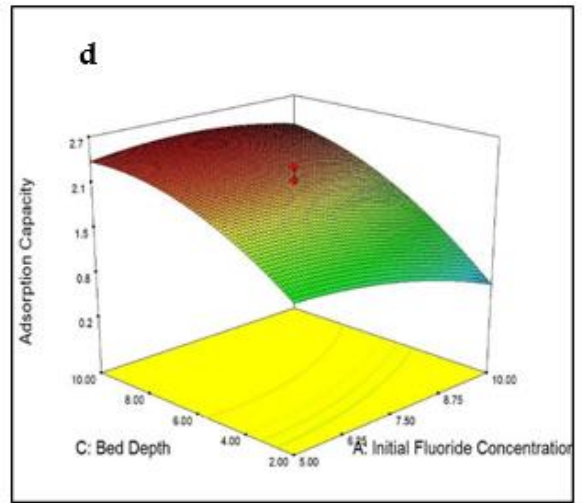
Fluoride removal

- ◆ Design points above predicted value
- ◇ Design points below predicted value



X1 = A: Initial Fluoride Concentraion
X2 = C: Bed Depth

Actual Factor
B: Flow Rate = 20.00



Design-Expert® Software

Adsorption Capacity

- ◆ Design points above predicted value
- ◇ Design points below predicted value



X1 = A: Initial Fluoride Concentraion
X2 = C: Bed Depth

Actual Factor
B: Flow Rate = 20.00

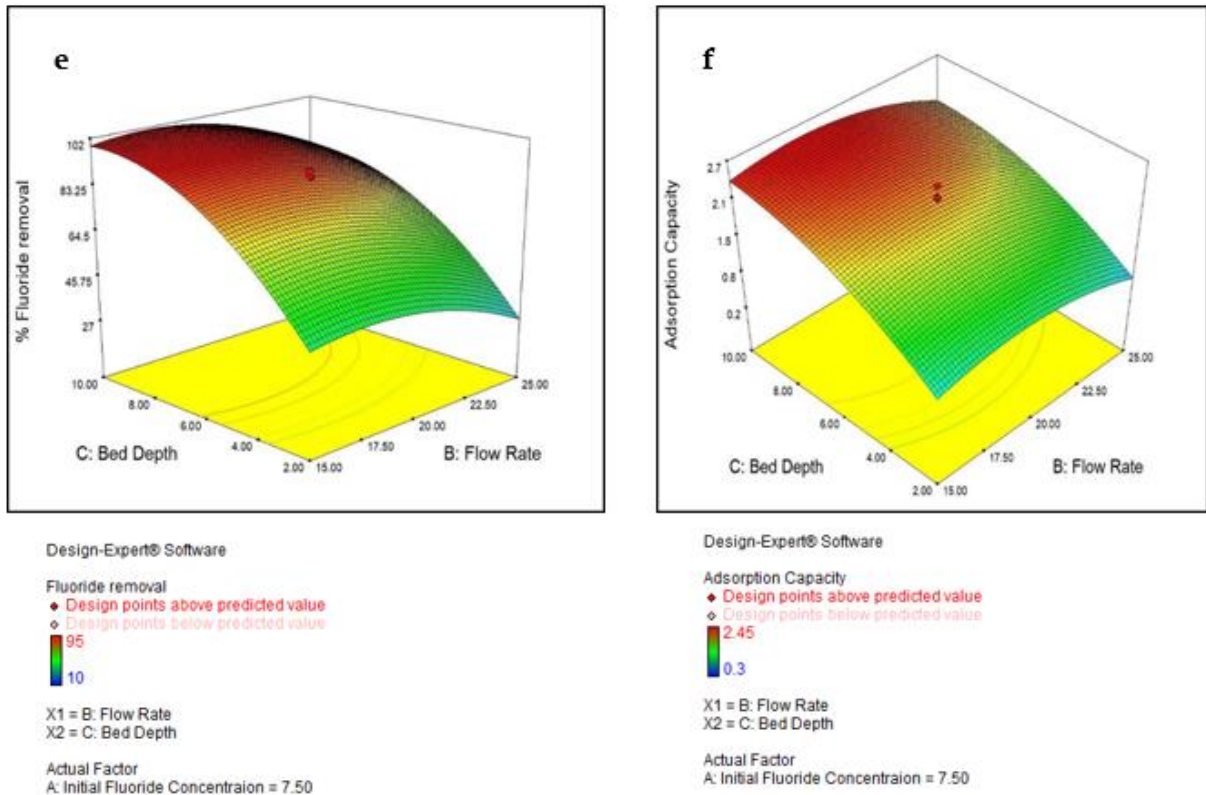


Figure 22:3D surface plots for interaction effect of operating conditions on Fluoride removal efficiency (R) and Adsorption Capacity (mg/g).

5.4. Optimization using the Desirability Function

It was examined the intended objective for each variable and the related response for numerical optimization [152]. Each objective was given a weight to change the form of its own desirability function. The initial fluoride concentration, flow rate, adsorbent packed bed depth, adsorption capacity, and fluoride removal are all things we want to achieve. In this study, the input variables were given specific ranged values, whereas the response was designed to achieve a maximum as shown in Table 5.3. A desired value for each input element and response can be selected via numerical optimization. The input variables in this study were given precise values, and the response was designed to attain a maximum. The obtained findings are consistent with the experimental data, which show that the optimal parameters for Fluoride removal are pH 7.2, bed depth of 8.88 cm, flow rate of 17.2 mL/min, and an initial fluoride content of 5.51 mg/L. At an initial fluoride concentration of 5.51 mg/L, a flow rate of 17.2 mL/min, and an adsorbent packed bed depth of 8.88 cm with desirability of 1.0, the maximum achievable fluoride adsorption capacity was 2.46 mg/g (Figure

5.4). Under identical circumstances at pH = 7.2, the optimum conditions were verified three times (n=3) (Table 5.3). The confirmatory experiment showed (Table 5.4) a fluoride removal efficiency of 100 % under optimal conditions compared with the fluoride removal percent of 99.05 % obtained by the model. This indicates the suitability and accuracy of the model.

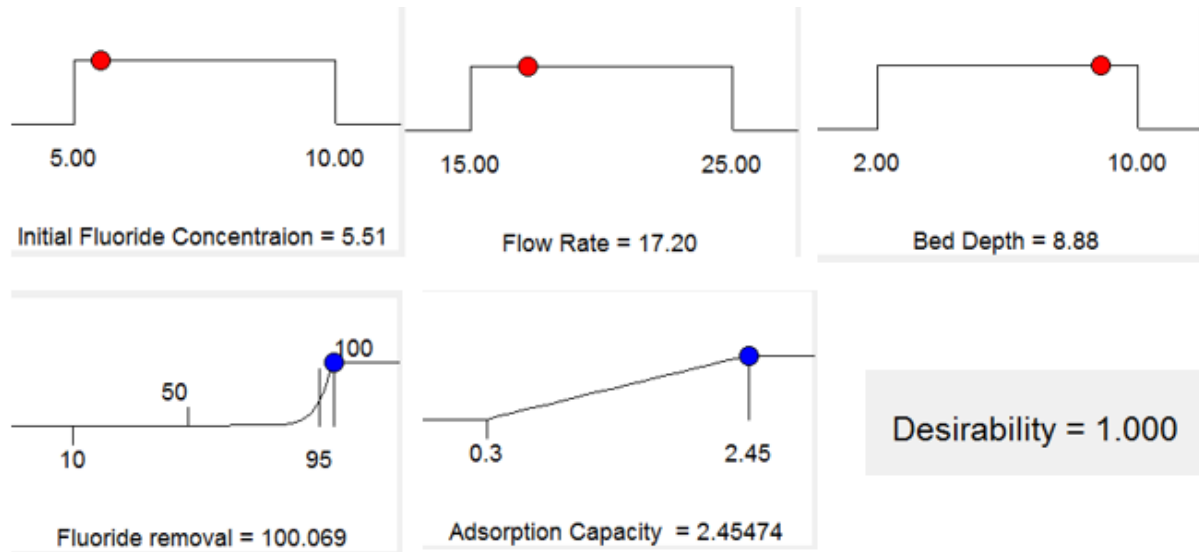


Figure 23:Desirability ramp for optimization (R = 100% & Desirability = 1.00)

Table 14:Constraints for desirability analysis selected.

Name	Goal	is	in	Lower	Upper	Weight	Weight	Importance
				Limit	Limit			
Initial Fluoride Concentration	is in range			5	10	1	1	2
Flow Rate	is in range			15	25	1	1	3
Bed Depth	is in range			2	10	1	1	3

Fluoride removal	maximize	50	100	10	1	3
Adsorption Capacity	maximize	0.3	2.45	1	1	3

Table 15: Optimization solutions provided by the model.

Number	Initial Fluoride Concentration	Flow Rate	Bed Depth	Fluoride removal	Adsorption Capacity	Desirability
1	6.84	18.22	8.59	100.505	2.46218	1
2	7.17	18	8.67	100.513	2.45742	1
3	5.51	17.2	8.88	100.069	2.45474	1
4	5.92	17.68	8.75	100.548	2.46739	1
5	6.62	17.01	8.78	101.153	2.46102	1
6	5.87	17.25	9.11	100.762	2.47643	1
7	6.83	18.38	9.98	100.797	2.51664	1
8	7.36	18.85	9.15	100.321	2.47696	1
9	6.9	16.46	9.86	101.19	2.48363	1
10	7.92	16.91	9.67	100.408	2.45459	1
11	7.81	16.65	9.81	100.504	2.45688	1
12	7.21	16.71	9.18	101.107	2.45836	1
13	7.94	16.75	9.82	100.305	2.45293	1
14	7.61	18.92	9.73	100.282	2.49188	1
15	5.81	16.62	9.06	100.661	2.45847	1
16	7.52	18.47	9.66	100.755	2.49698	1
17	7.08	18.29	9.73	101.104	2.5106	1
18	7.18	17.21	9.4	101.391	2.48524	1

Selecte
d

19	6.06	18.46	8.91	100.239	2.47605	1
20	6.74	16.43	9.74	101.228	2.48135	1
21	7.63	16.68	9.89	100.795	2.47035	1
22	6.12	18.26	9.7	100.351	2.50193	1
23	8.19	17.5	9.84	100.019	2.4607	1
24	6.4	16.53	8.83	101.059	2.45055	1
25	6.8	18.35	9.86	100.924	2.51484	1
26	5.71	17.94	8.98	100.142	2.47162	1
27	6.67	18	9.04	101.159	2.48933	1
28	7.39	16.8	9.54	101.136	2.47189	1
29	7.12	17.55	9.11	101.255	2.48051	1
30	5.8	16.75	9.09	100.657	2.46263	1
31	6.01	17.44	8.97	100.89	2.47735	1
32	7.88	18.57	9.7	100.251	2.48316	1
33	6.04	17.7	8.98	100.821	2.48062	1
34	6.31	16.68	9.31	101.251	2.47734	1
35	6.76	19.15	9.5	100.194	2.49312	1
36	5.51	16.65	9.2	100.072	2.45363	1
37	6.04	16.48	9.12	100.927	2.46062	1
38	6.34	17.6	9.33	101.24	2.49749	1
39	7.51	17.05	9.53	101.083	2.47487	1

5.5. Model Validation

Table 5.5 compares experimental data to anticipated values under optimal operating conditions. According to the table, the percentage error of experimental against anticipated value for adsorption capacity and removal efficiency is 2.43 percent and 1.00 percent, respectively. As a result, the models and optimal operating conditions created for the factors are valid and relevant in forecasting the response variables.

Table 16: Model validation.

Flowrate (mL/min)	Bed depth (cm)	Concentration (mg/L)	Experimental		Theoretical		Percentage error	
			q _e , (mg/g)	R (%)	(mg/g)	R (%)	q _e	R
17.2	8.88	5.51	2.2	99.05	2.46	10	2.43	1

3.8. Comparison of Fluoride Adsorption Capacities between ATB and Different Clay-based Adsorbents under Batch and Column Operations

The adsorption capacity of the adsorbent (ATB) was compared with different clay based-materials for fluoride adsorption as stated in Table 5.6 and it has relatively good result through packed fixed bed column experimentations.

Table 17: Bentonite based adsorbent were compared by their adsorptive capacity

Adsorbent	Mode of operation	Adsorption (mg/g)	capacity	References
Fired Clay pots	Batch	1.6		[153]
Granular acid-treated bentonite (GHB)	Batch & Column	0.094		[146]
Acid activated red mud (powdered)	Batch	5.06		[154]
Tunisian Kaolinite	Batch	1.48		[155]
Diatomite Modified with Aluminium hydroxide	Batch	1.67		[156]
Mn ²⁺ modified Bentonite Clay	Batch	0.08		[100]
Al ³⁺ -modified bentonite clay	Batch	5.7		[5]
Magnesium incorporated bentonite clay	Batch	2.26		[103]
Dicarboxylic acid (malic acid (A)), metal ion decorated bentonite clay (BC) modified with chitosan (CS)	Batch	9.87		[157]
Acid Treated Bentonite (ATB)	Column	2.46		This study

5.6. Summary

The adoption of an experimental design using RSM strategy allows for the speedy testing of a broad experimental domain for the optimization of acid treated bentonite adsorbent for fluoride adsorption capability. Under optimized condition, up to 99.05 % fluoride was removed from effluents using ATB adsorbent with initial fluoride concentrations of 5.51 mg/L, flow rate of 17.2 mL/min, bed depth of 8.88 cm with a 1.00 desirability. Results suggest that ATB adsorbent has potential for fluoride adsorption. All of the R^2 values indicate that the models match the experimental data well. As far as we know, no acid-treated bentonite clay has been used as an adsorbent in the RSM method using continuously flowing fixed bed column. This study shows that ATB are a potential adsorbent for the removal of fluoride ions from aqueous solution due to their high adsorption capacity and, more importantly, the fact that it is naturally and abundantly accessible at a reasonable cost.

**CHAPTER 6: EFFECTS OF CO-EXISTING IONS ON FLUORIDE
ADSORPTION AND RE-USABILITY**

6. Results and Discussions

6.1. Effect of coexisting anions

The effects of coexisting chloride, sulfate, phosphate and bicarbonate anions on fluoride adsorption were examined. It was taken into account that the interaction between ions found in natural water and fluoride ions on the clay surface. From the standpoint of industrial applications, it is critical to investigate the impact of anions that compete with fluoride adsorption through the application of fixed bed column operation. This is because fluoride in groundwater coexists with some anions, which are thought to interfere with the adsorption mechanism [158].

In the sequence of $\text{Cl}^- < \text{SO}_4^{2-} < \text{PO}_4^{3-} < \text{CO}_3^{2-}$, the anions decreased fluoride adsorption on to the ALUM-MBENT adsorbent through continuously flowing fixed bed column. This indicates that the adsorbent surface has a higher affinity for multivalent anions than monovalent anions. According to the literature, certain anions may increase coulombic repulsion forces and compete with fluoride for active sites, resulting in a rapid decrease in adsorption [159]. As shown in Figure 6.1, the carbonate ion had the most influence on fluoride removal, whereas chloride had the least.

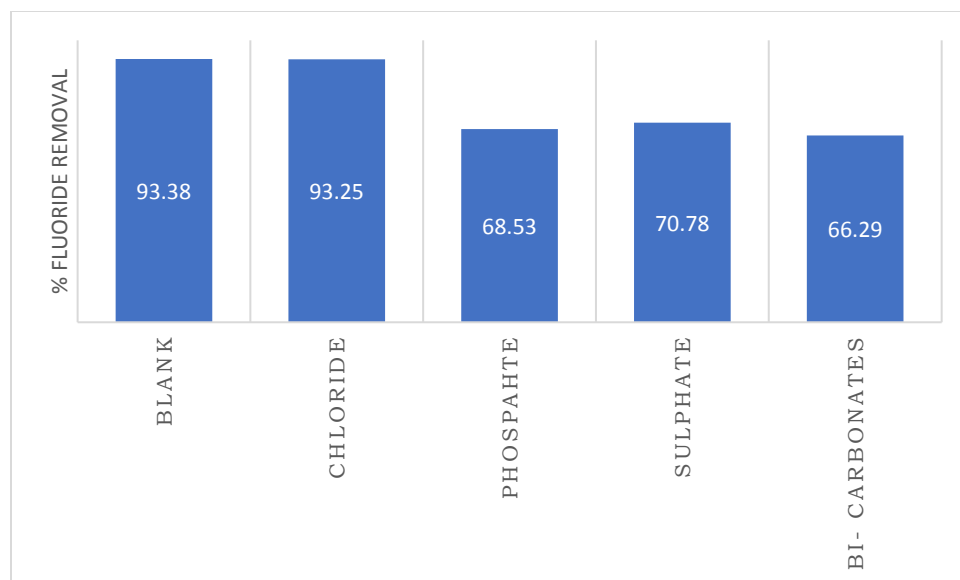


Figure 6.1: Effects of co-anions on fluoride removal by ALUM-MBENT co-ion concentrations for nitrate and phosphate that can be found in groundwater. Model water: Fluoride = 5mg/L, bed depth =10cm and Q = 15mL/min

Recognizing the competing adsorption mechanisms of other ionic species will also bring insight into the processes that occur at the interfaces of adsorbent materials, assisting in the creation of various adsorbent adsorption mechanisms. In this study, the effects of anions like chloride (Cl^-), which is monovalent, carbonates (CO_3^{2-}), which is divalent and Phosphates (PO_4^{3-}), which is multivalent were independently examined through continuously flowing fixed bed column packed with aluminum modified bentonite clay (ALUM-MBENT) adsorbent with the concentrations of anions 100, 10, and 0.1 mg/L with 10mg/L of fluoride concentration and the results presented in Table 6.1 & Figure 6.2.

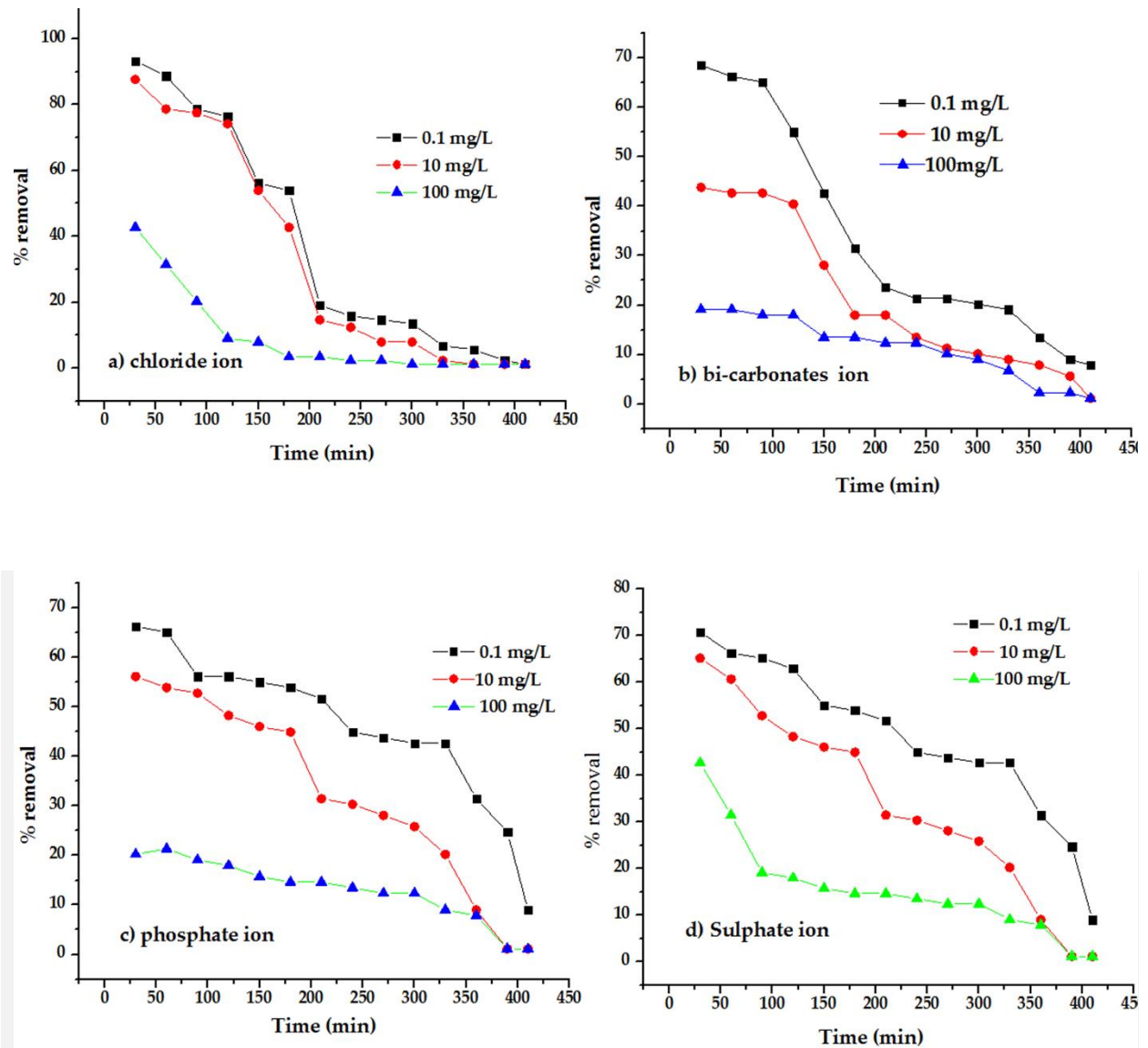


Figure 6.2: Effect of individual co-existing anions

The availability of competing anions resulted in a reduction in removal of fluoride; it's because the adsorbent robust locations are appropriate for having to attach the anions to the surface of the adsorbent.

Table 6.1: Effects of co-existing ions on adsorption of fluoride onto ALUM-MBENT: Model Water-Fluoride concentrations of 5mg/L, bed depth of 10cm and 15ml/min flowrate

Anions	Dose (mg/L)	% Fluoride removal	% Reduction
	Blank	94.38	
Chloride (Cl⁻)	0.1	93.25	1.13
	10	87.64	6.74
	100	56.17	37.21
Carbonates (CO₃²⁻)	0.1	66.29	28.09
	10	56.12	38.28
	100	20.22	74.16
Phosphate (PO₄)³⁻	0.1	68.53	25.85
	10	43.82	50.56
	100	19.10	75.28
Sulphate (SO₄)²⁻	0.1	70.78	22.6
	10	65.16	28.22
	100	42.19	51.19

The need of a competitive ion analysis in determining the adsorbent's actual effectiveness for a simulated groundwater sample is critical. Fluoride 5 mgL⁻¹ was held constant for the majority of the study, while each competing ion concentration varied between (0.1–100) mgL⁻¹ as shown in Table 6.1. Because HCO₃⁻ raises the pH of the solution and decreases the active sites for fluoride adsorption, HCO₃⁻ competes more effectively than other ions [12]. As a result of the comparable ionic radii of HCO₃⁻ (0.133 nm), the removal capability of fluoride

diminishes, and it is advised that HCO_3^- be replaced by the OH ion at higher pH. In comparison to bicarbonate, chloride has a less influence on alkaline pH because of its buffering effect. At all doses (0.1, 10 & 100) mgL^{-1} , HCO_3^- and $(\text{PO}_4)^{3-}$ primarily diminish fluoride adsorption percentage. When HCO_3^- concentration was increased from (0.1 to 100) mg/L , fluoride adsorption efficiency decreased from 94.38.0 % to 20.220 %. $(\text{PO}_4)^{3-}$ causes less adsorption, and fluoride competes for the same active site after inner-sphere complexation. By the addition of Cl^- shows no remarkable competition with fluoride during adsorption. Hence Cl^- bonding was weaker and less ligand affinity with the active site when compared to F^- . Chloride, carbonate, Sulphate and phosphate, among other major anions, decreased fluoride adsorption in the descending sense: $\text{Cl}^- < \text{SO}_4^{2-} < \text{PO}_4^{3-} < \text{CO}_3^{2-}$.

Since ALUM-MBENT fluoride adsorption is decreased with existence of different concentrations of bicarbonate, phosphate and chloride, its useful life cycle in groundwater with high ion concentrations is predicted to be shortened. As a result, these must be taken into account when planning for field use. In light of the fact that certain anions are often found in real groundwater, the evaluation of the ALUM-MBENT adsorbent for real ground water application was investigated for the combined effect of anions like sulphate, phosphate, carbonates, chloride and bi- carbonates. The percentage fluoride removal for fluoride only and with co-existing anions at initial fluoride concentration of 5 mg/L , flow rate of 15 mL/min and bed depth of 10 cm is 94.38 and 92.13 respectively. As depicted in Figure 6.3a & b, for the $C_0 = 5\text{mg/L}$, $Q = 25\text{mL/min}$

& bed depth of 10cm, the residual concentration reaches C_0 at 300min of analysis.

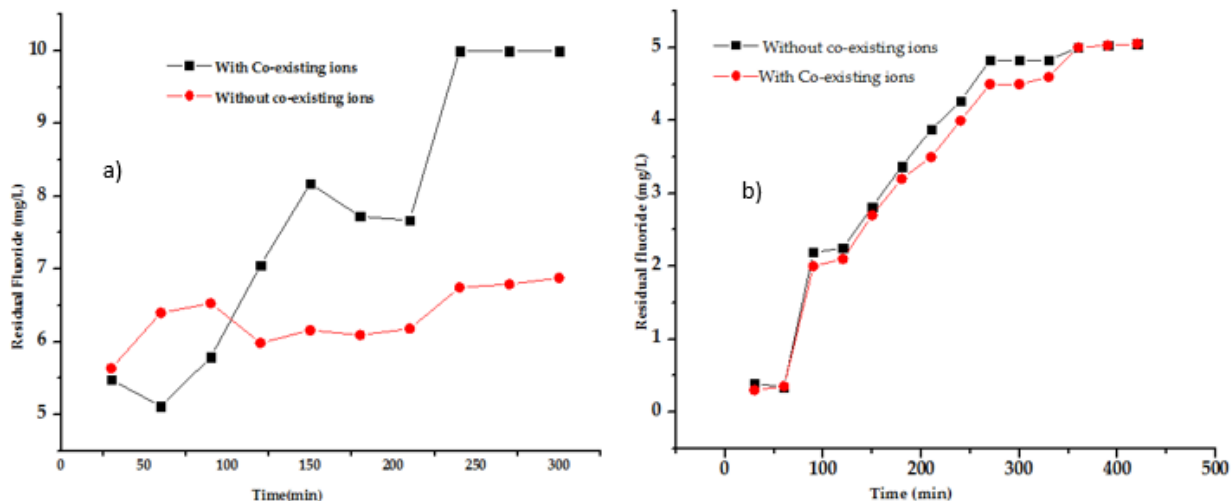


Figure 6.3: Effects of Co-existing anions a) $C_0 = 5\text{mg/L}$, $Q = 25\text{mL/min}$ & bed depth = 2cm b) $C_0 = 5\text{mg/L}$, $Q = 15\text{mL/min}$ & bed depth = 10cm.

6.2. Spent adsorbent regeneration.

Spent adsorbent regeneration plays a vital role in the application. The experiment was carried out for 5mgL^{-1} concentration, 15mL/min flowrate and 10cm bed depth for 410min. As shown in Figure 6.4, the blank removal (only Fluoride) rate was 94.5 percent, the first cycle removal rate was 86.2 percent, and the third cycle removal rate was 68.53 percent (1.57 mg/1 residual fluoride, which is close to the WHO guideline value) [160]. The removal efficiency decreases as the cycle progresses, which may be due to the adsorbent's binding sites being lost or the material losing its surface cations. The reusability study was carried out from 1–3 cycles presented in Figure 6.4. Effect of adsorption on ALUM-MBENT decreased from 94.5 to 68.53%. The overall detailed column study recommended that the adsorbent will effectively work for the first three cycles without considerable loss of adsorption efficiency for the first 150min.

Since fluoride removal decreases as the consumption period progresses, full adsorbent regeneration may not be appropriate.

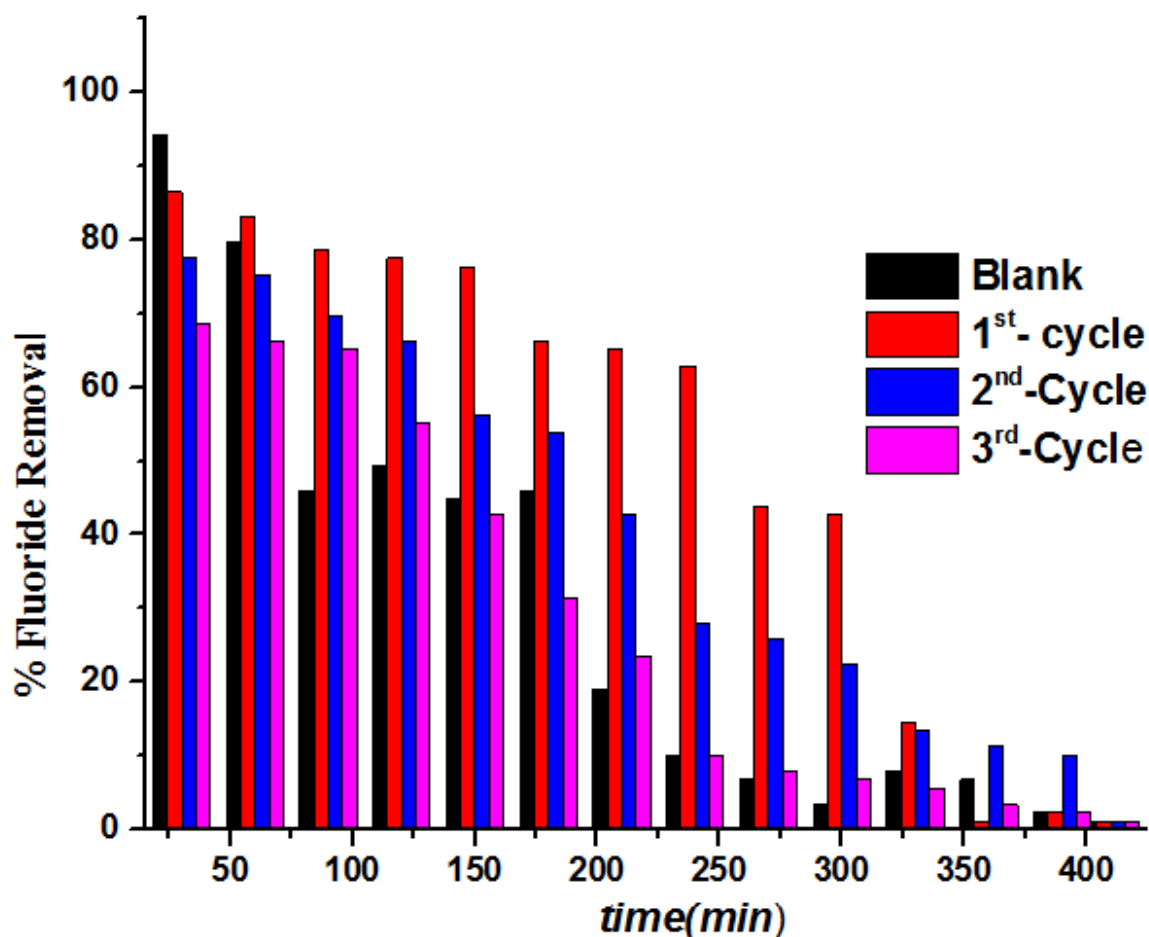


Figure 6.4: Removal percentage of fluoride obtained using 0.1MNaOH regenerants at 10cm column depth, 5mg/l of fluoride concentration and 15ml/min flowrate conducted with three de-fluoridation cycles

6.3. Summary

The aluminum amended bentonite clay (ALUM-MBENT) adsorbent is an effective adsorbent for fluoride removal from groundwater. Phosphate, sulphate, chloride, carbonates, and nitrate are among the ions found in drinking water. As a result, they will interact with fluoride anions for adsorbent active sites on the surface of the adsorbent. In column mode, the effects of anions on fluoride adsorption were investigated using concentrations of each anion of 0.1, 10, and 100 mg L⁻¹. When

competing anions were present, the adsorption capacity of the adsorbent reduced, according to the findings. multi valent anions are more easily absorbed than monovalent anions. Hence, Carbonates and phosphate were the main anions that had the greatest influence on fluoride adsorption. The fluoride adsorption is strongly affected by concentrations of competing anions. Phosphate, bicarbonate and sulfate greatly reduced fluoride adsorption. But Chloride had little effect on the sorption. The impact of major anions on fluoride adsorption followed the order of $\text{Cl}^- < \text{SO}_4^{2-} < \text{PO}_4^{3-} < \text{CO}_3^{2-}$.

CHAPTER 7: CONCLUSIONS AND RECOMMENDATIONS

7.1. Conclusion

Groundwater is the most significant source of community water supply in the East African Rift Valley zone, particularly in rural regions. However, one of the major issues related with its use is the presence of high quantities of fluoride. People in these places employ bone char and Nalgonda for defluoridation, however the methods are not effective in removing fluoride. The approaches appear to have flaws, since some local users reject them owing to cultural beliefs. There is therefore continuous interest to search for alternative adsorbents. Researchers are especially interested in the use of modified locally accessible materials as fluoride adsorbents since it may allow for local manufacture, which might contribute to both lower production costs and long-term sustainability. The purpose of this study was to look at a more cost-effective technique of removing fluoride from groundwater. The adsorptive removal of fluoride from aqueous solutions was examined using natural or modified low-cost adsorbents/bentonite clay [modified with acid and aluminum]. The findings may be useful to water providers in terms of strategic planning for the provision of safe drinking water to the research area's population in order to reduce the occurrence of fluorosis and other fluoride-related health problems. The study's analytical approach may be valuable to students and academics interested in undertaking comparable fluoride occurrence investigations in other similar sedimentary rock formations.

With regards to the interest in modifying the physico-chemical properties of locally available materials for groundwater defluoridation, bentonite is one such materials that is indigenous in many countries, which could possibly be used as a base material for the synthesis of a fluoride adsorbent, especially in regions where most adsorbents may not be locally available. Raw bentonite has known de-fluoridation properties; however, the fluoride adsorption capacity is limited and, modifications of its physico-chemical properties for improved performance appear not have been well studied. Moreover, some

studied and reported defluoridation materials are either of fine particles or powder that could make separation from aqueous solution difficult. Such materials could also cause clogging and/or low hydraulic conductivities when applied in fixed-bed adsorption systems. Raw bentonite on the other hand is robust and possess sufficient mechanical strength, and could be used as a base material for the production of a granular (upto 2mm in particle size) adsorbent with enhanced defluoridation capability that can also overcome limitations such as clogging and/or low hydraulic conductivities in fixed-bed adsorption systems. The properties of an adsorbent material, which may contribute to the number of available active sites for fluoride uptake may include both the surface area, as well as the nature of the surface (i.e. its reactivity/affinity for fluoride ions). Therefore, in the process of developing a fluoride adsorbent material, methods or process conditions that enhance both the surface area and reactivity/affinity of the produced adsorbent, require attention.

The study examines the efficacy of unmodified and modified with Aluminum/Acid bentonite clay as an adsorbent for adsorption technology. Thus, the findings of this study may aid in the search for alternative appropriate de-fluoridation materials that are sustainable for the treatment of fluoride-contaminated groundwater in underdeveloped nations. A series of essential adsorption tests (column mode) were undertaken to assess the potentiality of the adsorbents, and the findings of these investigations are given and analyzed in chapters 3–7. The extensive use of adsorption models in this thesis for the explanation of adsorption experimental data may be of benefit to scholars interested in the application of adsorption technology for water de-fluoridation and the removal of other pollutants from the aqueous phase in broad sense. In accordance with the specific objectives of the thesis, the study's findings can be summarized as follows.

- ✓ Since fluorosis is a permanent concern and there is no known effective cure, treatment of fluoride-contaminated water is required as a preventive strategy to avoid ingestion of excess fluoride. The adsorption approach is

deemed adequate among the technical choices for treating fluoride-contaminated groundwater; but, a major difficulty with the application of adsorption is the availability of a suitable adsorbent. Furthermore, a related problem linked with the usage of any particular fluoride adsorbent is its capacity to regenerate, allowing re-use, as this is required for its practical and economic feasibility. The proper disposal of a fluoride-saturated adsorbent when after it can no further be recycled to avoid groundwater pollution is also a concern.

- ✓ There are also substantial obstacles in developing a fluoride adsorbent capable of treating natural fluoride-contaminated groundwater in the field once it has been synthesized/produced and evaluated in the laboratory. Fluoride removal efficacy in the laboratory may not be reproducible in the field.
- ✓ This study also aptly illustrated that modifying the surfaces of indigenous/locally available materials (bentonite) through an Al modified/incorporation procedure, was a useful approach for developing innovative fluoride adsorbents. Even though batch adsorption tests are a quick and convenient way to evaluate adsorbent fluoride removal ability, the results are not as informative as those from continuous-flow column experiments. Under laboratory continuous flow settings employing a fixed bed column, both Aluminum and acid -modified local materials were capable of lowering fluoride concentrations in model water from 10 mg/L to 1.5 mg/L. Al-modified bentonite was shown to be the most successful and promising, with a generally strong potential for application in fluoritic areas of poor nations where charcoal is accessible for the treatment of fluoride-contaminated groundwater.
- ✓ pH, CEC, $pH_{p.z.c}$ measurements, FTIR, SEM, XRD, and EDX analyses, as well as physical adsorbent properties, revealed that the mechanism of fluoride adsorption onto the Al-modified and acid modified adsorbent materials was complex and involved both physisorption and chemisorption processes. The typical pH of bentonitic material tested is little below

neutral, about 6.8, and its cation exchange capacity is 28.78 meq/100g. The smaller particle provides more surface area and leading to more sorption sites and to greater sorption. The increase in particle size from 0.212mm to 1.25mm doesn't show any change in CEC per SSA values for the case of ALUM-MBENT and slight decrease for the case of RB. Both raw and Alum-Mbent clay have high pH_{pzc} indicative of clay dominated by alumino-silicate materials and other cations or oxides. Modification of the raw bentonite clay with acid and aluminum oxide increases the pH_{pzc} and which extends the pH range for adsorption of anions. Scanning electron microscopy (SEM) and Fourier transform infrared (FTIR) spectroscopy demonstrate that high fluoride adsorption favors a surface complexation process on the adsorbent surface. From the results of XRD analysis showed there were some phases that are characteristic of bentonite is quartz with trigonal crystal structure. Indications chemistry of bentonite samples were analyzed using Energy Dispersive X-ray analyzer (EDX). In this test was obtained CaCO₃, SiO₂, Al₂O₃, Fe₂O₃, Ti, and K as the content of bentonite. The impurity of bentonite is Ti and K. SEM was used to analyze the state morphology of bentonite particles. According to these images, agglomeration occurs on bentonite as a result of the interaction of bentonite with oxygen, and the particles have a spherical form.

- ✓ The study's findings demonstrated that surface modification of raw bentonite by aluminum and acid treatment technique might provide an adsorbent medium capable of treating fluoride-contaminated model water to achieve the WHO fluoride guideline value. Calcination of the raw bentonite base material at 300°C prior to aluminum amendment / acid treatment resulted in a considerable increase in the specific surface area of ALUM-MBENT/ATB, which contributed to a large increase in fluoride adsorption efficiency when compared to untreated raw bentonite. As a result of the research, it was discovered that the textural features (specific surface area) of the starting/base material might have a major impact in the fluoride adsorption effectiveness of the generated adsorbent.

- ✓ Laboratory-scale column experiments, as opposed to batch adsorption experiments, can simulate the dynamics of a fixed bed reactor, which may be used to provide parameters for improving the design of full-scale adsorption-based water treatment systems. Furthermore, the capacity of ALUM-MBENT to regenerate after being depleted is a characteristic that may contribute to its practical and economic feasibility. Furthermore, the ease (or difficulty) of securely disposing of used (fluoride-saturated) ALUM-MBENT without causing environmental contamination is a consideration that may contribute to its viability for use in practice.
- ✓ This study indicated that ALUM-MBENT and ATB adsorbents can successfully remove fluoride from groundwater by adsorption. The ALUM-MBENT removed 94.5 percent more fluoride than the ATB, which removed 79.5 percent more fluoride with a starting fluoride concentration of 5 mg/L, a bed depth of 10cm, and a flow rate of 15mL/min. According to the findings of this study, both adsorbents are efficient in lowering fluoride levels to the WHO permitted drinking water level of 1.5mg/L. This showed that the results of fluoride removal performance obtained in the laboratory were also reproducible under real field conditions.
- ✓ An empty bed contact time (EBCT) of 48 minutes was discovered to be an appropriate reference for the construction of full-scale water filtration systems that would allow effective utilization of the ALUM-MBENT fluoride adsorption capability.
- ✓ From the outputs of adsorption modelling, it was discovered that the Adam-Bohart model described the beginning portion of the breakthrough curves for the fluoride-ALUM-MBENT system quite well, while the Thomas and Clark models could effectively describe the whole breakthrough curve. The parameters found for these models might be useful to engineers interested in optimizing the design of ALUM-MBENT column filters for ground water de-fluoridation with less laboratory testing, thereby saving time and money. The models can also be beneficial for water treatment plant operators in predicting breakthrough times when the filters are in

use, allowing them to determine when adsorbent regeneration or replacement is necessary.

- ✓ One of the shortcomings of Nalgonda, bone char & RO systems at some places of the rift valley region, that are currently used for de-fluoridation, is the formation of large amounts of sludge, which makes disposal difficult and may result in secondary environmental concerns. For example, Nalgonda method may require 800 mg of chemicals to treat 10 mg/L of fluoride, which corresponds to 80 mg of alum per unit mass of fluoride treated. According to the findings of this study, the application of ALUM-MBENT can be regenerable for re-use thus avoiding the dumping of sludge. However, further study is needed to completely comprehend the processes that occur during regeneration.
- ✓ For column operation, central composite design (CCD) in response surface methodology (RSM) was used to evaluate the influence of different operational factors on fluoride removal and adsorptive capacity for optimization and assessment of interaction effects. The factors were discovered to have substantial influence on fluoride removal as well as adsorption capacity. Under optimized condition, up to 99.05 % fluoride was removed from effluents using ATB adsorbent with initial fluoride concentrations of 5.51 mg/L, flow rate of 17.2 mL/min, bed depth of 8.88 cm with a 1.00 desirability. The selected quadratic model's significance and appropriateness were tested using analysis of variance (ANOVA). And also, Contour and perturbation plots were used to project the effect of the experimental variables and their interactions on fluoride removal and adsorption capacity. The perturbation plot revealed that the fluoride removal and adsorption capacity of the column is more sensitive to flow rate and bed depth than initial fluoride concentration. Results suggest that ATB adsorbent has potential for fluoride adsorption. All of the R^2 values indicate that the models match the experimental data well. As far as we know, no acid-treated bentonite clay has been used as an adsorbent in the RSM method using continuously flowing fixed bed column. This

adsorbent's strong fluoride adsorptive removal capacity suggests its use in industrial/household systems, and the data obtained would aid in future upscaling of the adsorption process.

- ✓ The fluoride adsorption capabilities of the adsorbents presented in this thesis were found to be equivalent or greater than those of several fluoride adsorbents found in the literature. It was also discovered that the adsorbents synthesized could be regenerated when they were saturated, which might contribute to their cost feasibility in actual applications.
- ✓ In column mode, the effects of anions on fluoride adsorption were investigated using concentrations of each anion of 0.1, 10, and 100 mg/L. When competing anions were present, the adsorption capacity of the adsorbent reduced, according to the findings. multi valent anions are more easily absorbed than monovalent anions. Hence, Carbonates and phosphate were the main anions that had the greatest influence on fluoride adsorption. The fluoride adsorption is strongly affected by concentrations of competing anions. Phosphate, bicarbonate and sulfate greatly reduced fluoride adsorption. But Chloride had little effect on the sorption. The impact of major anions on fluoride adsorption followed the order of $\text{Cl}^- < \text{SO}_4^{2-} < \text{PO}_4^{3-} < \text{CO}_3^{2-}$
- ✓ According to the US-Toxicity EPA's characterization leaching method (TCLP), wasted adsorbent (i.e. when the manufactured adsorbent is exhausted and cannot be re-used) was found to be non-hazardous and may be securely disposed of into the environment using a simple landfill.
- ✓ This study component's results and conclusions discussed the development of various novel adsorbents for the treatment of fluoride-contaminated groundwater. The information presented may be useful for water service providers, such as the government, non-governmental organizations (NGOs), and engineers, who are looking for a possible adsorbent for the treatment of fluoride-contaminated groundwater, particularly in poor nations.

- ✓ Overall, it can be concluded that the current findings can open up a new option in the removal of fluoride from fluoride polluted water employing various low-cost adsorbents/clay minerals, both in home and commercial settings. The data reported in these experiments can be extrapolated further to build and implement an effective fluoride removal plan while treating potentially polluted groundwater.
- ✓ Despite effective data gathering to accomplish the research objectives, the study experienced significant difficulties, such as a lack of appropriate circumstances for pilot-scale field testing.

7.2. General outlook, Recommendations and Limitations

This work has given some insights on a low-cost adsorption technique for removing fluoride from groundwater. It also discussed the removal procedures related with fluoride contamination, as well as the impact of co-existing ions on the technology's effectiveness.

Thus, the findings of this study may aid in the search for alternative appropriate de-fluoridation materials that are sustainable for the treatment of fluoride-contaminated groundwater in underdeveloped nations. The comprehensive use of kinetic models in this thesis for the interpretation of adsorption experimental results may be useful to students interested in using adsorption technology for water de-fluoridation and the removal of other pollutants from the aqueous phase in general. Despite the fact that the research covered many aspects of fluoride, such as the development of fluoride adsorbent materials, regeneration when exhausted, and safe disposal, there are still many aspects that were either not covered or require further understanding, as indicated below, and recommendations for future research studies.

- ✓ More research into the adsorption capability of clay-based fluoride adsorbents like bentonite is needed to increase its practical and economic feasibility, as well as its potential usage in large centralized systems. In this regard, greater research into the surface chemistry and other important qualities (e.g. textural properties) of the clay, as well as the

processes involved in the surface modification process utilizing aluminum and an acid, is needed to gain a better understanding.

- ✓ Because just three cycles of adsorbent regeneration were performed in this study using a small size column, more research on the feasibility of repeated regeneration on a pilot scale in the field is required.
- ✓ A detailed/complete cost evaluation of the production of aluminol or an acid functionalized bentonite clay for fluoride removal, regeneration, and disposal is required, based on a situation in which optimized production is done in a typical developing country setting, using locally available bentonite.
- ✓ When coexisting ions are present simultaneously, they have opposing impacts on the performance of ALUM-MBENT in terms of fluoride removal. However, more research is needed to increase the removal capabilities of the ALUM-MBENT technology when co-existing ions present in the groundwater.
- ✓ Applying the adsorbents for column performance using real contaminated groundwater at field scale for household purposes is required (as the fluoride is urgent).
- ✓

REFERENCES

1. Prystupa, J., *Fluorine—a current literature review. An NRC and ATSDR based review of safety standards for exposure to fluorine and fluorides*. Toxicology mechanisms and methods, 2011. 21(2): p. 103-170.
2. Singh, K., et al., *Removal of fluoride from aqueous solution: status and techniques*. Desalination and Water Treatment, 2013. 51(16-18): p. 3233-3247.
3. Srimurali, M., A. Pragathi, and J. Karthikeyan, *A study on removal of fluorides from drinking water by adsorption onto low-cost materials*. Environmental pollution, 1998. 99(2): p. 285-289.
4. Bhatnagar, A., E. Kumar, and M. Sillanpää, *Fluoride removal from water by adsorption—a review*. Chemical Engineering Journal, 2011. 171(3): p. 811-840.
5. Vhahangwele, M., G.W. Mugeru, and N. Tholiso, *Defluoridation of drinking water using Al³⁺-modified bentonite clay: optimization of fluoride adsorption conditions*. Toxicological & Environmental Chemistry, 2014. 96(9): p. 1294-1309.
6. Kamble, S.P., et al., *Defluoridation of drinking water using chemically modified bentonite clay*. Desalination, 2009. 249(2): p. 687-693.
7. Fewtrell, L., et al., *An attempt to estimate the global burden of disease due to fluoride in drinking water*. Journal of water and health, 2006. 4(4): p. 533-542.
8. Organization, W.H., *Boron in drinking-water: Background document for development of WHO Guidelines for Drinking-water Quality*, 2009, Geneva: World Health Organization.
9. Rasool, A., et al., *Co-occurrence of arsenic and fluoride in the groundwater of Punjab, Pakistan: source discrimination and health risk assessment*. Environmental Science and Pollution Research, 2015. 22(24): p. 19729-19746.
10. Smedley, P., et al., *Hydrogeochemistry of arsenic and other inorganic constituents in groundwaters from La Pampa, Argentina*. Applied geochemistry, 2002. 17(3): p. 259-284.
11. Vithanage, M. and P. Bhattacharya, *Fluoride in the environment: sources, distribution and defluoridation*. Vol. 13. 2015.
12. Tekle-Haimanot, R., et al., *The geographic distribution of fluoride in surface and groundwater in Ethiopia with an emphasis on the Rift Valley*. Science of the Total Environment, 2006. 367(1): p. 182-190.
13. Dessalegne, M., et al., *Effective fluoride adsorption by aluminum oxide modified clays: Ethiopian bentonite vs commercial montmorillonite*. Bulletin of the Chemical Society of Ethiopia, 2018. 32(2): p. 199-211.

14. Gevera, P. and H. Mouri, *Natural occurrence of potentially harmful fluoride contamination in groundwater: an example from Nakuru County, the Kenyan Rift Valley*. Environmental Earth Sciences, 2018. 77(10): p. 365.
15. Kloos, H. and R.T. Haimanot, *Distribution of fluoride and fluorosis in Ethiopia and prospects for control*. Tropical Medicine & International Health, 1999. 4(5): p. 355-364.
16. Viswanathan, N. and S. Meenakshi, *Role of metal ion incorporation in ion exchange resin on the selectivity of fluoride*. Journal of hazardous materials, 2009. 162(2-3): p. 920-930.
17. Waghmare, S.S., et al., *Preparation and characterization of polyalthia longifolia based alumina as a novel adsorbent for removing fluoride from drinking water*. Asian J. Adv. Basic Sci, 2015. 4(1): p. 12-24.
18. Zhang, S., et al., *Removal of fluoride ion from groundwater by adsorption on lanthanum and aluminum loaded clay adsorbent*. Environmental Earth Sciences, 2016. 75(5): p. 401.
19. Mourabet, M., et al., *Removal of fluoride from aqueous solution by adsorption on Apatitic tricalcium phosphate using Box-Behnken design and desirability function*. Applied Surface Science, 2012. 258(10): p. 4402-4410.
20. Chen, N., et al., *An excellent fluoride sorption behavior of ceramic adsorbent*. Journal of Hazardous Materials, 2010. 183(1-3): p. 460-465.
21. Loganathan, P., et al., *Defluoridation of drinking water using adsorption processes*. Journal of hazardous materials, 2013. 248: p. 1-19.
22. Karthikeyan, G., A. Pius, and G. Alagumuthu, *Fluoride adsorption studies of montmorillonite clay*. 2005.
23. Moges, G., F. Zewge, and M. Socher, *Preliminary investigations on the defluoridation of water using fired clay chips*. Journal of African Earth Sciences, 1996. 22(4): p. 479-482.
24. Walther, I., *Fluoride contamination in the main Ethiopian Rift Valley*, 2009.
25. South Africa, D.M.E.A.V.N., *Bentonite, pyrophyllite and talc in the Republic of South Africa, 2004*. 2005, Pretoria: Directorate : Mineral Economics, Department of Minerals and Energy.
26. Ma, Y., et al., *Characteristics and defluoridation performance of granular activated carbons coated with manganese oxides*. Journal of hazardous materials, 2009. 168(2-3): p. 1140-1146.
27. Bradley, G. and D. Weils, *Elements of nature*, 2004, Blackflies and Sons, USA.
28. Beneberu, S., Z. Feleka, and C. Sing, *Removal of excess fluoride from water by aluminium hydroxide*. Bull. Chem. Soc. Ethiopia, 2006. 20(1): p. 17-34.

29. Eren, E. and B. Afsin, *Removal of basic dye using raw and acid activated bentonite samples*. Journal of hazardous materials, 2009. 166(2-3): p. 830-835.
30. Alexander, J.A., et al., *Surface modification of low-cost bentonite adsorbents—A review*. Particulate Science and Technology, 2019. 37(5): p. 534-545.
31. Rosenqvist, J., *Surface chemistry of Al and Si (hydr)oxides, with emphasis on nano-sized gibbsite (α -Al(OH)₃)*, 2002. p. 66.
32. Tekle-Haimanot, R., *Study of fluoride and fluorosis in Ethiopia with recommendations on appropriate defluoridation technologies*. Consultancy report, UNICEF—Ethiopia. Faculty of medicine, Addis Ababa University, 2005.
33. Jha, S.K., et al., *Fluoride in groundwater: toxicological exposure and remedies*. J Toxicol Environ Health B Crit Rev, 2013. 16(1): p. 52-66.
34. Yadav, K.K., et al., *Fluoride contamination, health problems and remediation methods in Asian groundwater: A comprehensive review*. Ecotoxicol Environ Saf, 2019. 182: p. 109362.
35. Keesari, T., et al., *Fluoride Geochemistry and Exposure Risk Through Groundwater Sources in Northeastern Parts of Rajasthan, India*. Arch Environ Contam Toxicol, 2021. 80(1): p. 294-307.
36. Onipe, T., J.N. Edokpayi, and J.O. Odiyo, *A review on the potential sources and health implications of fluoride in groundwater of Sub-Saharan Africa*. J Environ Sci Health A Tox Hazard Subst Environ Eng, 2020. 55(9): p. 1078-1093.
37. Brunt, R.V.L.G.J.I.G.R.A.C., *Fluoride in groundwater : probability of occurrence of excessive concentration on global scale*. 2004, Utrecht: IGRAC.
38. Apambire, W.B., D.R. Boyle, and F.A. Michel, *Geochemistry, genesis, and health implications of fluoriferous groundwaters in the upper regions of Ghana*. Environmental Geology, 1997. 33(1): p. 13-24.
39. Liu, X., B. Wang, and B. Zheng, *Geochemical process of fluorine in soil*. Chinese Journal of Geochemistry, 2014. 33(3): p. 277-279.
40. Li, P., et al., *Occurrence and hydrogeochemistry of fluoride in alluvial aquifer of Weihe River, China*. Environmental earth sciences, 2014. 71(7): p. 3133-3145.
41. Bharti, V.K., *Fluoride Sources, Toxicity and Its Amelioration: A Review*. Peertechz Journal of Environmental Science and Toxicology, 2017: p. 021-032.
42. Annadurai, S.T., et al., *Batch and column approach on biosorption of fluoride from aqueous medium using live, dead and various pretreated Aspergillus niger (FS18) biomass*. Surfaces and Interfaces, 2019. 15: p. 60-69.
43. García-Sánchez, J.J., et al., *Experimental study of the adsorption of fluoride by modified magnetite using a continuous flow system and numerical simulation*. Process Safety and Environmental Protection, 2017. 109: p. 130-139.

44. N. Janardhana Raju¹, Sangita Dey¹, and, and K. Das², *Fluoride contamination in groundwaters of Sonbhadra District, Uttar Pradesh, India* CREENT SCIENCE, 2009. 96.
45. Marília Afonso Rabelo Buzalafa, G.M.W., *Fluoride Metabolism*. Monogr Oral Sci. Basel, Karger, 2011. 22: p. 20–36.
46. Tomar, V. and D. Kumar, *A critical study on efficiency of different materials for fluoride removal from aqueous media*. Chemistry Central Journal, 2013. 7(1): p. 51.
47. Chen, N., et al., *Investigations on the batch and fixed-bed column performance of fluoride adsorption by Kanuma mud*. Desalination, 2011. 268(1-3): p. 76-82.
48. Gitari, W.M., et al., *Defluoridation of groundwater using Fe³⁺-modified bentonite clay: optimization of adsorption conditions*. Desalination and Water Treatment, 2013. 53(6): p. 1578-1590.
49. Assaoui J*, K.A.a.H.Z., *Defluoridation of Wastewater by Natural Bentonite Clay in Batch Reactor*. INorganic chemistry - An indian Journal, 2018. 13.
50. Zhang, Y., et al., *Adsorption of Fluoride from Aqueous Solution Using Low-Cost Bentonite/Chitosan Beads*. American Journal of Analytical Chemistry, 2013. 04(07): p. 48-53.
51. Zhang, Y., et al., *La(III)-loaded bentonite/chitosan beads for defluoridation from aqueous solution*. Journal of Rare Earths, 2014. 32(5): p. 458-466.
52. Singh, J., P. Singh, and A. Singh, *Fluoride ions vs removal technologies: A study*. Arabian Journal of Chemistry, 2016. 9(6): p. 815-824.
53. Abdollah Dargahi, Z.A., Mitra Mohammadi, Ali Azizi³, Ali Almasi^{2*}, Mir Mohammad Hoseini Ahagh⁴, *STUDY THE EFFICIENCY OF ALUM COAGULANT IN FLUORIDE REMOVAL FROM DRINKING WATER*. International Journal of Pharmacy & Technology. 8 p. 16772-16778
54. Ayoob, S., A. Gupta, and V.T. Bhat, *A conceptual overview on sustainable technologies for the defluoridation of drinking water*. Critical reviews in environmental science and technology, 2008. 38(6): p. 401-470.
55. Yami, T., et al., *Performance enhancement of Nalgonda technique and pilot testing electrolytic defluoridation system for removing fluoride from drinking water in East Africa*. Vol. 12. 2018. 357-369.
56. Ingole, D.N. and D. S.S.Patil, "Studies on defluoridation: A Critical Review" (2012). Journal of Engineering Research and Studies, vol3, issue 1, Jan-Mar 2012, page 111-119., 2012. 3: p. 111-119.
57. Ktari, T., C. Larchet, and B. Auclair, *Mass transfer characterization in Donnan dialysis*. Journal of membrane science, 1993. 84(1-2): p. 53-60.
58. Hichour, M., et al., *Défluoruration des eaux par dialyse de Donnan et électrodialyse*. Revue des sciences de l'eau / Journal of Water Science, 1999. 12(4): p. 671-686.

59. Zarrabi, M., *Removal of fluoride ions by ion exchange resin: kinetic and equilibrium studies*. Environmental engineering and management journal, 2014. 13: p. 205-214.
60. Sandoval, M., et al., *Fluoride removal from drinking water by electrocoagulation in a continuous filter press reactor coupled to a flocculator and clarifier*. Separation and Purification Technology, 2014. 134: p. 163–170.
61. Grich, N.B., et al., *Fluoride removal from water by electrocoagulation: Effect of the type of water and the experimental parameters*. Electrochimica Acta, 2019.
62. Ullah, R., M.S. Zafar, and N. Shahani, *Potential fluoride toxicity from oral medicaments: A review*. Iran J Basic Med Sci, 2017. 20(8): p. 841-848.
63. Barbier, O., L. Arreola-Mendoza, and L.M. Del Razo, *Molecular mechanisms of fluoride toxicity*. Chem Biol Interact, 2010. 188(2): p. 319-33.
64. Zuo, H., et al., *Toxic effects of fluoride on organisms*. Life Sci, 2018. 198: p. 18-24.
65. Sun, Z., et al., *Effects of Fluoride on SOD and CAT in Testis and Epididymis of Mice*. Biol Trace Elem Res, 2018. 184(1): p. 148-153.
66. Wei, R., et al., *Chronic fluoride exposure-induced testicular toxicity is associated with inflammatory response in mice*. Chemosphere, 2016. 153: p. 419-25.
67. Gan, Y., et al., *Coagulation removal of fluoride by zirconium tetrachloride: Performance evaluation and mechanism analysis*. Chemosphere, 2019. 218: p. 860-868.
68. Yu, W.H., et al., *Clean production of CTAB-montmorillonite: formation mechanism and swelling behavior in xylene*. Applied Clay Science, 2014. 97-98: p. 222-234.
69. Guan, X., et al., *Studies on modified conditions of biochar and the mechanism for fluoride removal*. Desalination and Water Treatment, 2015. 55(2): p. 440-447.
70. Zhaolun, W., et al., *Decolouring mechanism of Zhejiang diatomite. Application to printing and dyeing wastewater*. Environmental Chemistry Letters, 2005. 3(1): p. 33-37.
71. Kumar, E., et al., *Defluoridation from aqueous solutions by nano-alumina: Characterization and sorption studies*. Journal of Hazardous Materials, 2011. 186(2): p. 1042-1049.
72. Mudzielwana, R., et al., *Synthesis, characterization, and potential application of Mn 2+-intercalated bentonite in fluoride removal: adsorption modeling and mechanism evaluation*. Applied Water Science, 2017. 7(8): p. 4549-4561.
73. Vadivelan, V. and K.V. Kumar, *Equilibrium, kinetics, mechanism, and process design for the sorption of methylene blue onto rice husk*. Journal of colloid and interface science, 2005. 286(1): p. 90-100.

74. Ghorbani, F., et al., *Application of response surface methodology for optimization of cadmium biosorption in an aqueous solution by Saccharomyces cerevisiae*. Chemical Engineering Journal, 2008. 145(2): p. 267-275.
75. Zhou, C.-H., et al., *Paper-like composites of cellulose acetate–organo-montmorillonite for removal of hazardous anionic dye in water*. Chemical Engineering Journal, 2012. 209: p. 223-234.
76. Onyango, M.S., et al., *Uptake of fluoride by Al³⁺ pretreated low-silica synthetic zeolites: adsorption equilibrium and rate studies*. Separation Science and Technology, 2006. 41(4): p. 683-704.
77. Paudyal, H., et al., *Adsorptive removal of fluoride from aqueous medium using a fixed bed column packed with Zr(IV) loaded dried orange juice residue*. Bioresour Technol, 2013. 146: p. 713-720.
78. Maity, J.P., et al., *Removal of fluoride from water through bacterial-surfactin mediated novel hydroxyapatite nanoparticle and its efficiency assessment: Adsorption isotherm, adsorption kinetic and adsorption Thermodynamics*. Environmental Nanotechnology, Monitoring & Management, 2018. 9: p. 18-28.
79. Kofa, G.P., et al., *Removal of Fluoride from Water by Adsorption onto Fired Clay Pots: Kinetics and Equilibrium Studies*. Journal of Applied Chemistry, 2017. 2017: p. 1-7.
80. Bharat, G.K., M.K.N. Yenkie, and G.S. Natarajan, *Influence of Physico-Chemical Characteristics of Adsorbent and Adsorbate on Competitive Adsorption Equilibrium and Kinetics*, in *Fundamentals of Adsorption: Proceedings of the Fifth International Conference on Fundamentals of Adsorption*, M.D. LeVan, Editor. 1996, Springer US: Boston, MA. p. 91-99.
81. Biswas, K., K. Gupta, and U.C. Ghosh, *Adsorption of fluoride by hydrous iron(III)–tin(IV) bimetal mixed oxide from the aqueous solutions*. Chemical Engineering Journal, 2009. 149(1-3): p. 196-206.
82. Gebrewold, B.D., et al., *Fluoride removal from groundwater using chemically modified rice husk and corn cob activated carbon*. Environ Technol, 2018: p. 1-15.
83. Ye, Y., et al., *Fluoride removal from water using a magnesia-pullulan composite in a continuous fixed-bed column*. J Environ Manage, 2018. 206: p. 929-937.
84. Lee, C.-G., et al., *Comparative analysis of fixed-bed sorption models using phosphate breakthrough curves in slag filter media*. Desalination and Water Treatment, 2015. 55(7): p. 1795-1805.
85. Onyango, M.S., et al., *Breakthrough Analysis for Water Defluoridation Using Surface-Tailored Zeolite in a Fixed Bed Column*. Industrial & Engineering Chemistry Research, 2009. 48(2): p. 931-937.
86. Talat, M., et al., *Effective removal of fluoride from water by coconut husk activated carbon in fixed bed column: Experimental and*

- breakthrough curves analysis*. Groundwater for Sustainable Development, 2018. 7: p. 48-55.
87. Patel, H., *Fixed-bed column adsorption study: a comprehensive review*. Applied Water Science, 2019. 9(3): p. 45.
 88. Moyo, M., V.E. Pakade, and S.J. Modise, *Biosorption of lead (II) by chemically modified Mangifera indica seed shells: adsorbent preparation, characterization and performance assessment*. Process Safety and Environmental Protection, 2017. 111: p. 40-51.
 89. Sathasivam, K. and M.R.H.M. Haris, *Adsorption kinetics and capacity of fatty acid-modified banana trunk fibers for oil in water*. Water, Air, & Soil Pollution, 2010. 213(1): p. 413-423.
 90. López-Cervantes, J., et al., *Study of a fixed-bed column in the adsorption of an azo dye from an aqueous medium using a chitosan-glutaraldehyde biosorbent*. Adsorption Science & Technology, 2018. 36(1-2): p. 215-232.
 91. Sheng, L., et al., *Mesoporous/microporous silica materials: preparation from natural sands and highly efficient fixed-bed adsorption of methylene blue in wastewater*. Microporous and Mesoporous Materials, 2018. 257: p. 9-18.
 92. Teutscherova, N., et al., *Leaching of ammonium and nitrate from Acrisol and Calcisol amended with holm oak biochar: A column study*. Geoderma, 2018. 323: p. 136-145.
 93. Zou, W., L. Zhao, and L. Zhu, *Adsorption of uranium (VI) by grapefruit peel in a fixed-bed column: experiments and prediction of breakthrough curves*. Journal of Radioanalytical and Nuclear Chemistry, 2013. 295(1): p. 717-727.
 94. Ahmed, M. and B. Hameed, *Removal of emerging pharmaceutical contaminants by adsorption in a fixed-bed column: a review*. Ecotoxicology and Environmental Safety, 2018. 149: p. 257-266.
 95. Ye, Y., et al., *Fluoride removal from water using a magnesia-pullulan composite in a continuous fixed-bed column*. Journal of environmental management, 2018. 206: p. 929-937.
 96. Ma, Y., et al., *Preparation of granular Zr-loaded bentonite and its defluoridation properties from aqueous solutions*. Harbin Institute of Technol.(New Series), 2005. 12: p. 236-240.
 97. Temuujin, J., et al., *Characterisation of acid activated montmorillonite clay from Tuulant (Mongolia)*. Ceramics International, 2004. 30(2): p. 251-255.
 98. Tor, A., *Removal of fluoride from an aqueous solution by using montmorillonite*. Desalination, 2006. 201(1-3): p. 267-276.
 99. Thakre, D., et al., *Magnesium incorporated bentonite clay for defluoridation of drinking water*. Journal of Hazardous Materials, 2010. 180(1-3): p. 122-130.
 100. Mudzielwana, R., et al., *Performance of Mn²⁺ modified Bentonite Clay for the Removal of Fluoride from Aqueous Solution*. South

- African journal of chemistry. Suid-Afrikaanse tydskrif vir chemie, 2018. 71: p. 15-23.
101. Gitari, W., et al., *Defluoridation of groundwater using Fe³⁺-modified bentonite clay: optimization of adsorption conditions*. Desalination and Water Treatment, 2015. 53(6): p. 1578-1590.
 102. Assaoui, J., A. Kheribech, and Z. Hatim, *Defluoridation of Wastewater by Natural Bentonite Clay in Batch Reactor*. Inorg. Chem. Ind. J., 2018. 13(1): p. 121.
 103. Thakre, D., et al., *Magnesium incorporated bentonite clay for defluoridation of drinking water*. J Hazard Mater, 2010. 180(1-3): p. 122-30.
 104. Temuujin, J., et al., *Characterization and bleaching properties of acid-leached montmorillonite*. Journal of Chemical Technology & Biotechnology: International Research in Process, Environmental & Clean Technology, 2006. 81(4): p. 688-693.
 105. Farooq, M., A. Ramli, and D. Subbarao, *Physiochemical Properties of γ -Al₂O₃-MgO and γ -Al₂O₃-CeO₂ Composite Oxides*. Journal of Chemical & Engineering Data, 2012. 57(1): p. 26-32.
 106. Allen, R., *Standard test methods for determining average grain size (F112)*. Annual Book of ASTM Standards, Metal-Mechanical Testing; Elevated and Low Temperature Tests; Metallography, 1999.
 107. Huerta-Pujol, O., et al., *Bulk density determination as a simple and complementary tool in composting process control*. Bioresource technology, 2010. 101(3): p. 995-1001.
 108. Kahr, G. and F. Madsen, *Determination of the cation exchange capacity and the surface area of bentonite, illite and kaolinite by methylene blue adsorption*. Applied Clay Science, 1995. 9(5): p. 327-336.
 109. Hang, P.T. and G. Brindley, *Methylene blue absorption by clay minerals. Determination of surface areas and cation exchange capacities (clay-organic studies XVIII)*. Clays and clay minerals, 1970. 18(4): p. 203-212.
 110. Rihayat, T., et al., *Determination of CEC value (Cation Exchange Capacity) of Bentonites from North Aceh and Bener Meriah, Aceh Province, Indonesia using three methods*. IOP Conference Series: Materials Science and Engineering, 2018. 334: p. 012054.
 111. Lataye, D.H., I.M. Mishra, and I.D. Mall, *Removal of Pyridine from Aqueous Solution by Adsorption on Bagasse Fly Ash*. Industrial & Engineering Chemistry Research, 2006. 45(11): p. 3934-3943.
 112. Nwosu, F.O., et al., *Preparation and characterization of adsorbents derived from bentonite and kaolin clays*. Applied Water Science, 2018. 8(7): p. 195.
 113. Thomas, H.C., *Heterogeneous Ion Exchange in a Flowing System*. Journal of the American Chemical Society, 1944. 66(10): p. 1664-1666.

114. Yoon, Y.H. and J.H. Nelson, *Application of Gas Adsorption Kinetics I. A Theoretical Model for Respirator Cartridge Service Life*. American Industrial Hygiene Association Journal, 1984. 45(8): p. 509-516.
115. Goel, J., et al., *Removal of lead(II) by adsorption using treated granular activated carbon: Batch and column studies*. Journal of Hazardous Materials, 2005. 125(1): p. 211-220.
116. García-Sánchez, J., et al., *Removal of fluoride ions from drinking water and fluoride solutions by aluminum modified iron oxides in a column system*. Journal of colloid and interface science, 2013. 407: p. 410-415.
117. Biswas, S. and U. Mishra, *Continuous Fixed-Bed Column Study and Adsorption Modeling: Removal of Lead Ion from Aqueous Solution by Charcoal Originated from Chemical Carbonization of Rubber Wood Sawdust*. Journal of Chemistry, 2015. 2015: p. 9.
118. Goel, J., et al., *Removal of lead (II) by adsorption using treated granular activated carbon: batch and column studies*. Journal of hazardous materials, 2005. 125(1-3): p. 211-220.
119. Kumar Gupta, V., et al., *Application of response surface methodology to optimize the adsorption performance of a magnetic graphene oxide nanocomposite adsorbent for removal of methadone from the environment*. J Colloid Interface Sci, 2017. 497: p. 193-200.
120. Alkhatib, M.F.R., A.A. Mamun, and I. Akbar, *Application of response surface methodology (RSM) for optimization of color removal from POME by granular activated carbon*. International Journal of Environmental Science and Technology, 2014. 12: p. 1295-1302.
121. Prakash Kumar, B.G., et al., *Preparation of steam activated carbon from rubberwood sawdust (Hevea brasiliensis) and its adsorption kinetics*. J Hazard Mater, 2006. 136(3): p. 922-9.
122. Bhatti, M.S., et al., *Modeling and optimization of voltage and treatment time for electrocoagulation removal of hexavalent chromium*. Desalination, 2011. 269(1-3): p. 157-162.
123. Biswas, G., et al., *Application of response surface methodology for optimization of biosorption of fluoride from groundwater using Shorea robusta flower petal*. Applied Water Science, 2017. 7(8): p. 4673-4690.
124. Ghosh, S.B., R. Bhaumik, and N.K. Mondal, *Optimization study of adsorption parameters for removal of fluoride using aluminium-impregnated potato plant ash by response surface methodology*. Clean Technologies and Environmental Policy, 2016. 18(4): p. 1069-1083.
125. Feng, Q., et al., *Synthesis of LiAl₂(OH)₆⁺ intercalated montmorillonite by a hydrothermal soft chemical reaction*. Journal of Materials Chemistry, 2000. 10(2): p. 483-488.
126. Madejová, J., et al., *Comparative FT-IR study of structural modifications during acid treatment of dioctahedral smectites and*

- hectorite*. *Spectrochimica Acta Part A: Molecular and Biomolecular Spectroscopy*, 1998. 54(10): p. 1397-1406.
127. Farmer, V.C., *Infrared spectra of minerals*. 1974: Mineralogical society.
 128. Temuujin, J., K. Okada, and K.J. MacKenzie, *Preparation of porous silica from vermiculite by selective leaching*. *Applied Clay Science*, 2003. 22(4): p. 187-195.
 129. Kim, D.S., *Measurement of point of zero charge of bentonite by solubilization technique and its dependence of surface potential on pH*. *Environmental Engineering Research*, 2003. 8: p. 222-227.
 130. Taty-Costodes, V.C., et al., *Removal of lead (II) ions from synthetic and real effluents using immobilized Pinus sylvestris sawdust: Adsorption on a fixed-bed column*. *Journal of Hazardous Materials*, 2005. 123(1): p. 135-144.
 131. Gupta, S. and B. Babu, *Experimental investigations and theoretical modeling aspects in column studies for removal of Cr (VI) from aqueous solutions using activated tamarind seeds*. *Journal of Water Resource and Protection*, 2010. 2(08): p. 706.
 132. Nur, T., et al., *Batch and column adsorption and desorption of fluoride using hydrous ferric oxide: Solution chemistry and modeling*. *Chemical Engineering Journal*, 2014. 247: p. 93-102.
 133. Shih, T.C., M. Wangpaichitr, and M. Suffet, *Evaluation of granular activated carbon technology for the removal of methyl tertiary butyl ether (MTBE) from drinking water*. *Water Research*, 2003. 37(2): p. 375-385.
 134. Han, R., et al., *Adsorption of methylene blue by phoenix tree leaf powder in a fixed-bed column: experiments and prediction of breakthrough curves*. *Desalination*, 2009. 245(1-3): p. 284-297.
 135. Kumari, U., et al., *Effective defluoridation of industrial wastewater by using acid modified alumina in fixed-bed adsorption column: Experimental and breakthrough curves analysis*. *Journal of Cleaner Production*, 2021. 279: p. 123645.
 136. Chen, S., et al., *Adsorption of hexavalent chromium from aqueous solution by modified corn stalk: a fixed-bed column study*. *Bioresour Technol*, 2012. 113: p. 114-20.
 137. Ghorai, S. and K. Pant, *Equilibrium, kinetics and breakthrough studies for adsorption of fluoride on activated alumina*. *Separation and purification technology*, 2005. 42(3): p. 265-271.
 138. Baharlouei, A., E. Jalilnejad, and M. Sirousazar, *Fixed-bed column performance of methylene blue biosorption by *Luffa cylindrica*: statistical and mathematical modeling*. *Chemical Engineering Communications*, 2018. 205(11): p. 1537-1554.
 139. Hanen, N. and O. Abdelmottaleb, *Modeling of the dynamics adsorption of phenol from an aqueous solution on activated carbon produced from olive stones*. *Journal of Chemical Engineering & Process Technology*, 2013. 4(3).

140. Chowdhury, A.N., et al., *Cobalt–nickel mixed oxide surface: A promising adsorbent for the removal of PR dye from water*. Appl. Surf. Sci., 2010. 256: p. 3718.
141. Yadav, M., et al., *Adsorption of fluoride from aqueous solution by Bio-F sorbent: a fixed-bed column study*. Desalination and Water Treatment, 2016. 57(14): p. 6624-6631.
142. Aksu, Z. and F. Gönen, *Biosorption of phenol by immobilized activated sludge in a continuous packed bed: Prediction of breakthrough curves*. Process Biochemistry, 2004. 39: p. 599-613.
143. Quintelas, C., et al., *Removal of Ni(II) from aqueous solutions by an Arthrobacter viscosus biofilm supported on zeolite: From laboratory to pilot scale*. Bioresource technology, 2013. 142C: p. 368-374.
144. Abu Bakar, A.H., et al., *Column Efficiency of Fluoride Removal Using Quaternized Palm Kernel Shell (QPKS)*. International Journal of Chemical Engineering, 2019. 2019: p. 5743590.
145. Kumar, H., M. Patel, and D. Mohan, *Simplified Batch and Fixed-Bed Design System for Efficient and Sustainable Fluoride Removal from Water Using Slow Pyrolyzed Okra Stem and Black Gram Straw Biochars*. ACS Omega, 2019. 4(22): p. 19513-19525.
146. Ma, Y., et al., *Removal of fluoride from aqueous solution using granular acid-treated bentonite (GHB): Batch and column studies*. Journal of hazardous materials, 2011. 185(2-3): p. 1073-1080.
147. Cronje, K., et al., *Optimization of chromium (VI) sorption potential using developed activated carbon from sugarcane bagasse with chemical activation by zinc chloride*. Desalination, 2011. 275(1-3): p. 276-284.
148. Yahaya, N., et al., *Process optimisation for Zn (II) removal by activated carbon prepared from rice husk using chemical activation*. Int J Eng Technol, 2010. 10: p. 132-136.
149. Elibol, M., *Response surface methodological approach for inclusion of perfluorocarbon in actinorhodin fermentation medium*. Process Biochemistry, 2002. 38(5): p. 667-673.
150. Can, M.Y., Y. Kaya, and O.F. Alger, *Response surface optimization of the removal of nickel from aqueous solution by cone biomass of Pinus sylvestris*. Bioresource technology, 2006. 97(14): p. 1761-1765.
151. Pehlivan, E., T. Altun, and S. Parlayici, *Utilization of barley straws as biosorbents for Cu²⁺ and Pb²⁺ ions*. J Hazard Mater, 2009. 164(2-3): p. 982-6.
152. Chang, L., S. Chen, and X. Li, *Synthesis and properties of core-shell magnetic molecular imprinted polymers*. Applied Surface Science, 2012. 258(17): p. 6660-6664.
153. Kofa, G.P., et al., *Removal of Fluoride from Water by Adsorption onto Fired Clay Pots: Kinetics and Equilibrium Studies*. Journal of Applied Chemistry, 2017. 2017: p. 6254683.

154. Cengeloglu, Y., E. Kır, and M. Ersoz, *Removal of Fluoride from Aqueous Solution by Using Red Mud*. Separation and Purification Technology, 2002. 28: p. 81-86.
155. Ben Amor, T., et al., *STUDY OF DEFLUORIDATION OF WATER USING NATURAL CLAY MINERALS*. Clays and Clay Minerals, 2018. 66(6): p. 493-499.
156. Akafu, T., A. Chimdi, and K. Gomoro, *Removal of Fluoride from Drinking Water by Sorption Using Diatomite Modified with Aluminum Hydroxide*. Journal of Analytical Methods in Chemistry, 2019. 2019: p. 4831926.
157. Nagaraj, A., et al., *Dicarboxylic acid cross-linked metal ion decorated bentonite clay and chitosan for fluoride removal studies*. RSC Advances, 2020. 10(28): p. 16791-16803.
158. He, Z.L., et al., *Effects of Co-Existing Anions on Fluoride Adsorption onto Magnesia-Amended Activated Carbon*. Advanced Materials Research, 2012. 463-464: p. 47-51.
159. Bhaumik, M., et al., *Enhanced removal of Cr(VI) from aqueous solution using polypyrrole/Fe₃O₄ magnetic nanocomposite*. J Hazard Mater, 2011. 190(1-3): p. 381-90.
160. Edition, F., *Guidelines for drinking-water quality*. WHO chronicle, 2011. 38(4): p. 104-8.